Investigation into frontal and occipital scalp dermal signatures to identify the cause of follicle miniaturisation in androgenetic alopecia

A thesis submitted by

Summik Limbu

For the degree of

Doctor of Philosophy

Department of Bioengineering

Imperial College London

January 2022

Declaration of originality

I hereby declare that this thesis is entirely the result of my own work.

Summik Limbu

January 2022

Copyright declaration

The copyright of this thesis rests with the author. Unless otherwise indicated, its contents are licensed under a Creative Commons Attribution-Non Commercial 4.0 International Licence (CC BY-NC).

Under this licence, you may copy and redistribute the material in any medium or format. You may also create and distribute modified versions of the work. This is on the condition that: you credit the author and do not use it, or any derivative works, for a commercial purpose.

When reusing or sharing this work, ensure you make the licence terms clear to others by naming the licence and linking to the licence text. Where a work has been adapted, you should indicate that the work has been changed and describe those changes.

Please seek permission from the copyright holder for uses of this work that are not included in this licence or permitted under UK Copyright Law.

Acknowledgements

First and foremost, I would like to thank my supervisors Dr Claire Higgins and Dr Paul Kemp. To Claire, thank you so much for all the support that you have provided me for the past four years. I am grateful for your guidance and all the opportunities that you have given me. To Paul, thank you for always helping me and kindly hosting me at Birmingham.

Thanks to all the current and previous members of the Higgins lab for creating a stimulating and wonderful environment to be in. Special thanks to Sharad, Helena and Krysia for all your help and for making the lab such an enjoyable place to be in. I will always fondly remember our movie and pizza night sessions and late-night conversations.

I gratefully acknowledge the funding from Engineering and Physical Sciences Research Council and my industrial sponsor, HairClone, which granted me the opportunity to undertake this PhD.

Lastly, I would like to thank my family and friends for always believing in me. I am grateful to my Mum and Dad for always encouraging me and being supportive. I am deeply thankful to Gully for always being there for me and for always having an unlimited belief in me. I am also thankful to Nand for always being so supportive and providing me with motivation as I was writing up my thesis. I am forever grateful to Manju, Susan, and Ashok especially in the last couple of months as I was finishing off my thesis. Thank you for always being supportive of me and helping me in your own unique ways.

Abstract

The hair follicle is a dynamic mini organ which undergoes phases of periodic cycling. It consists of mainly epithelial cells with a small population of mesenchymal cells. Mesenchymal-epithelial signalling drives hair follicle morphogenesis and postnatally similar mesenchymal-epithelial signalling is recapitulated to produce new hair at the start of a new hair cycle. Regeneration of a hair follicle is mainly attributed to inductive signals from the dermal papilla, which are specialised mesenchymal cells found at the base of the hair follicle. Dysregulation of the hair cycle can lead to hair disorders such as androgenetic alopecia in which terminal follicles miniaturise into vellus follicles as a result of aberrant signalling in response to androgens. The hair follicle cycling, and growth is also influenced by the macroenvironment surrounding the follicle. In the first section of this thesis, the macroenvironment of hair follicles in androgenetic alopecia is investigated through whole-mount immunolabelling and volumetric imaging. I found that follicles have reduced innervation and blood vessels but there is an increase in lymphatic vessels in androgenetic alopecia. I observed network of nerves and blood vessels connecting hair follicles in a follicular unit pointing towards a follicular unit macroenvironmental regulation of hair growth. The next part of the thesis investigated the role of the dermal papilla in miniaturisation of hair follicles. Assessing the ability of frontal and occipital dermal papilla cells using an *in vitro* double spheres model revealed decreased ability of frontal dermal papilla cells to differentiate bulge cells into follicular keratinocytes. Transcriptional profiling of patient-matched intact frontal and occipital dermal papilla and dermal sheath showed inherent differential gene expression between frontal and occipital dermal papilla and dermal sheath with each cell type defined by expression of unique signature genes. Occipital dermal papilla signature contained genes that maintain dermal papilla identity, but also novel genes were identified, whose roles in the hair follicle have not been defined. TRPS1 was selected as the gene of interest as it has been shown to have a role in both hypotrichosis and hypertrichosis implicating it in control of follicle size. The data suggests that TRPS1 potentially is involved in the maintenance of dermal papilla identity, while

its expression is required for bulge cell activation to promote a new growth phase. Regulation of TRPS1 expression by the androgen receptor further supports the role of TRPS1 in providing protection against miniaturisation of occipital hair follicles.

Table of Contents

Declaration of originality 2
Copyright declaration 3
Acknowledgements 4
Abstract 5
List of figures 10
List of tables 12
List of abbreviations 13
Chapter 1: General Introduction 16
1.1. Skin and it's appendages 17
1.2. Hair follicle 18
1.3. Hair follicle morphogenesis 21
1.3.1. Hair follicle induction capability of dermal papilla cells 24
Dermal papilla inductivity. A) Adult intact human DP have the ability to induce new hair follicles. B) Human DP cells cultured *in vitro* lose their inductivity and cannot form new follicles. C) Inductiveness of cultured human DP cells can be restored through addition of keratinocyte conditioned media, WNT, BMP and FGF activators, overexpression of alkaline phosphatase, culturing as 3D spheres and addition of DP spheres exosomes. 26
1.4. Hair cycle 26
1.4.1. Anagen phase 27
1.4.2. Catagen phase 27
1.4.3. Telogen phase 28
1.4.4. Macroenvironment of the hair follicle 30
1.5. Androgenetic alopecia 33
1.5.1. Mechanism of miniaturisation in androgenetic alopecia 34
1.5.2. Role of the androgen receptor in androgenetic alopecia 38
1.5.3. Genome-wide association studies of androgenetic alopecia 40
1.5.4. Current treatments for androgenetic alopecia 41
1.5.5. Development of a commercial cell therapeutic product for androgenetic alopecia 44
1.5.6. Clinical trials involving follicular cells for hair regeneration 46
1.6. Aims of the PhD 49
Chapter 2: Investigating the macroenvironment of hair follicles in androgenetic alopecia 50
2.1. Introduction 51
2.1.1. Changes in the follicular macroenvironment in androgenetic alopecia 51
2.1.2. Whole-mount immunolabelling and volumetric imaging 52
2.2. Specific aims in Chapter 2 54
2.3. Materials and Methods 55
2.3.1. Collection of frontal and occipital hair follicles 55
2.3.2. iDISCO whole-mount immunostaining 55
2.3.3. Whole-mount imaging of hair follicles 58

2.3.4. Immunofluorescence quantification 58
2.3.5. Statistical analysis 59

2.4. Results **59**
2.4.1. Innervation around the hair follicle macroenvironment 59
2.4.2. Innervation of hair follicles is decreased in frontal hair follicles 68
2.4.3. Characterisation of blood vessels in hair follicles 69
2.4.4. Frontal hair follicles contain less blood vessels 72
2.4.5. Characterisation of lymphatic vessels in hair follicles 74
2.4.6. There is an increase in lymphatic vessels in frontal hair follicles 78

2.5. Summary **80**

Chapter 3: Transcriptomic analysis to elucidate the protective nature of occipital hair follicles ***83***

3.1. Introduction **84**
3.1.1. Differences between balding and non-balding dermal papilla 85
3.1.2. *In vitro* co-culture systems 86

3.2. Specific aims in Chapter 3 ..... **88**

3.3. Materials and Methods **89**
3.3.1. Collection of human tissue 89
3.3.2. Isolation and culture of dermal papilla and dermal sheath cells 89
3.3.3. Isolation and culture of papillary and reticular fibroblasts 90
3.3.4. Isolation and culture of human bulge cells 90
3.3.5. Isolation and culture of skin keratinocytes 91
3.3.6. Transcriptomic analysis of intact dermal papilla and dermal sheath 92
3.3.7. Establishment of frontal and occipital dermal papilla cells as spheres 93
3.3.8. *In vitro* inductivity model 93
3.3.9. Collection of 3D dermal papilla conditioned media 94
3.3.10. *In vitro* miniaturisation model 94
3.3.11. siRNA transfection 95
3.3.12. Compounds 95
3.3.13. RNA extraction, reverse transcription, and quantitative RT-PCR 95
3.3.14. Immunofluorescence 97
3.3.15. Bisulfite sequencing 98

3.4. Results **100**
3.4.1. Dermal papilla cells reprogramme skin keratinocytes towards a follicular fate 100
3.4.2. Dermal papilla induces highest expression of keratin 75 compared to papillary and reticular fibroblasts 104
3.4.3. Frontal and occipital dermal papilla cells have different hair inducing ability 107
3.4.4. Frontal and occipital follicular mesenchyme have inherently different gene expression 110
3.4.5. Identification of signature genes of follicular mesenchyme 115
3.4.6. TRPS1 regulates expression of BLCAP 122
3.4.7. TRPS1 knockdown decreases K75 expression 124
3.4.8. TRPS1 does not affect the age of dermal papilla cells 126
3.4.9. Expression of TRPS1 is regulated by the androgen receptor 129

3.5. Summary **131**

Chapter 4: Discussion and future directions ***133***

4.1. Changes in nerves, blood vessels and lymphatic vessels in AGA **134**

4.2. *In vitro* models are useful to test for inductivity **139**

4.3. Miniaturisation can be modelled *in vitro* **140**

4.4. Transcriptomic analysis of frontal and occipital hair follicle mesenchyme reveals inherent differential gene expression.....141

4.5. Potential role of TRPS1 in androgenetic alopecia 143

4.6. Androgenic regulation of TRPS1 145

4.7. Conclusions 146

4.8. Future directions 149

References..... 150

Appendix..... 176

List of figures

Figure 1.1: Structure of the skin. 18
Figure 1.2: Hair follicle anatomy. 20
Figure 1.3: Hair follicle morphogenesis. 24
Figure 1.4: Dermal papilla inductivity. 26
Figure 1.5: The hair cycle. 29
Figure 1.6: Macroenvironment of the hair follicle. 33
Figure 1.7: Miniaturisation of a hair follicle. 37
Figure 1.8: Mechanism of action of the androgen receptor. 39
Figure 1.9: Regeneration versus Rejuvenation. 44
Figure 1.10: Differences between hair multiplication process and hair transplantation. 46
Figure 1.11: Timeline of major research conducted which helped to understand the basis of hair regeneration and the companies involved in the development of a cell therapeutic product for androgenetic alopecia. 48

Figure 2.1: Hair follicles before and after tissue clearing. 60
Figure 2.2: Innervation around the hair follicle macroenvironment. 62
Figure 2.3: Innervation of eccrine gland, sebaceous gland and vessel/gland. 63
Figure 2.4: Specialised nerve endings in human hair follicles. 64
Figure 2.5: Same nerve branches off to innervate multiple hair follicles in a follicular unit. 65
Figure 2.6: Close interactions between nerves and epithelial cells. 67
Figure 2.7: Comparison of mean fluorescence intensity of NFH in frontal and occipital hair follicles. 68
Figure 2.8: Hair follicles are highly vascularised. 70
Figure 2.9: Blood vessels around the hair follicle. 72
Figure 2.10: Comparison of mean fluorescence intensity of CD31 in frontal and occipital hair follicles. 73
Figure 2.11: Lymphatic vessels of a hair follicle. 75
Figure 2.12: LYVE-1 staining of the hair follicle. 76
Figure 2.13: Lymphatic vessels and blood vessels are in close association with each other. 77
Figure 2.14: Comparison of mean fluorescence intensity of LYVE-1 in frontal and occipital hair follicles. 79

Figure 3.1: DP-KC spheres formed using KC grown under feeder-free and feeder-dependent culture conditions. 101
Figure 3.2: DP reprogrammes skin KC into follicular KC. 103
Figure 3.3: Comparison of K75 induction across different dermal fibroblast cell types. 105
Figure 3.4: Assessment of DP cell contact and paracrine factors for inductivity. 106
Figure 3.5: Development of an *in vitro* miniaturisation model. 109
Figure 3.6: Differential gene expression in frontal and occipital follicular mesenchyme. 111
Figure 3.7: Fold enrichment of biological processes upregulated (A) and downregulated (B) in FDP compared to ODP. 113
Figure 3.8: Fold enrichment of biological processes upregulated (A) and downregulated (B) in FDS compared to ODS. 114
Figure 3.9: Identifying unique cell type signatures. 115
Figure 3.10: Gene ontology analysis of signature FDP and ODP signature genes. 116
Figure 3.11: Protein class categorisation and RT-PCR validation of ODP signature genes. 121
Figure 3.12: Effect of TRPS1 knockdown on ODP signature genes. 123
Figure 3.13: Effect of TRPS1 knockdown on K15 and K75 expression. 125
Figure 3.14: Effect of TRPS1 knockdown on ELOVL2 methylation status. 128
Figure 3.15: Effect of androgen receptor activation and inactivation on DKK-1 and TRPS1 expression. 130

Figure 4.1: A model of hair follicle macroenvironment. 138
Figure 4.2: Expression of HHIP and SOSTDC1 in intact DP, cultured DP cells at P0, P1, P3, P5 and spheres. (From Higgins et al., 2013) 143
Figure 4.3: Schematic diagram of macroenvironmental and AR-dependent signalling changes in frontal and occipital follicle and DP. 148

Figure A.1. In situ hybridisation of ODP signature genes. 176
Figure A.2. Venn diagram to identify TRPS1 regulated genes in the follicular mesenchyme. 177

List of tables

Table 2.1: Patient information. 55
Table 2.2: Components and suppliers for PTx.2. 56
Table 2.3: Components and suppliers for permeabilization buffer, blocking solution and PTwH. 57
Table 2.4: Primary and secondary antibodies used for immunolabelling. 57

Table 3.1: FAD media components. 92
Table 3.2: Primer sequences used for quantitative RT-PCR. 96
Table 3.3: List of primary and secondary antibodies used for immunofluorescence staining. 98
Table 3.4: Primer sequences and the sequence to analyse for ELOVL2. 99
Table 3.5: Knockdown efficiency of siTRPS1 after 24, 48, 72, 96 and 125 hours of transfection. 124

List of abbreviations

2D	Two-dimensional
3D	Three-dimensional
ABAM	Antibiotic-antimycotic
AGA	Androgenetic alopecia
APM	Arrector pili muscle
AR	Androgen receptor
ARI	Aderans Research Institute
BC	Bulge cells
BMP	Bone morphogenetic protein
CD31	Cluster of differentiation 31
CLARITY	Cleared lipid-extracted acryl-hybridized rigid immunostaining/ in situ hybridization-compatible tissue hydrogel
CM	Conditioned media
COL4	Collagen 4
CSFBS	Charcoal stripped FBS
CSFBS	Charcoal stripped FBS
CTRTH2	Chemoattractant receptor-homologous molecule expressed on TH2 cells
CTS	Connective tissue sheath
DBD	DNA binding domain
DBE	Dibenzyl ether
DC	Dermal condensate
DCM	Dichloromethane
DHT	Dihydrotestosterone
DMEM	Dulbecco’s minimal essential medium
DMEM	Dulbecco’s minimal essential medium
DMSO	Dimethyl sulfoxide
DP	Dermal papilla
DS	Dermal sheath
DUPA	Diffuse unpatterned alopecia
dWAT	Dermal white adipose tissue
ECM	Extracellular matrix
eHFSC	Epithelial hair follicle stem cells
EVAL	Ethylene-co-vinyl alcohol

FBS	Foetal bovine serum
FDA	Food and Drug Administration
FDP	Frontal DP
FDP	Frontal DP
FDS	Frontal dermal sheath
FGF	Fibroblast growth factor
FNA	Follicular network A
FNB	Follicular network B
FU	Follicular units
gDNA	Genomic DNA
GFP	Green fluorescent protein
GMP	Good manufacturing practice
GWAS	Genome-wide association studies
HFDSCs	Hair follicle dermal stem cells
HMVECs	Human microvascular endothelial cells
iDISCO	Immunolabeling-enabled three-dimensional imaging of solvent-cleared organs
IP	Intellectual property
IRS	Inner root sheath
K15	Keratin 15
KC	Keratinocytes
KEGF	Keratinocyte serum-free medium
K14	Keratin 14
K17	Keratin 17
K74	Keratin 74
K75	Keratin 75
K85	Keratin 85
KRT15	Cytokeratin15
LF	Lung fibroblasts
LTMR	Low threshold mechanoreceptors
LYVE-1	Lymphatic vessel endothelial hyaluronan receptor 1
MEFs	Mouse embryonic fibroblasts
Mx	Matrix
NF	Neurofilament
NFH	Neurofilament heavy
NFL	Neurofilament light

NFM	Neurofilament medium
NGS	Normal goat serum
OCT	Optimal Cutting Temperature
ODP	Occipital DP
ODP	Occipital DP
ODS	Occipital dermal sheath
ORS	Outer root sheath
PACT	Passive CLARITY
PBS	Dulbecco′s Phosphate Buffered Saline
PBS	Dulbecco′s Phosphate Buffered Saline
PECAM-1	Platelet endothelial cell adhesion molecule 1
PFA	Paraformaldehyde
PFI	Papillary fibroblasts
PGD2	Prostaglandin D2
RFI	Reticular fibroblasts
RSPO	R-spondin
SHG	Secondary hair germ
siRNA	Small interfering RNA
TRPS	Tricho-rhino-phalangeal syndrome
VEGF	Vascular endothelial growth factor
Wls	Wntless
Wnt	Wingless-type MMTV integration site family member

Chapter 1: General Introduction

1.1. Skin and it's appendages

The skin is a complex multi-layered tissue and the largest organ of the body. It functions as a protective barrier against pathogens, chemicals, sun rays, and mechanical and environmental insults. The skin consists of three layers (Figure 1.1). The outermost layer is called the epidermis which is further subdivided into the basal layer, spinous layer, granular layer, and the stratum corneum (bottom to top). Depending on the location of the body, the epidermis can be as thin as 0.05 mm on the eyelids and as thick as 1.55 mm on palms and soles (Fenner and Clark, 2016). The epidermis also contains other cell types such as melanocytes, merkel cells and Langerhans cells (Kolarsick and Goodwin, 2018). The next layer is called the dermis, which is connected to the epidermis via the basement membrane consisting of collagen XVII, integrin α6β4, and laminin 332. The dermal layer is composed of collagen and elastic fibres and is subdivided into papillary and reticular dermis. It is populated by fibroblasts (papillary and reticular fibroblasts according to their location) along with mast cells, lymphocytes and contains various appendages such as sebaceous glands, nerves, blood vessels, lymphatic vessels, hair follicles and apocrine or eccrine glands depending on the body site (Lai-Cheong and McGrath, 2017). The deepest layer of the skin is the hypodermis which acts as an energy storage, provides insulation for the body, and is also involved in regulation of the hair cycle and wound healing. It is composed of numerous cell types such as adipocytes, adipose-derived stem cells and immune cells (Nicu *et al.*, 2018).

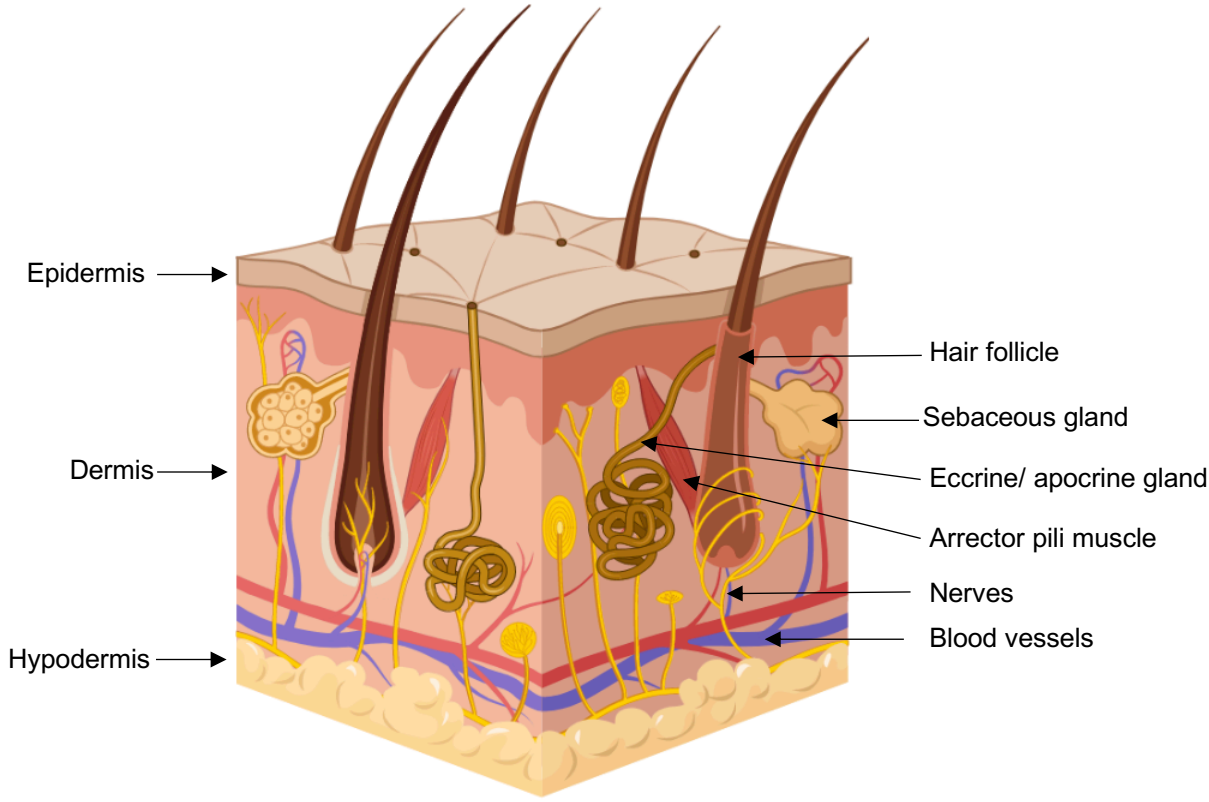


Figure 1.1: Structure of the skin.

The skin is divided into three layers: epidermis, dermis, and hypodermis. Within the skin, there are various appendages present such as hair follicles, eccrine/ apocrine and sebaceous glands, arrector pili muscle, nerves, and blood vessels. (Image from BioRender).

1.2. Hair follicle

The hair follicle is a complex mini organ which regenerates itself throughout a person's lifetime. It is primarily an ectodermal appendage consisting of small population of mesenchyme-derived fibroblasts called the dermal papilla (DP) at the bottom of the hair follicle. The hair follicle can be divided into upper, permanent portion while the lower portion regenerates at every cycle (Figure 1.2). The upper part consists of the infundibulum and isthmus. The lower part of the infundibulum is the insertion point for sebaceous glands while the lower part of the isthmus is where the arrector pili muscle is inserted. Epithelial hair follicle stem cells (eHFSC),

also known as bulge cells (BC), and melanocytic hair follicle stem cells are located in the lower part of the isthmus. The lower, cycling part of the hair follicle consists of suprabulbar epithelium and the DP. The DP is surrounded by BC-derived progenitor cells called matrix cells which receive signalling from the DP to proliferate and differentiate into different layers of the hair follicle such as the outer root sheath (ORS), inner root sheath (IRS) and the hair shaft (Schneider, Schmidt-Ullrich and Paus, 2009). The hair follicle is encapsulated by connective tissue sheath (CTS) or the dermal sheath (DS) (Martino, Heitman and Rendl, 2021).

Hair has many functions for mammals. It provides insulation, helps to conceal against predators and can also be used by some mammals to sense the environment around them through specialised type of sensory follicles called vibrissae. Unlike other primates, humans have lost their thick body hair over the course of evolution, which has been replaced by fine, unpigmented, vellus hairs; however, humans have retained thick, pigmented, terminal hairs on the scalp, eyebrows, armpits, and pubic areas. There are several theories to the evolution of hair loss in humans. One of the theories is the aquatic ape theory which argues that as humans lived on the savannahs of Africa, it was not beneficial to be covered in thick hairs during the dry season that required hunting in shallow waters and lakesides; thus, humans lost their body hair and developed a fat layer instead. However, this theory is not accepted as widely as the theory of loss of body hair for thermoregulation. As humans moved from the cool shady forests into the savannah, humans lost their body hair to be able to hunt during the day without overheating. This also led to a dramatic increase in eccrine sweat glands which helps to regulate body temperature through water loss (Kamberov *et al.*, 2015).

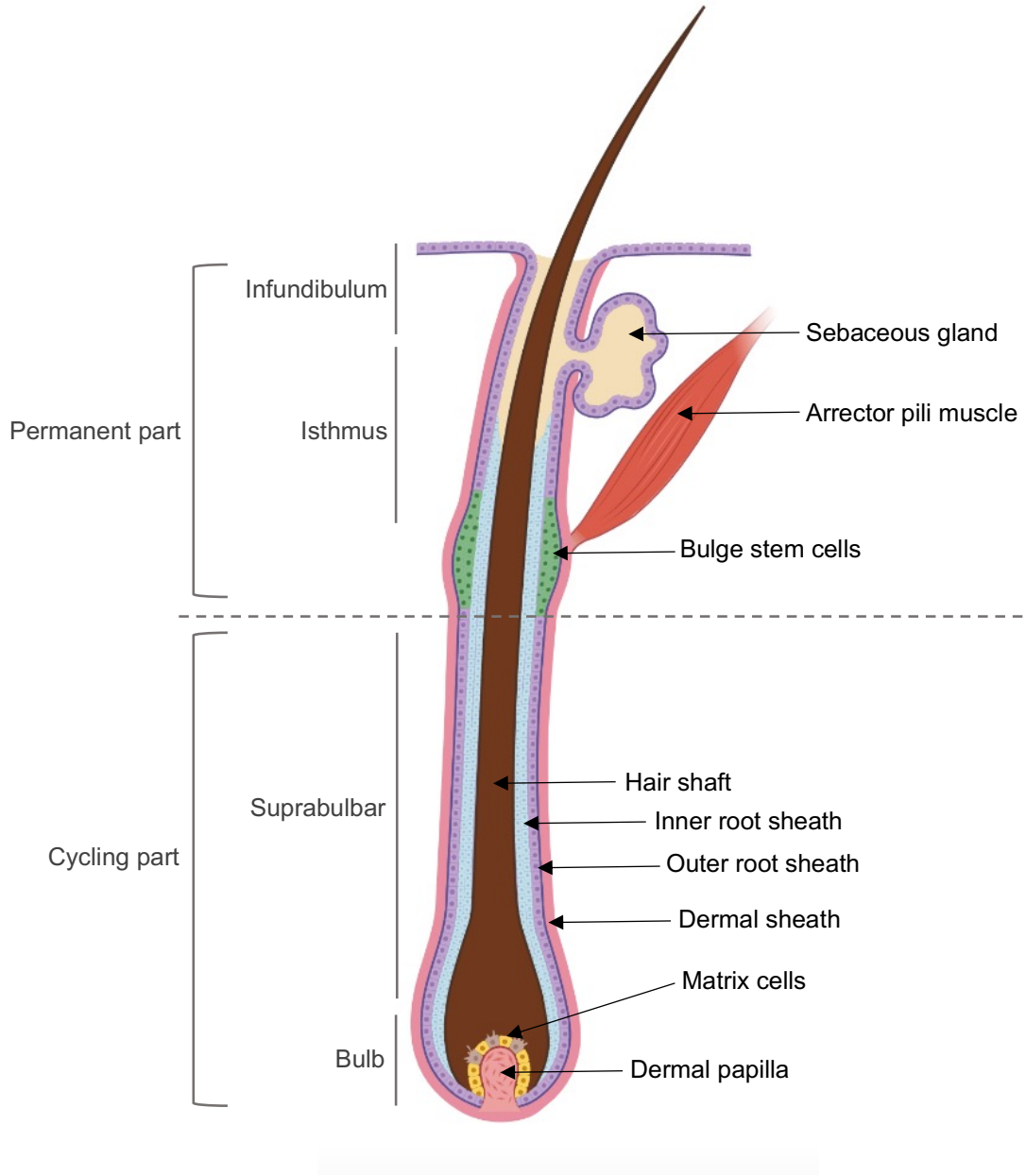


Figure 1.2: Hair follicle anatomy.

The hair follicle can be divided into two parts: upper, permanent part consisting of infundibulum and isthmus. The lower, cycling part contains the suprabulbar epithelium and the bulb which consists of dermal papilla and matrix cells. The dermal papilla directs the differentiation of matrix cells into the outer root sheath, inner root sheath and the hair shaft. Image from BioRender.

1.3. Hair follicle morphogenesis

Hair follicle morphogenesis begins during embryogenesis and requires complex epithelial and mesenchymal interactions. All hair follicles are formed before birth and no new follicles are formed postnatally. Hair follicle morphogenesis in mice has been well-characterised and recently, this process has been categorised into 10 stages taking into account the molecular and signalling events that occur in precursor cells before any morphological changes are seen. Even though the type, pattern and distribution of hair is different between mice and humans, the underlying mechanisms required for hair formation is thought to be similar.

Hair follicle induction starts with an initial signal arising from the dermis (known as “first dermal signal”) which signals to the epithelial cells in the overlying epidermis to cluster and form regularly, spaced placodes. After placode formation, the epithelial cells signal back to the dermis which leads to migration and clustering of fibroblasts under the placode to form the dermal condensate (DC). A second dermal signal arises from the DC which leads to proliferation and invasion of placode cells into the dermis. Further epithelial and mesenchymal interactions leads to the formation of a hair germ then a hair peg and eventually a mature hair follicle in which the DC is surrounded by epithelial cells and becomes the DP (Figure 1.3) (Reddy *et al.*, 2001).

It is known that the first signal for hair follicle morphogenesis arises from the dermis through tissue recombination studies *in vivo*. The dermis has the ability to reprogram non-hair bearing epidermis to form hair follicles as recombination of mouse dermis from a hairy site with mouse footpad epidermis (non-hair bearing site) leads to formation of placodes in footpad epithelium suggesting that the first signal for initiating appendage formation comes from the dermis (Dhouailly, 1973). Recombination of mouse dermis with chick foot epidermis and lizard epidermis leads to initiation of feather buds and scale placodes respectively showing that this dermal signal is conserved across appendage types (Dhouailly, 1973; Hardy, 1992).

Additionally, the origin of the dermis determines the number and size of the appendage that is formed. Smaller and higher number of feather rudiments are induced in the chick epidermis when combined with dorsal mouse dermis while vibrissae dermis induced larger but fewer feather rudiments (Dhouailly, 1973).

It is still unknown what the first dermal signal is; however, there is evidence to suggest that Wingless-type MMTV integration site family member (Wnt) signalling pathway is the earliest signal involved. Wnt signalling is activated in the upper dermis around E12.5 before hair follicle morphogenesis begins (Zhang *et al.*, 2009). Epidermal Wnt ligands are required to activate the Wnt pathway in the underlying dermis as loss of epidermal Wntless (Wls), a transmembrane protein involved in secretion of Wnt proteins, leads to inhibition of hair follicle formation (Chen et al., 2012). Epidermal Wnts activate the Wnt pathway in the dermis which leads to release of the "first dermal signal" and initiation of hair follicle formation (Chen *et al.*, 2012; de Groot *et al.*, 2021).

Wnts are secreted glycoproteins which bind to Frizzled receptors and other co-receptors such as low-density lipoprotein receptor-related protein 5 (LRP5) and LRP6 (Niehrs, 2012). Activation of the Wnt pathway leads to dissociation of ß-catenin from ß-catenin destruction complex which include Axin, adenomatosis polyposis coli (APC), protein phosphatase 2A (PP2A), glycogen synthase kinase 3 (GSK3) and casein kinase 1α (CK1α). This leads to translocation of ß-catenin into the nucleus where it binds LEF/TCF family protein which leads to activation of target genes (Komiya and Habas, 2008). Forced activation of ß-catenin in the dermis leads to formation of thickened dermis along with larger and more hair follicle placodes (Chen et al., 2012). Absence of dermal ß-catenin activity prevent placode formation (Chen et al., 2012). Inhibition of Wnt activity through overexpression of epidermal DKK-1 also results in loss of placode formation (Andl *et al.*, 2002). Wnt activity is also important in epidermis for hair follicle formation. Ablation of ß-catenin in the epidermis results in patchy hair loss at birth in mice and complete loss of hairs after the first hair cycle (Huelsken *et al.*, 2001). Deletion of

Wls in the epidermis also display patchy hair loss suggesting impaired placode formation in absence of Wls (Huang *et al.*, 2012).

The first dermal signal from the dermis induces Wnt signalling in pre-placode cells which activates EDA/EDAR/NF-κB signalling in pre-placode cells (Zhang *et al.*, 2009a). This helps to refine the borders of the hair placodes as NF-κB upregulates expression of Wnt inhibitor, DKK4, which is required for correct patterning of regularly spaced hair placodes (Sick *et al.*, 2006). The pre-placode signals back to the dermis through release of Fgf20 which specifies DC fate in pre-condensate cells which are predetermined to contribute to the condensate. Signalling from the pre-placode cells causes pre-condensate cells to aggregate under the placodes and form the DC (Biggs *et al.*, 2018; Mok *et al.*, 2019).

After establishment of physically identifiable placode and DC, there is more reciprocal signalling which leads to formation of HFSC and matrix (Mx) cells precursors. The HFSC precursors differentiate into all parts of the epithelial portion of the hair follicle along with the sebaceous gland and merkel cells (Nguyen *et al.*, 2018). As hair follicle formation progresses, continued Wnt signalling in the DC is required to form a mature hair follicle (Tsai *et al.*, 2014).

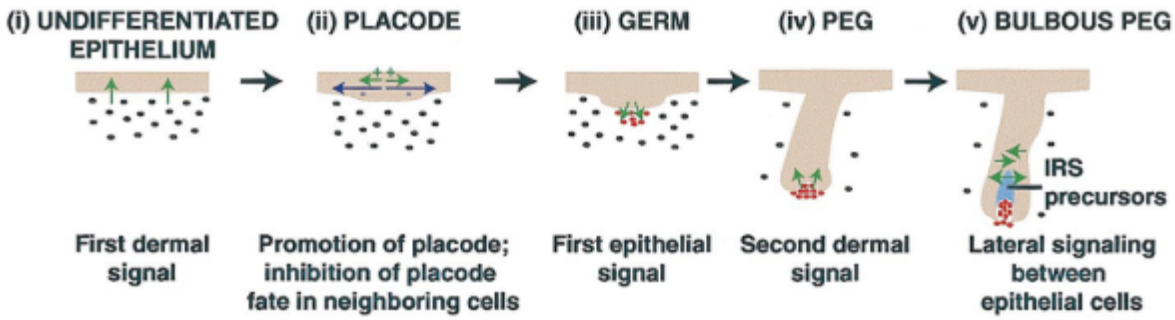


Figure 1.3: Hair follicle morphogenesis.

(i) Hair follicle morphogenesis begins with an unknown "first dermal signal" to an undifferentiated epithelium. (ii) This dermal signal results in localised clustering and thickening of the epithelium to form regularly spaced placodes. (iii) The placode signals back to the dermis ("first epithelial signal") which causes fibroblasts in the dermis to migrate under the placode and form the dermal condensate (red dots). (iv) Signalling back from the dermal condensate induces proliferation of the epithelial cells, downward growth of the follicle and envelopment of the DC by epithelial cells. (v) The DC acquires a DP fate and further reciprocal signalling leads to differentiation of the epithelial cells into IRS and formation of a mature hair follicle. (Image from Reddy et al., 2001).

1.3.1. Hair follicle induction capability of dermal papilla cells

The complex epithelial-mesenchymal interactions which occur during hair follicle morphogenesis are recapitulated postnatally during hair follicle regeneration and cycling. Research from the 1960's and 1970's showed that this regenerative ability can be attributed to the DP which maintains its inductive ability postnatally. Similarly to embryonic dermis, transplantation of adult vibrissae DP into the ear induces a large whisker follicle as appose to a small ear hair follicle (Jahoda, 1992). Oliver (1970) also showed that vibrissae DP combined with scrotal sac skin or oral epithelium transplanted into rat ear dermis form hair follicles suggesting that signalling from the adult DP can reprogramme glabrous skin into hair-bearing skin. This research opened the possibility of using human DP for cell therapy to treat hair loss disorders such as androgenetic alopecia. Transplanting intact DP into the balding scalp does

not provide any more benefit than transplanting individual hair follicles as there is not an increase in the overall number of hair follicles; however, theoretically the culture and expansion of DP cells could provide millions of cells which could be used to induce new hair follicles in the balding scalp.

Vibrissae DP cells were first cultured *in vitro* in 1981 and this was soon followed by culturing of human DP cells *in vitro* in 1984 (Jahoda & Oliver, 1981; Messenger, 1984). Similarly to intact DP, cultured vibrissae DP cells were shown to induce hair growth and reprogramme glabrous skin such as the footpad epithelium to produce hair follicles (Reynolds and Jahoda, 1992). However, this inductive ability is restricted to early passage vibrissae DP cells as late passage vibrissae DP cells cannot produce new hair follicles (Jahoda et al., 1993). Unlike cultured vibrissae DP cells, cultured human DP cells do not have inductive potential without the addition of growth factors or modifications to their culture conditions.

Numerous methods have been developed to increase hair inducing ability of cultured human DP cells such as culturing human DP cells with keratinocyte-conditioned media from newborn foreskin epidermis (Qiao et al., 2009), addition of small molecules that activate Wnt, bone morphogenetic protein (Bmp) and fibroblast growth factor (Fgf) pathways (Ohyama *et al.*, 2012), overexpression of alkaline phosphatase (Kwack et al., 2019) and culturing human DP cells as three-dimensional (3D) spheres (Higgins *et al.*, 2010, 2013; Kang *et al.*, 2012). Recently, it was shown that culturing human DP cells under hypoxic (2% O_2) conditions (Zheng et al., 2019) and addition of exosomes derived from human DP spheres can increase the hair-inductive capacity of human DP spheres (Kwack et al., 2019) (Figure 1.4).

Higgins et al., (2013) showed that the two-dimensional (2D) culture leads to significant changes in the transcriptome of human DP cells even at passage 0, while culturing DP cells as spheres restores around 22% of the gene expression which enables them to be inductive again. Culturing DP cells as spheres restores some of the DP signature genes such as HEY1,

BMP2, FGF7 and SFRP2. Similarly, other methods of restoring DP inductivity also leads to an increase in wnt, bmp and fgf target genes showing the importance of these signalling pathways for DP inductivity. Culturing DP cells under hypoxic conditions decreased expression of ß-galactosidase, which is a marker of cellular senescence, suggesting that passaging of DP cells as 2D cultures could increase their ageing (Zheng et al., 2019).

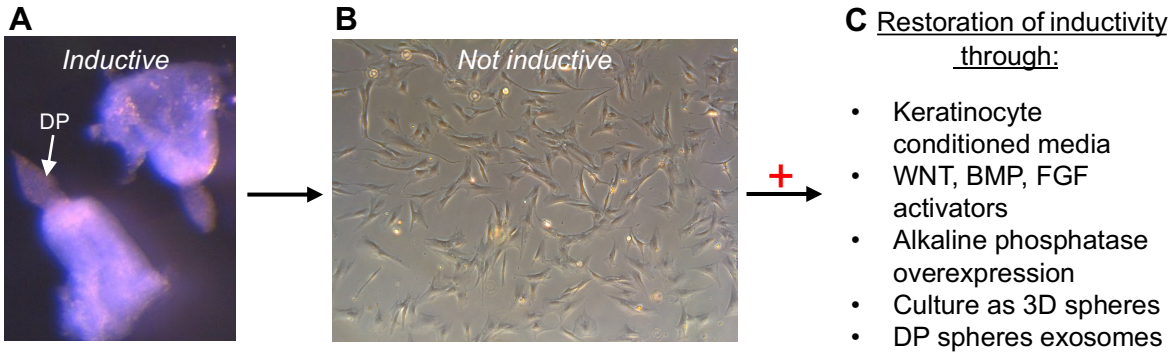


Figure 1.4: Dermal papilla inductivity.

Dermal papilla inductivity. A) Adult intact human DP have the ability to induce new hair follicles. B) Human DP cells cultured *in vitro* lose their inductivity and cannot form new follicles. C) Inductiveness of cultured human DP cells can be restored through addition of keratinocyte conditioned media, WNT, BMP and FGF activators, overexpression of alkaline phosphatase, culturing as 3D spheres and addition of DP spheres exosomes.

1.4. Hair cycle

The hair follicle undergoes periodic cycling of growth (anagen), regression (catagen) and rest (telogen) (Figure 1.5). Human hair cycle is synchronised for the first few weeks after birth; however, the cycling becomes asynchronous after 3 months (Oh *et al.*, 2016). In young mice, the first two hair cycles on the dorsal skin are synchronised and occur in waves. In older mice, the cycle becomes less synchronised so that only patches of hair follicles grow in synchronised manner creating a mosaic pattern on the dorsal skin (Chase, 1954; Stenn and Paus, 2001; Lin *et al.*, 2004). The length of each phase of a hair cycle varies depending on the body site and determines the length of the hair shaft that is produced. In humans, hair follicles on the scalp have long anagen phase (2-7 years) while eyebrow hairs have shorter anagen phase of

few weeks. Catagen lasts for few weeks while telogen normally lasts for 3 months (Duverger and Morasso, 2014). In mice, dorsal skin hair follicles are in anagen for 2-3 weeks, catagen for 3-4 days and telogen for 2 weeks for the first hair cycle and more than 2 weeks in the second hair cycle (Müller-Röver *et al.*, 2001; Alonso and Fuchs, 2006).

1.4.1. Anagen phase

During the anagen phase, the DP, a flame-shaped structure at the bottom of the follicle, signals to the overlying heterogenous population of matrix cells to proliferate and differentiate into different layers of the hair follicle such as the ORS, companion layer, IRS and the hair shaft (Stenn and Paus, 2001). The volume of the DP determines the size of the hair shaft that is produced (Chi, Wu and Morgan, 2013). The extracellular matrix and number of cells in the DP influences the volume of the DP with anagen scalp human DP each containing around 1000 cells (Chi, Wu and Morgan, 2013). Wnt signalling pathway is important for anagen maintenance. Elliott and Messenger (1999) cultured DP cells expressing green fluorescent protein (GFP) from anagen DP and showed that constant expression of GFP (which suggests DP are in anagen state) requires Wnt3a as GFP expression is lost in culture without Wnt3a.

Anagen phase is subdivided into 6 stages in mice and humans. Between anagen I and anagen IV, there is enlargement of the DP along with formation of a pigmented hair shaft and downward growth into the adipose layer. Anagen V and anagen VI are characterised by further growth of the hair shaft and emergence of the hair shaft through the hair canal (Figure 1.5) (Müller-Röver *et al.*, 2001; Oh *et al.*, 2016).

1.4.2. Catagen phase

At the end of the anagen phase, the matrix cells stop proliferation and differentiation. They undergo apoptosis along with ORS, IRS, hair shaft and DS. Apoptosis has not been observed

in the DP (Lindner *et al.*, 1997; Soma *et al.*, 1998; Botchkareva, Ahluwalia and Shander, 2006) but the DP starts condensing and the DP volume decreases during catagen. A club hair and an epithelial strand is formed during catagen. At the end of the epithelial strand is a compacted DP and recently, it was shown that the DS contracts at the club hair-epithelial strand interface pulling the DP towards the bulge region where it rests below the secondary hair germ (SHG) at the end of the catagen phase (Lindner *et al.*, 1997; Soma *et al.*, 1998; Botchkareva, Ahluwalia and Shander, 2006). FGF5 has been shown to be a major regulator of catagen induction as addition of FGF5 to organ cultured human hair follicles results in early catagen entry. Mutations in FGF5 also result in the opposite with elongation of the anagen phase and delayed catagen entry (Heitman *et al.*, 2020).

In mice, the catagen phase can be subdivided into 8 stages (catagen I- catagen VIII), whilst in humans it is classified into 3 stages (early, mid and late catagen) (Müller-Röver *et al.*, 2001; Oh *et al.*, 2016). In early catagen (equivalent to mice catagen stages I-IV), there is decrease in DP size along with loss of pigmentation in the hair shaft closest to the DP. In mid-catagen (equivalent to mice catagen stages V-VI), there is condensation of the DP into an almond-shape with formation of a club hair, epithelial strand and thickening of the DS. In late catagen (mice catagen stages VII-VIII), the DP further condenses into a ball shape with fully formed club hair and a prominent trail in the DS (Müller-Röver *et al.*, 2001; Oh *et al.*, 2016).

1.4.3. Telogen phase

At telogen, the DP is a compacted ball of cells resting below the SHG and is surrounded by hair follicle dermal stem cells (HFDSCs) (Higgins *et al.*, 2014). The BC are in a state of quiescence which is maintained by the niche surrounding them such as the DP, DS, dermal fibroblasts, and adipocytes (Rahmani *et al.*, 2014). At the start of the telogen phase, the BC are in a refractory phase and are unresponsive to anagen-inducing signals from neighbouring anagen hair follicles. They are kept in their refractory phase by high expression of inhibitory

molecules such as FGF18 from the inner bulge (Plikus, 2012) and BMP2 and BMP4 from the dermis and subcutaneous adipocytes with low expression of activating factors such as FGF7 and Wnts (Kimura-Ueki *et al.*, 2012). In late telogen, the BC are in a competent state and become responsive to anagen-activating signals. BMP2 and BMP4 expression is downregulated with a concomitant increase in BMP antagonists, Wnts and TGF-ß2 (Plikus *et al.*, 2008; Geyfman *et al.*, 2015). Release of FGF7 from the DP causes the SHG to proliferate and stimulates hair follicles to enter a new anagen (Alonso and Fuchs, 2006).

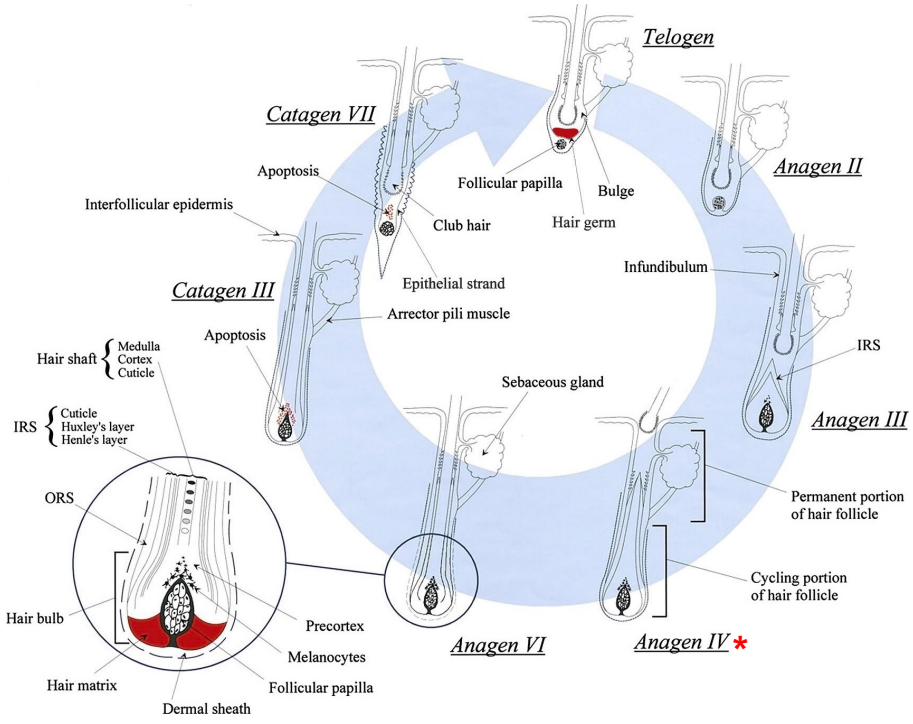


Figure 1.5: The hair cycle.

The hair follicle undergoes cycles of growth (anagen), regression (catagen) and rest (telogen). In anagen, the matrix cells receive signalling from the DP to proliferate and differentiate to produce different layers of the hair follicle such as the inner root sheath and the hair shaft. During catagen, these matrix cells and the outer root sheath cells undergo apoptosis which forms an epithelial strand. The DP compacts and is pulled up towards the secondary germ where it rests at telogen. Anagen and catagen are subdivided into further stages. There are 6 stages (anagen I- anagen VI). Each stage varies in duration, size of the dermal papilla, length of the hair follicle, and pigmentation and length of the hair shaft with the hair shaft being fully mature in anagen IV (marked by red asterisk). The catagen phase is subdivided into 8 stages (catagen I- catagen VIII). Image modified from Panteleyev (2018).

1.4.4. Macroenvironment of the hair follicle

The macroenvironment surrounding the hair follicle consists of vast network of blood vessels originating from the deep dermal vascular plexus, lymphatic vessels, neurons, intradermal adipocytes, and immune cells (Figure 1.6). The macroenvironment changes as the hair follicle cycles and studies have shown that various components of the follicular macroenvironment can have a direct influence on the cycling of the hair follicles. In mice, the skin thickness changes during the hair cycle. At early anagen, there is a large increase in the thickness of the epidermis (2-3X more compared to telogen epidermis). At anagen IV, there is an unexpected decrease in the epidermis thickness as it returns to the thickness seen at telogen; however, the dermal thickness increases by about one-half, and the adipose layer thickens by 2-3X due to an increase in blood supply and tissue fluid. During the catagen phase, the adipose layer and the dermis thickness returns to the thickness seen at telogen (Chase, Montagna and Malone, 1953).

1.4.4.1. Vasculature of the hair follicle

During anagen, the hair follicle is vascularised by network of vessels arising from the deep dermal vascular plexus. The blood vessels are embedded in the CTS of the hair follicle with a small network of capillaries found within the DP. At early catagen, this network of capillaries within the DP are still present but show signs of degeneration while the network in the CTS remains intact. By the end of catagen, there are no capillaries found in the DP while the network of blood vessels from the CTS form a tight bundle around and underneath the DP (Chase, Montagna and Malone, 1953).

Studies have shown that angiogenesis can regulate hair follicle regeneration and size. Vascular endothelial growth factor (VEGF) is a potent angiogenic factor and is expressed in ORS, IRS, and DP of human hair follicles (Kozlowska *et al.*, 1998). Inhibition of angiogenesis

through addition of an angiogenesis inhibitor drug, TNP-470, delayed anagen initiation in mice (Kozlowska *et al.*, 1998). TNP-470 inhibits proliferation of endothelial cells by arresting cells in the G1 phase of the cell cycle (Castronovo and Belotti, 1996). It has been shown to inhibit mRNA expression of cyclin-dependent kinases and cyclin D1 (Kruger and Figg, 2005). TNP-470 binds to type 2 methionine aminopeptidase (MetAP2) and inhibits cell proliferation through activation of the p53 pathway (Griffith *et al.*, 1997; Zhang *et al.*, 2000). Overexpression of VEGF in transgenic mice accelerated anagen initiation along with size of the follicles (Mecklenburg *et al.*, 2000).

1.4.4.2. Lymphatic system of the hair follicle

The major function of the lymphatic system is to transport lymph from tissues to the bloodstream. It is a major part of the body's immune system as immune cells use the lymphatic system as a transport route to tissues. The lymphatic system consists of lymph nodes, lymphatic capillaries and lymphatic vessels (Yano, Brown and Detmar, 2001). Recently, it was shown that lymphatic vessels are localised closely to the anterior side of bulge and bulb of murine hair follicles. Overexpression of VEGF-C, which promotes growth of lymphatic vessels, led to an increase in number of hair follicles at anagen phase suggesting increase in lymphatic vessels prolongs anagen phase (Swartz, 2001). The close association of lymphatic vessels with the bulge requires BC-derived WNTs as ablation of Wls from BC results in delocalisation of lymphatic vessels from the bulge and instead being localised parallel to the epidermis (Yoon *et al.*, 2019). (Peña-Jimenez *et al.*, 2019) showed that BC are involved in remodelling the lymphatic vessels during the hair cycle. At telogen, quiescent BC release angiopoietin-like protein 7 (ANGPTL7) which keeps the BC in a quiescent state and maintains hair follicles in a telogen state. ANGPTL7 is a secreted glycoprotein which belongs to a class of angiopoietin-like proteins. It has been implicated in glaucoma, inflammation, haematopoietic stem cell expansion, angiogenesis, and lipid metabolism (Hato, Tabata and Oike, 2008; Xiao *et al.*, 2015; Praveen *et al.*, 2022). In order to regenerate hair, the BC undergo a secretome switch

where they downregulate expression of Angptl7 and instead upregulate Angptl4, which causes dissociation of the lymphatic vessels from the bulge transiently allowing activation of the BC and regeneration of the hair follicle.

1.4.4.3. Innervation of the hair follicle

Hair follicles are innervated by sensory and sympathetic neurons and therefore act as a sensory touch organ. In mice, different types of hair follicles (vibrissae, guard, awl/auchene and zigzag) have different innervation. Vibrissae are densely innervated while pelage follicles tend to have lanceolate nerve endings or free nerve endings. Innervation of pelage follicles in mice have also been shown to undergo remodelling during different phases of the hair cycle (Botchkarev *et al.*, 1997). At telogen, unorganised nerve fibres arising from the subepidermal nervous plexus enwrap the infundibulum of the hair follicle (referred to as follicular neural network A, FNA). There is also another network of fibres arising from the deep cutaneous nerve plexus (referred to as FNB) which form longitudinal and circular endings around the bulge region. There is a large increase in fibres in FNA during anagen. In FNB, the number of circular fibres increase the most at early anagen, but no changes are seen in longitudinal fibres. Less innervation was seen in the lower, non-permanent portion of the hair follicle during anagen (Botchkarev *et al.*, 1997).

In vellus human hair follicles, large nerve fibres are present around the hair follicle which divide into smaller nerve fibres along the hair follicle and form circular and longitudinal endings around the level of sebaceous gland, where the highest level of innervation is seen. These nerve endings surround the ORS of the hair follicles and are embedded in the CTS (Botchkarev *et al.*, 1997). Similarly to mice, finer nerve fibres also surround the infundibulum which branch out to the epidermis (Hashimoto, Ito and Suzuki, 1990; Halata, 1993).

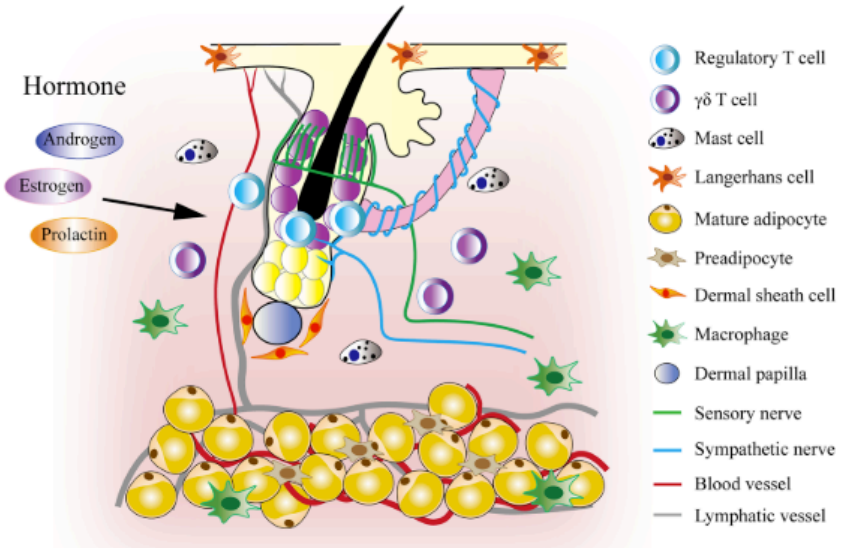


Figure 1.6: Macroenvironment of the hair follicle.

The hair follicle is closely associated with its surrounding environment. It is innervated by sensory and sympathetic nerves at the upper region near the bulge. Similarly, lymphatic vessels are closely associated along the bulge region of the hair follicle. Blood vessels arising from the deep dermal vascular plexus is embedded in the connective tissue sheath with the DP having its own supply of blood capillaries. Hair follicles are embedded within the intradermal white adipose tissue layer during anagen and the specialised immune environment around the hair follicle can modulate its activity during the hair cycle. (Image from (Hordinsky and Ericson, 1996).

1.5. Androgenetic alopecia

In section 1.4, I have described a normal hair cycle which is required throughout a person's lifetime to maintain a scalp with a normal number of hairs and even coverage. However, dysfunction of the hair cycle can lead to hair loss, otherwise known as alopecia. Androgenetic alopecia (AGA) is a common hair loss disorder impacting both genders. At least 50% of men are affected by AGA by the time they reach 50 years old and up to 40% of women are affected by age 70 (Trüeb, 2002). In males, AGA is characterised by thinning on the temples, vertex, and frontal scalp (Trüeb, 2002), while in females, it is characterised by overall hair thinning and hair loss especially from the central, frontal, and parietal scalp regions (Cranwell and Sinclair, 2016). Although AGA is not considered a life-threatening medical condition, hair loss

can have a significant psychological impact. It is well-known that androgens, especially dihydrotestosterone (DHT), can affect the growth of follicles in the balding scalp, leading to the production of small, fine hairs and eventually hair loss. It is believed that the follicles in the frontal scalp are androgen-sensitive due to the pattern of hair loss that is observed, while the follicles in the occipital scalp are androgen-insensitive. Androgens mediate their effects through the androgen receptors (AR) and AR has been shown to be expressed in the frontal hair follicles but not the occipital hair follicles (Fabbrocini *et al.*, 2018). It is thought that the site of AR action is the DP as androgen-sensitive follicles have higher levels of AR (Itami *et al.*, 1995; Sawaya and Price, 1997). Therefore, the DP has become a target of emerging cell therapies for AGA.

1.5.1. Mechanism of miniaturisation in androgenetic alopecia

In AGA, androgen-sensitive follicles undergo a process known as miniaturisation which is the transformation of thick, pigmented terminal hairs into thin, unpigmented vellus hairs (Figure 1.7), resulting in less coverage and appearance of a bald scalp (Hibberts, Howell and Randall, 1998). The precise mechanism behind miniaturisation is not well understood; however, androgens have been shown to have a crucial role in AGA (Hamilton, 1942) and for the induction of miniaturisation (Hamilton, 1942). In androgen-sensitive follicles, circulating androgens are converted to DHT by 5α-reductase in the DP. DHT binds to AR and activates androgen-responsive genes such as TGF-β1, TGF-β2, DKK-1, and IL-6. TGF-β1 inhibits proliferation of keratinocytes *in vitro* (Inui *et al.*, 2002) while TGF-β2 activates caspase-9 and caspase-3 leading to apoptosis of keratinocytes and suppression of hair growth in follicle organ cultures (Inui *et al.*, 2002). DKK-1, whose expression is higher in the balding scalp (Hibino and Nishiyama, 2004), induces apoptosis of keratinocytes *in vitro* and in cultured hair follicles (Fawzi *et al.*, 2016). Similarly, IL-6 inhibits hair growth *in vitro* and injection of recombinant IL-6 into the hypodermis induces catagen onset in mice (Kwack et al., 2012). This suggests that activation of androgen-responsive genes promotes transition of the DP

from a growth state to a regression state which contributes to the onset of miniaturisation. Moreover, it has been hypothesised that miniaturisation could occur due to lack of conversion of BC into progenitors that fuel hair growth during anagen. Garza et al., (2011) showed that hair follicles from the balding scalp retained $KRT15^{hi}$ $ITGA6^{hi}$ stem cells but the levels of $CD200^{hi}$ $ITGA6^{hi}CD34^{hi}$ progenitor cells diminished. The reason for this lack of conversion in AGA is unknown.

Miniaturisation does not occur during anagen but occurs when follicles transition through the hair cycle phases. In miniaturised follicles, there are also changes to the hair cycle. The duration of the anagen phase is shorter while the telogen phase is extended. This results in a higher percentage of follicles in the telogen phase (Jahoda, 1998; Whiting, 2001). Courtois et al., (1994) used phototrichogram to track hairs on the vertex of 10 men with none to severe alopecia for between 9 and 14 years. They observed that the balding men had highest proportion (40% or more) of fine (35-50 μm) to very fine hairs (<35 μm). The anagen phase of these fine to very fine hairs were significantly shorter as it lasted less than 6 months compared to thick (66-80 μm) or very thick (>80 μm) terminal hairs whose anagen phase lasted for more than 2 years. Miniaturisation is also observed within 6 to 12 months clinically. This has led to the suggestion that miniaturisation may occur abruptly in one hair cycle (Whiting, 2001).

There is also evidence to suggest that after exogen (shedding of the hair shaft), unlike normal hair follicles which transition into anagen, miniaturised hair follicles remain empty without formation of a new hair shaft for longer. This latency period, also known as kenogen, was observed to affect 22% of hair follicles in women with AGA while it affected up to 80% of hair follicles in men with AGA (Whiting, 2001).

Along with changes in the hair cycle, a decrease in both the volume of the DP and the number of cells within the DP has been observed in miniaturised follicles (Rebora and Guarrera, 2002; Guarrera and Rebora, 2019). This is important as the volume of the DP is proportionally linked

to the size of the hair matrix and the width of the hair shaft produced as mentioned in section 1.4.1 (Chi, Wu and Morgan, 2013). It has been proposed that the reduction in DP cell numbers could be due to a larger than normal number of cells moving out of the DP during the anagen to catagen phase or due to a lower number of cells moving into the DP from the DS during the telogen to anagen phase (Chi, Wu and Morgan, 2013). If the DP cell number cannot be replenished at early anagen, then this will result in a smaller DP and miniaturisation of a follicle in one hair cycle. This suggests that it might be possible to reverse miniaturisation quickly by stimulating an increase in DP cell numbers or by inhibiting cell movements out of the DP at the end of anagen. Another strategy to prevent, but not reverse, hair follicle miniaturisation would be to maintain follicles in anagen phase for longer. If the follicles cannot cycle, they cannot miniaturise.

A study by (Pantelireis and Higgins, 2018) showed that the DP from the frontal follicle, which miniaturise, are also less inductive. DP cells were cultured from frontal and occipital hair follicles and inductivity was assessed by creating spheres from cultured 2D DP cells. The spheres were injected into nude mice with neonatal mice epidermis in an *in vivo* patch assay. They showed that the frontal DP spheres were less inductive compared to occipital DP spheres as they produced fewer hair follicles.

Parts of sections 1.5 and 1.5.1 has been copied verbatim from **Limbu S**, Kemp PK. Hair regeneration and rejuvenation: pipeline of medical and technical strategies. Cell based strategies for hair follicle regeneration. Springer, Cell Based Therapies for Hair Regeneration, In Press, 2021

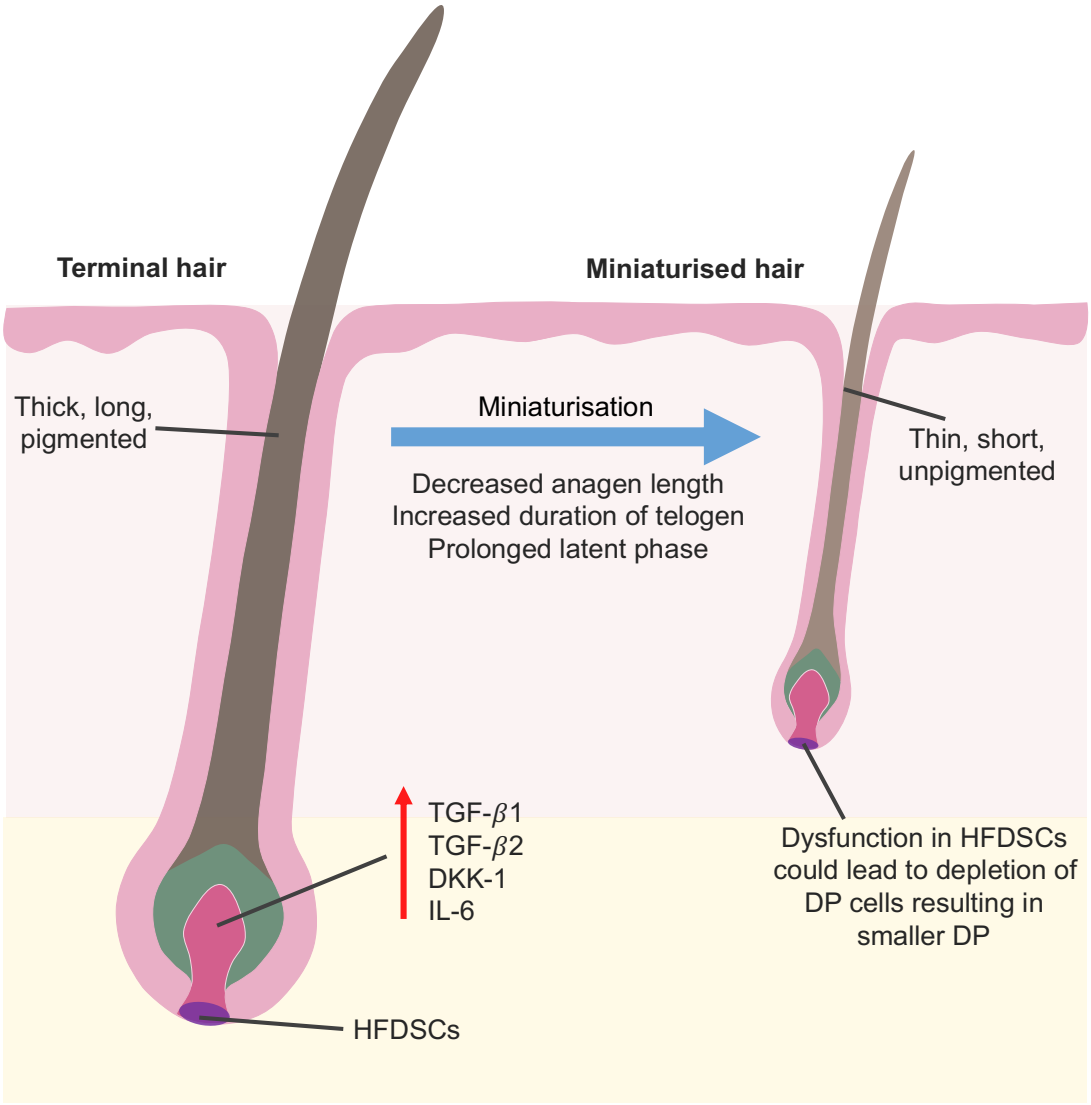


Figure 1.7: Miniaturisation of a hair follicle.

In the balding scalp, the androgen-sensitive terminal follicles transition into miniaturised vellus-like hairs. This transition is accompanied by changes in the hair shaft as well as the duration of different stages of the hair cycle. The anagen phase decreases, the telogen phase increases with a prolonged latent phase. In response to androgen-mediated signalling, there is an increase in secretion of TGF-β1, TGF-β2, DKK-1, and IL-6 from the DP, which all contribute to shorten hair growth. Finally, it has been hypothesised that the impairment in differentiation of hair follicle dermal stem cells (HFDSCs) could lead to decreased number of DP cells resulting in a smaller DP and production of a smaller hair shaft (Pantelireis and Higgins, 2018).

1.5.2. Role of the androgen receptor in androgenetic alopecia

The role of androgens in the pathogenesis of AGA has been well-established and as previously mentioned in section 1.5., androgens mediate their actions through the AR. The AR is expressed in various tissues such as the prostate, sebaceous glands, sweat glands, muscle, bone and adipose tissue (De Winter *et al.*, 1991; Davey and Grossmann, 2016). The AR is located on the X-chromosome (Xq11-12), contains eight exons, and has three functional domains- N-terminal transcriptional domain, DNA binding domain and ligand binding domain. The DNA binding domain recognises AR-consensus sequence on promoters of AR-regulated genes which allows it to activate or repress expression of its target genes (De Winter *et al.*, 1991; Davey and Grossmann, 2016). The AR is a nuclear receptor and is bound to heat shock proteins and other chaperone proteins in the cytoplasm in the absence of a ligand. Upon ligand binding such as testosterone or DHT, the ligand-bound AR translocates to the nucleus where the dimerised AR binds promoter of its target genes (Figure 1.8).

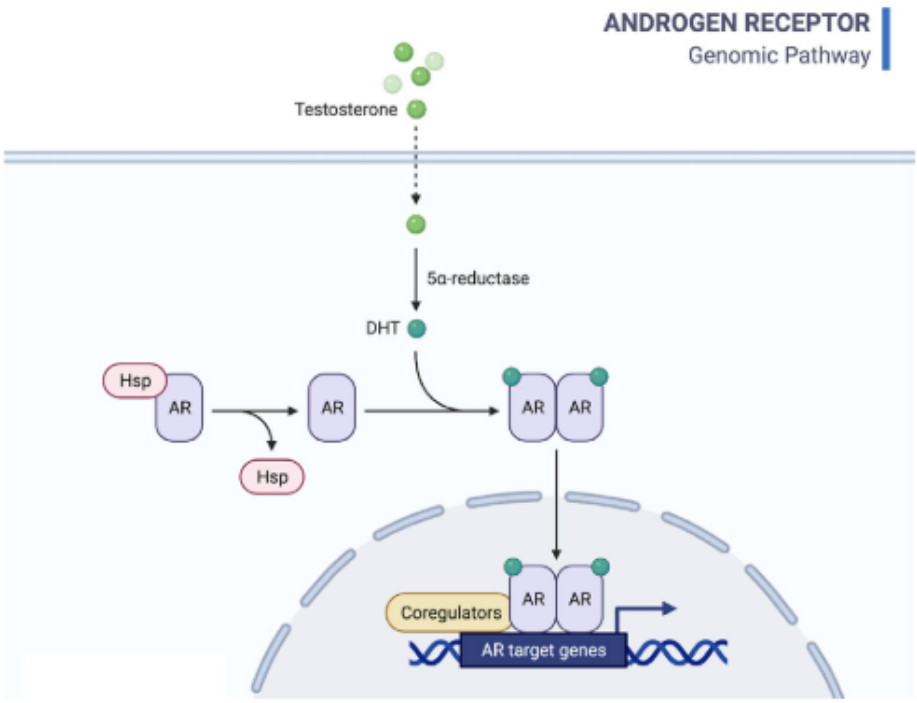


Figure 1.8: Mechanism of action of the androgen receptor.

The AR is present in the cytoplasm bound to heat shock proteins and other chaperone proteins which keep it in an inactivated state. Circulating testosterone is converted into DHT in the cytoplasm of DP cells by the enzyme 5α-reductase. DHT binds the AR which leads to dissociation of heat shock proteins and chaperone proteins. The DHT-bound AR dimerises and is translocated to the nucleus where it binds promoters of its target genes to activate or repress their expression. (Image from (Davey and Grossmann, 2016).

In AGA, frontal hair follicles contain higher levels of AR compared to occipital follicles in both men and women (Sawaya and Price, 1997). Epigenetic modification such as DNA methylation of CpG islands on a gene promoter can regulate its expression and these modifications can be inherited (Sawaya and Price, 1997). Hypermethylation of CpG islands promotes silencing of the gene while hypomethylation of same CpG islands leads to overexpression (Teama, 2018). (Moore, Le and Fan, 2012) found higher methylation of the AR promoter in occipital hair follicles compared to vertex balding follicles suggesting AR promoter is hypomethylated in androgen-sensitive hair follicles which could explain the increase in AR expression in androgen-sensitive follicles.

In addition, the AR has a major role in the development of prostate cancer and several mutations have been discovered which affect the function of AR. It has been hypothesised that similar mutations in AR may exist in people with AGA that could predispose or contribute to pathogenesis of AGA. Indeed, it has been shown that there is a link between vertex baldness and risk of developing prostate cancer (Giles *et al.*, 2002; Amoretti, Laydner and Bergfeld, 2013). Mutations around the N-terminal region of AR have been identified in prostate cancer. Polymorphisms in the two trinucleotide regions (CAG and GGC repeats) in the N-terminal region (within exon 1) alters transcriptional activity of AR and is associated with higher risk of prostate cancer (Giles *et al.*, 2002; Amoretti, Laydner and Bergfeld, 2013). The same polymorphisms have been identified in people with AGA. (Irvine *et al.*, 1995) found that men with AGA had shorter CAG and GGC repeats. Shorter CAG repeats have been shown to correlate with increased AR mRNA and protein levels (Choong *et al.*, 1996).

1.5.3. Genome-wide association studies of androgenetic alopecia

AGA is a highly heritable condition, and its inheritance is polygenic (Choong *et al.*, 1996). Twin studies have estimated that heredity accounts for approximately 80% of the predisposition to AGA (Heilmann *et al.*, 2013). Genome-wide association studies (GWAS) are used to identify genetic variants associated with common diseases with polygenic inheritance. In a GWAS, genomes of large number of people with a certain disease are compared against people without the disease in order to identify associations between variant inheritance patterns that could explain the cause of the disease or could be used as a marker to predict the severity of the disease (Nyholt *et al.*, 2003). GWAS have identified over 375 risk loci associated with AGA (Visscher *et al.*, 2017) and AR/ EDAR is consistently one of the most significantly associated risk loci for AGA (Hochfeld *et al.*, 2021) showing the important role of variations in AR for the pathogenesis of AGA.

Through GWAS, other AGA candidate genes have been discovered such as PAX1, FOXA2 (Richards *et al.*, 2008; Brockschmidt *et al.*, 2011a; Hagenaars *et al.*, 2017; Heilmann-Heimbach *et al.*, 2017), AUTS2, SETBP1 (Hillmer *et al.*, 2008; Richards *et al.*, 2008; Li *et al.*, 2012) and HDAC9 (Brockschmidt *et al.*, 2011b). Recently, (Brockschmidt *et al.*, 2011b) showed that EBF1 and WNT10A, both identified as risk loci for AGA through GWAS (Heilmann-Heimbach *et al.*, 2017), may have a functional role in AGA. Luciferase reporter assay showed that EBF1 binds to the WNT10A promoter but the presence of WNT10A AGA risk allele (rs3856551-T) leads to decreased promoter activation by EBF1; thus, less WNT10A is produced. As WNT10A is required for anagen maintenance, they conclude that decreased WNT10A production leads to anagen shortening which is one of the hallmarks of AGA.

1.5.4. Current treatments for androgenetic alopecia

There are only two Food and Drug Administration (FDA)-approved pharmacological treatments available for AGA: minoxidil and finasteride. Minoxidil can be used by both men and women. It is a potassium channel opener that triggers follicles in telogen to enter anagen phase, and also increases the duration of the anagen phase which increases the length of the hair produced (Heilmann-Heimbach *et al.*, 2017). Finasteride is an inhibitor of 5α-reductase type II enzyme, which metabolises testosterone into DHT, and is only approved for use by men (Fabbrocini *et al.*, 2018). Both drugs must be used indefinitely as hair loss can occur upon discontinuation. Both drugs prevent, but not reverse, miniaturisation of hair follicles. Moreover, in some cases, usage of these drugs can have undesirable side effects. Oral minoxidil can induce hair growth on the face and limbs (Fabbrocini *et al.*, 2018), while treatment with finasteride has been reported to cause sexual side effects (Peluso *et al.*, 1997); however, this remains controversial as many other studies have found no significant link between usage of finasteride and sexual dysfunctions (Mella *et al.*, 2010; Irwig and Kolukula, 2011; Traish, 2020).

Both minoxidil and finasteride were discovered serendipitously when the drugs caused hypertrichosis as an unwanted side effect. Minoxidil was originally developed to treat hypertension (Tosti, Piraccini and Soli, 2001; Haber *et al.*, 2019; Pallotti *et al.*, 2020) while finasteride was developed to treat men with benign prostatic hyperplasia (Dargie, Dollery and Daniel, 1977). However, in recent years, targeted analysis has uncovered potential new drugs. Through microarray analysis of balding and haired scalp of men with AGA, (Gormley *et al.*, 1992) identified elevated levels of prostaglandin D_2 synthase along with its product prostaglandin D_2 (PGD_2) in the balding scalp. Setipiprant was identified as a drug to block PGD_2 receptor, Chemoattractant receptor-homologous molecule expressed on TH2 cells (CRTH2). It was originally trialled to treat allergic rhinitis and asthma; however, a Phase 3 trial concluded that it provided no more benefit than the placebo (Ratner *et al.*, 2017). Thus, setipiprant was discontinued for use for allergic rhinitis and asthma and was repurposed to treat hair loss in AGA. A Phase 2a trial on 169 individuals found that there was no significant hair growth using setipiprant compared with placebo (Ratner *et al.*, 2017). Even though, setipiprant did not improve hair growth as expected, the study by Garza et al., (2012) shows that targeted analysis can be a useful method to identify specific drug targets for AGA. This study also showed that there are changes in the intrafollicular skin which impact the follicle.

A popular treatment for AGA is hair transplantation surgery which involves transferring follicles from the occipital scalp (donor zone) into the frontal scalp (recipient zone). The occipital hair follicles have “donor dominance” which is the concept that these donor follicles maintain their original characteristics such as texture, colour, and length of anagen phase when transferred into the frontal scalp. As the occipital follicles are less sensitive to androgens, they remain in the frontal scalp without undergoing miniaturisation (DuBois *et al.*, 2021). Even though hair transplantation surgeries are performed with local anaesthesia and are relatively quick, many people have concerns undergoing surgeries. Moreover, hair transplantation involves one-to-one relocation, and therefore, it is difficult to use for patients who are beginning to notice hair loss as the eventual extent of hair miniaturisation and receding is unknown. Also, some women

exhibit diffuse unpatterned alopecia (DUPA) in which hair miniaturisation occurs throughout the entire scalp including the donor area making hair transplantation unsuitable as a treatment (Orentreich, 1959; Dinh, Sinclair and Martinick, 2008). Thus, alternative therapies are required which can give similar results to hair transplantations without the need to undergo surgery.

Effective therapy for AGA would address two main concerns: 1) replacing lost hair follicles through follicle regeneration, and 2) converting existing miniaturised hairs into terminal ones through rejuvenation (Figure 1.9A and 1.9B). A cell therapy treatment would be beneficial for people with advanced AGA with insufficient amounts of donor hairs for transplantation. It would be permanent, like transplantations, but would not require the use of long-term medications. A drug-based therapy would not change the identity of the frontal follicles as they are still androgen sensitive and will likely miniaturise at a later hair cycle. In comparison, cell therapy with DP cells would theoretically alter the identity of the frontal follicles to make them more like occipital follicles, thus, making them insensitive to androgens and miniaturisation (Jimenez *et al.*, 2021). Also, a cell therapy would be useful for both men and women making cell therapy an attractive alternative treatment for AGA.

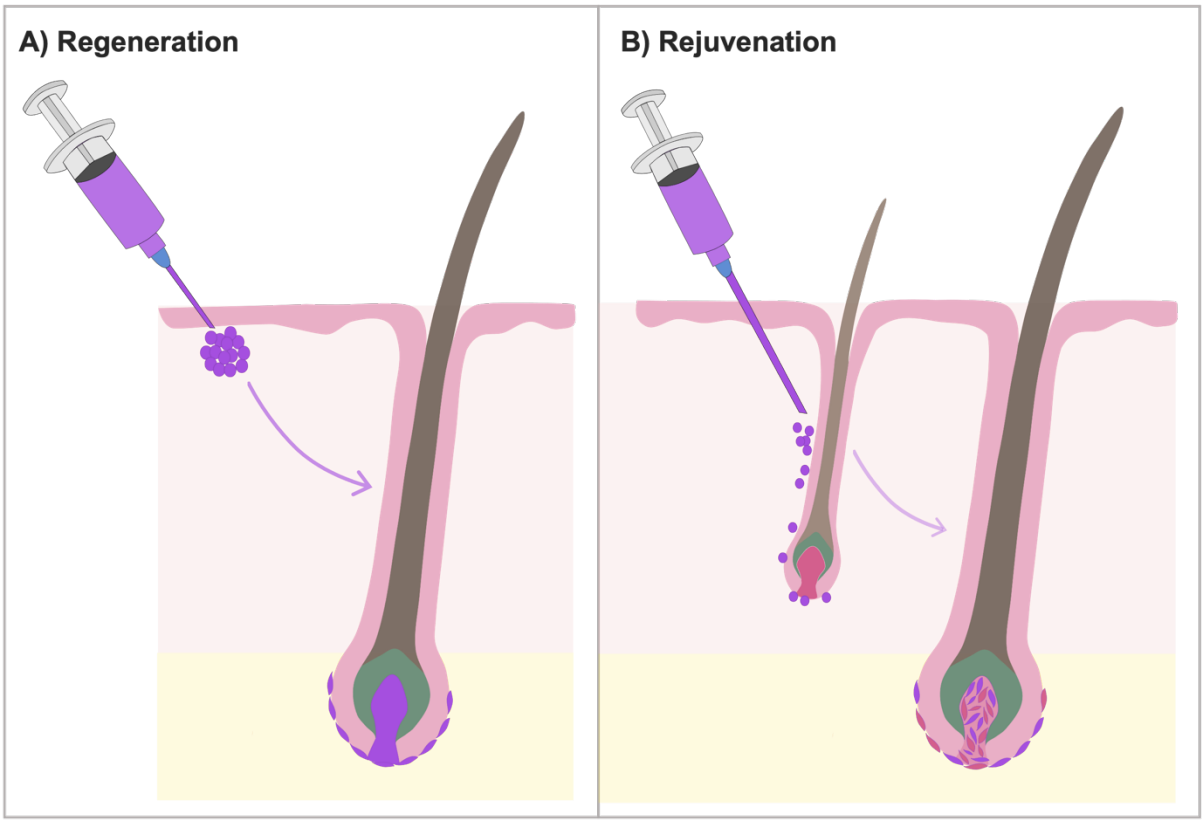


Figure 1.9: Regeneration versus Rejuvenation.

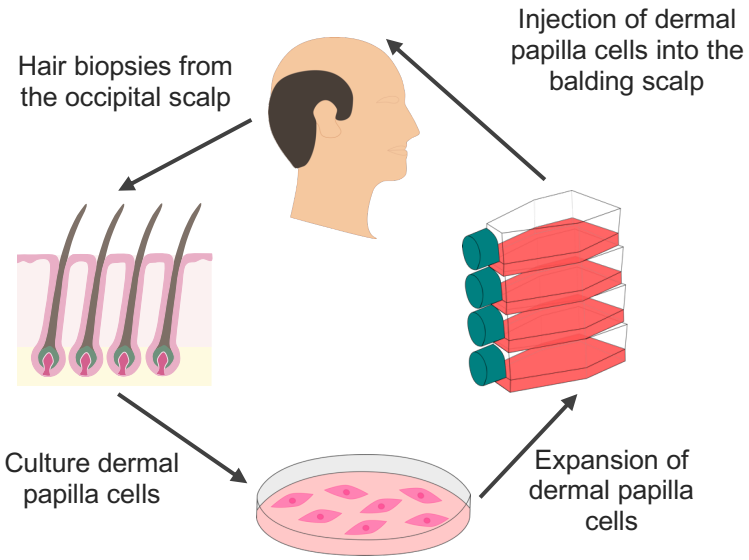
A) Regeneration is the process of producing new hair follicles through injection of DP cells. These cells induce the overlying epidermis into a follicular state, thereby producing a new hair follicle. B) During rejuvenation of a hair follicle, the injected cells are thought to migrate to miniaturised follicles and replenish the DP. This increases DP size resulting in transition of vellus follicles into terminal ones.

1.5.5. Development of a commercial cell therapeutic product for androgenetic alopecia

Studies have shown that the DP is critical for the induction of new hair follicles (Topouzi and Higgins, 2016). The inductive ability retained by cultured DP cells raised the possibility of using DP cells to treat AGA (Jahoda & Oliver, 1984; Jahoda et al., 1993). Currently, several companies are working on developing commercial products for AGA using DP cells as well as other follicular cells such as the DS cup cells. One of the earliest companies involved in developing cell therapeutic products was Intercytex. From its founding in 1997, Intercytex was interested in taking advantage of the inductive capability of cultured DP cells to treat hair loss.

Their process would involve taking biopsies of few hair follicles from the occipital scalp, expanding DP cells to obtain sufficient number of cells, and then injecting the cells back into the balding scalp where the intention was that they would interact with local epithelial cells to induce the formation of new hairs as seen in rodent model systems. This process is known as “hair multiplication” as small numbers of hair follicles could be used to create indefinite number of new hair follicles in theory (Figure 1.10A) and is different to hair transplantation surgeries which requires good quality and intact hair follicles (Figure 1.10B).

A) Hair multiplication



B) Hair transplantation

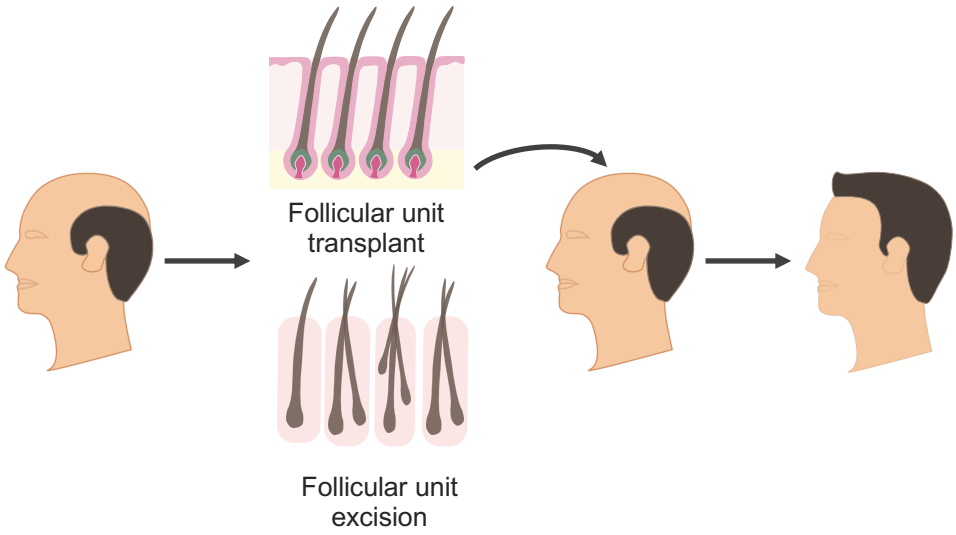


Figure 1.10: Differences between hair multiplication process and hair transplantation.

A) For hair multiplication process, skin biopsies containing hair follicles are taken from the occipital scalp of a patient. The DP is microdissected out of the hair follicle and cultured in a good manufacturing practice (GMP) laboratory. The DP cells are expanded to obtain large number of cells. After sufficient number of cells have been cultured, DP cells are injected back into the patient's balding scalp to induce hair regeneration. B) During the surgery, hair follicles are harvested from the occipital scalp either as a strip of donor skin (strip harvesting follicular unit transplantation) or as individual follicular units (follicular unit excision). The donor follicular units are inserted into the balding scalp leading to hair growth after few months of surgery.

1.5.6. Clinical trials involving follicular cells for hair regeneration

Intercytex licensed the technology from Hiroshima University, where the work by Mutsumi Inamatsu was carried out. In 2002, they built their manufacturing facility and developed a good manufacturing practice (GMP) process to culture autologous human DP cells. Several millions of cultured DP cells would be injected intradermally into the patient's scalp. Phase I clinical trials started in 2003 intending to regenerate new hair follicles in completely balding regions of patients with AGA. Results showed an increase in hair numbers with no adverse side effects (personal communication with Farjo Hair Institute). Phase II trials conducted in the UK with DP cell injections showed some efficacy and produced new hair follicles (Adams, 2011); however, these were mainly fine vellus-type hairs which did not offer a cosmetic benefit. In 2010, Intercytex stopped research into the hair multiplication process and sold their assets to Aderans Research Institute (ARI).

ARI was founded in 2002 as a subsidiary of Aderans, a leading global wig manufacturer. Their original intellectual property (IP) was based on research from (Adams, 2011) in which mice neonatal epidermal and dermal cells are injected together to form new hair follicles. ARI conducted Phase II clinical trials using autologous, cultured dermal cells combined with epidermal cells which were injected into the balding scalp of men and women. Their Phase II

trials involved comparing the efficacy of injecting dermal and epidermal cells with injecting dermal cells only or with topical minoxidil and number of injections required (Sousa and Tosti, 2013). No results of the clinical trials have been published and Aderans stopped funding this research in 2013 (Figure 1.11).

*Parts of sections 1.5.4, 1.5.5 and 1.5.6 has been copied verbatim from **Limbu S**, Kemp PK. Hair regeneration and rejuvenation: pipeline of medical and technical strategies. Cell based strategies for hair follicle regeneration. Springer, Cell Based Therapies for Hair Regeneration, In Press, 2021

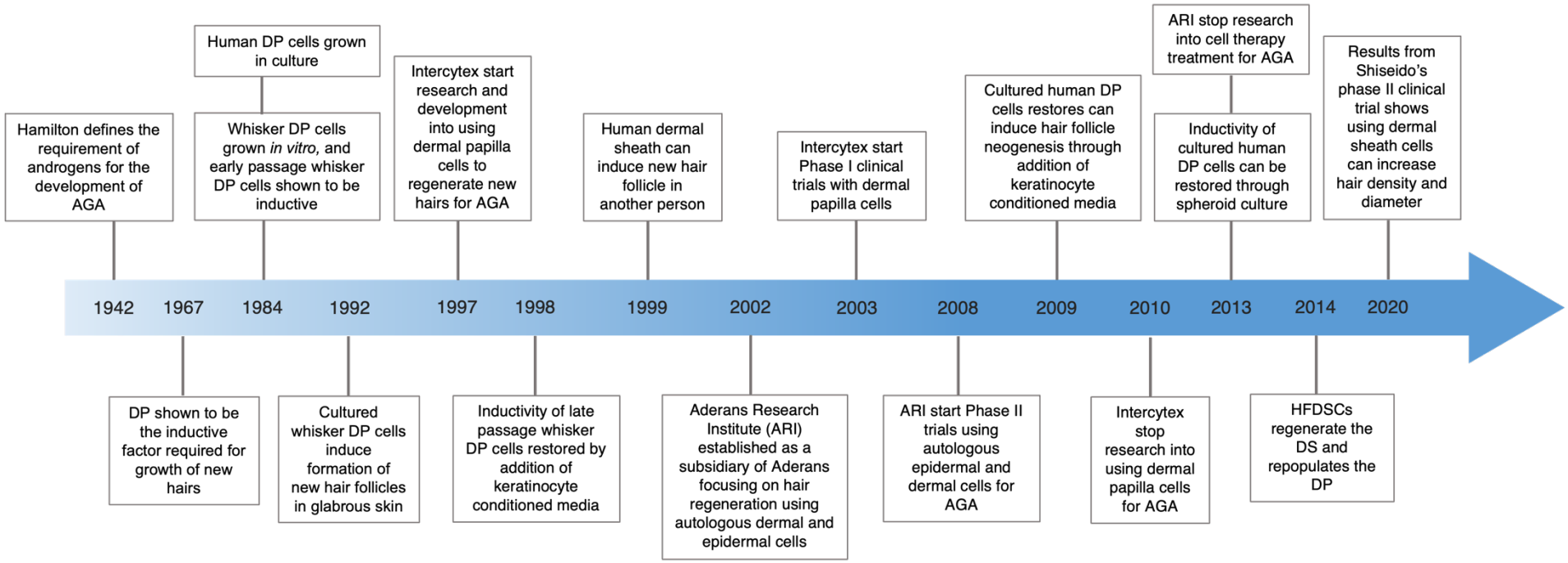


Figure 1.11: Timeline of major research conducted which helped to understand the basis of hair regeneration and the companies involved in the development of a cell therapeutic product for androgenetic alopecia.

1.6. Aims of the PhD

Collectively, the literature shows that there are inherent differences between frontal hair follicles (which are susceptible to miniaturisation in AGA) and occipital hair follicles (which do not miniaturise). Numerous genetic studies have implicated a role of the AR in driving AGA pathogenesis. The dynamics of the hair follicle cycle is known to shift in AGA while in recent years the role of the follicular macroenvironment has also emerged as a regulator of the hair cycle. I hypothesise that follicles on the occipital scalp do not miniaturise as they are 'protected' from miniaturisation. This would explain the concept of donor dominance observed when occipital follicles are transplanted into the frontal scalp. There are two main aims to address this hypothesis.

Aim 1:

The hair follicle is a dynamic mini organ which can regenerate itself throughout a person's lifetime. This regenerative potential is influenced by numerous environmental components that surround the hair follicle. In AGA, hair follicles miniaturise with changes to its regenerative properties. The first aim of this thesis is to characterise the macroenvironment of the hair follicle from the frontal and occipital scalp in order to determine whether the innervation, vasculature or lymphatic vessels are modified in AGA. This work is discussed in Chapter 2.

Aim 2:

In AGA, occipital hair follicles are transplanted into the frontal scalp do not miniaturise showing inherent differences between frontal and occipital hair follicles. Given that the DP is the main signalling centre of the hair follicle and is thought to be the main target of androgens, the second aim of this thesis is to determine whether there are transcriptional changes in the hair follicle mesenchyme from the frontal and occipital scalp. This would help us to elucidate the cause of follicular miniaturisation in AGA. This work is discussed in Chapter 3.

Chapter 2: Investigating the macroenvironment of hair follicles in androgenetic alopecia

2.1. Introduction

2.1.1. Changes in the follicular macroenvironment in androgenetic alopecia

The biggest morphological change in AGA is the reduction in the size of the hair follicle where terminal hair follicles transform to a vellus state. In humans, hair follicles exist in follicular units (FU) of up to 3 follicles and sometimes up to 4 or 5 hairs. A FU consists of both primary and secondary follicles which are attached to arrector pili muscle (APM) and sebaceous glands. The APM is attached tightly to the primary follicle but is also in contact with the secondary follicles (Sousa and Tosti, 2013). The hair shafts of all follicles in a FU emerge from the same infundibulum in the scalp and follicles in a FU can be at different stages of the hair cycle.

In AGA, the secondary follicles miniaturise first resulting in reduced density while miniaturisation of the primary follicle gives rise to a bald appearance (Song *et al.*, 2006). Not only are there changes within a FU but there are also changes to the components surrounding miniaturised hair follicles in AGA. There is a consistent loss of APM attachment to miniaturised hairs in AGA (Yazdabadi *et al.*, 2012) with APM degenerating and being replaced with fat (Yazdabadi *et al.*, 2012). The sebaceous gland has been shown to be enlarged (Torkamani *et al.*, 2014) and contain more lobules in a FU in AGA (Kim *et al.*, 2014). Moreover, eccrine sweat glands number and volume increase in AGA (Kure, Isago and Hirayama, 2015).

There are other macroenvironmental structures, namely blood vessels, nerves and lymphatic vessels which are also associated with the hair follicle. These are known to change during the hair cycle in mice and can influence follicle growth (Poblet *et al.*, 2018), so logically these may also be altered in AGA follicles. Expression of VEGF has been shown to be decreased in AGA (Botchkarev *et al.*, 1997; Mecklenburg *et al.*, 2000; Yoon *et al.*, 2019) which would suggest that there would be less blood vessels present in miniaturised hair follicles. (Goldman *et al.*, 1995) have reported, through alkaline phosphatase staining, that miniaturised vellus-type hair

follicles have smaller capillaries and are “less numerous”. They conclude that this is due to a smaller hair follicle requiring less blood supply. Additionally, Lattanand & Johnson, (1975) observed variations in the nerve plexus of miniaturised hair follicles. Some follicles had intact or “completely withdrawn” nerve plexus while in some follicles, nerves were found in the streamers below the miniaturised follicle. However, they did not mention if there were changes in the nerve fibres that innervate the follicle. They might not have detected finer nerve fibres as they used acetylcholine to detect nerves which can diffuse from smaller fibres (Hordinsky and Ericson, 1996).

2.1.2. Whole-mount immunolabelling and volumetric imaging

Cells, tissues, and organs are complex 3D structures, but they are commonly visualised in 2D as flat sections. Sectioned samples are useful as it has allowed researchers to probe cellular localisation of proteins, visualise tissue organisation and arrangement of vessels and nerves around tissues. However, thin sections do not capture the networks that are formed by nerves and vessels around tissues as they are usually on different object planes and become separated on slides. Imaging of serial sections can permit reconstruction of tissues in 3D; nevertheless, sectioning can lead to loss of samples due to individual sections becoming folded or torn apart. This can result in distorted or out of focus final volumetric image if sections are missing (Hordinsky and Ericson, 1996).

Imaging intact samples without sectioning can create 3D images of an entire sample without any loss of information. It also results in less tissue structural damage and preserves tissue morphology. Advances in fluorescence microscopy, computational imaging software and tissue clearing techniques have enabled volumetric imaging of large tissues such as mouse embryo, adult mouse brain and even whole adult mouse (Richardson and Lichtman, 2015). Volumetric imaging can be used to visualise the complex organisation of neural and vessel networks around and deep within tissues at a high resolution. This can help us to see if these

networks are disrupted or changed in diseases and developmental disorders (Renier *et al.*, 2014; Cai *et al.*, 2019)

Normally, tissues are opaque and certain proteins in cells can produce pigments such as melanin while some tissues naturally produce autofluorescence. This reduces the amount of light that can pass through a sample and hinders the depth to which the sample can be imaged (Gómez-Gaviro *et al.*, 2020). Light scattering from nuclei, ribosomes, membranes, lipids, and extracellular matrix (ECM) prevents deeper imaging, however making the tissue transparent allows deeper fluorescent imaging. Tissues can be made transparent by tissue clearing techniques which homogenises the refractive index throughout the tissue (Richardson and Lichtman, 2015).

Several tissue clearing techniques have been developed to make tissues transparent such as hydrogel-based clearing, aqueous-based clearing, and solvent-based clearing. In hydrogel-based clearing such as Cleared lipid-extracted acryl-hybridized rigid immunostaining/ in situ hybridization-compatible tissue hydrogel (CLARITY) and passive CLARITY (PACT), fixed tissues are infused with hydrogel monomers to form tissue-hydrogel hybrid. Tissue is cleared by removing lipids using sodium dodecyl sulfate and immersed in FocusClear or 80% glycerol to clear the tissue (Molbay *et al.*, 2021). Aqueous-based clearing techniques use water-soluble agents such as sucrose, fructose, urea and amino alcohols to clear the tissue while solvent-based clearing methods use organic solvents such as benzyl alcohol/ benzyl benzoate and dichloromethane/ dibenzyl ether to clear tissues (Reveles Jensen and Berg, 2017). Different tissue clearing methods are used depending on the type and size of tissue.

Immunolabeling-enabled three-dimensional imaging of solvent-cleared organs (iDISCO) is a solvent-based tissue clearing technique that can be used to immunolabel large tissues for volume imaging. It allows antibodies to diffuse deeply into tissues, immunolabel with multiple antibodies and takes around 8-18 days depending on the size of the sample (Richardson and

Lichtman, 2015). The iDISCO protocol also uses common laboratory reagents which are inexpensive and has been shown to clear tissues containing connective tissues such as skin (Renier *et al.*, 2014).

2.2. Specific aims in Chapter 2

The hair follicle has dynamic interactions with its macroenvironment as discussed in section 1.4.4. During the hair cycle, there is active remodelling of the hair follicle along with its macroenvironment such as the vasculature, nerves, dermis, and the dermal white adipose tissue (dWAT). There is also active signalling between the hair follicle and its macroenvironment which enables hair regeneration and cycling. In AGA, changes in hair follicle macroenvironment occur such as the loss of APM attachment resulting in fat accumulation near APM attachment site which has been correlated with irreversibility of hair loss. However, only differences in nerve plexus between terminal and vellus hair follicles has been observed (Azaripour *et al.*, 2016). To my knowledge, the differences in innervation between androgen-sensitive and androgen-insensitive hair follicles has not been investigated. Moreover, the only literature on differences in blood vessels between androgen-sensitive and androgen-insensitive hair follicles was by Lattanand & Johnson (1975) which was not quantified. It is unknown whether there are changes in density and size of blood vessels in AGA. Finally, there is no known literature looking at the lymphatic vessels in AGA.

I hypothesise that miniaturisation of the hair follicle in AGA changes the level of innervation along with amount and density of blood vessels and lymphatic vessels. Thus, the aim of this chapter is to characterise the nerves, blood vessels and lymphatic vessels in androgen-sensitive (frontal) and androgen-insensitive (occipital) hair follicles. This will be conducted through whole-mount immunolabelling and volume imaging to gain spatial and architectural information of the nerves, blood vessels and lymphatic vessels in and around the hair follicles.

2.3. Materials and Methods

2.3.1. Collection of frontal and occipital hair follicles

Fifteen frontal (combination of large and miniaturised in size) and fifteen occipital hair follicles were donated by three patients undergoing hair transplantation surgeries at the Farjo Hair Institute at Manchester, U.K. Consent was taken from patients using IC-REC approved consent forms. Information on the patients used in this chapter are listed in table 2.1. The hair follicles were placed in 4% paraformaldehyde (PFA, Agar Scientific) for 24 hours at 4°C. After 24 hours, hair follicles were washed with Dulbecco′s Phosphate Buffered Saline (PBS, Sigma-Aldrich) with shaking 3 times for 30 minutes each at room temperature. Then, the hair follicles were stored in PBS with 0.02% sodium azide (Sigma-Aldrich) at 4°C.

Table 2.1: Patient information.

Patient	Date of birth	Age	Gender
1	10/89	31	M
2	09/62	58	M
3	04/56	65	M

2.3.2. iDISCO whole-mount immunostaining

The iDISCO protocol from (Lattanand and Johnson, 1975) was used. The whole-mount immunostaining protocol is divided into 3 main sections: pre-treatment, immunolabelling and clearing.

2.3.2.1. Pre-treatment

Firstly, the fixed hair follicles were washed in buffer PTx.2 twice for 1 hour each at room temperature with shaking. Then, the hair follicles were incubated in 1XPBS/ 0.2% Triton X-

100/ 20% dimethyl sulfoxide (DMSO, Sigma-Aldrich) at 37°C overnight. The next day, the hair follicles were incubated in 1xPBS/ 0.1% Tween-20 (Sigma-Aldrich)/ 0.1% TritonX-100/ 0.1% Deoxycholate (Sigma-Aldrich)/ 0.1% NP40 (Sigma-Aldrich)/ 20% DMSO at 37°C overnight. Then, the hair follicles were washed in PTx.2 twice for 1 hour each at room temperature with shaking. The components and suppliers for PTx.2 are listed in table 2.2.

Table 2.2: Components and suppliers for PTx.2.

Reagent	Volume for 1L	Supplier
PBS (10X)	100 mL	Sigma-Aldrich
Triton X-100	2 mL	Sigma-Aldrich
Water	898 mL	-

2.3.2.2. Immunolabelling

The hair follicles were incubated in permeabilization solution at 37°C overnight. Then, they were blocked in blocking solution at 37°C overnight. The hair follicles were incubated in primary antibodies in PTwH/ 5% DMSO/ 3% normal goat serum (NGS, Vector Laboratories) at 37°C overnight. Then, they were washed in PTwH with shaking for 4-5 times for 24 hours. Next, the hair follicles were incubated in secondary antibodies in PTwH/ 3% NGS at 37°C overnight. The hair follicles were washed in PTwH with shaking for 4-5 times for 24 hours. The components and suppliers for buffers are listed in table 2.3. The list of primary and secondary antibodies used in this chapter are in table 2.4.

Table 2.3: Components and suppliers for permeabilization buffer, blocking solution and PTwH.

Permeabilisation solution	**Volume for 500 mL**	**Supplier**
PTx.2	400 mL	-
Glycine	11.5 g	Sigma-Aldrich
DMSO	100 mL	Sigma-Aldrich
Blocking solution	**Volume for 500 mL**	**Supplier**
PTx.2	42 mL	-
Normal goat serum	3 mL	Vector Laboratories
DMSO	5 mL	Sigma-Aldrich
PTwH	**Volume for 1L**	**Supplier**
PBS (10X)	100 mL	Sigma-Aldrich
Tween-20	2 mL	Sigma-Aldrich
Heparin (10mg/mL)	1 mL	Sigma-Aldrich
Water	897 mL	-

Table 2.4: Primary and secondary antibodies used for immunolabelling.

Name	**Host species**	**Supplier**	**Catalogue number**	**Dilution**
NFH	Chicken	Sigma-Aldrich	AB5539	1:1000
K15	Rabbit	Proteintech	10137-1-AP	1:500
K15	Mouse	Abcam	ab80522	1:500
CD31	Rabbit	Abcam	ab32457	1:500
LYVE-1	Mouse	Thermo Fisher Scientific	14-0443-80	1:100
488 anti-mouse	Goat	Thermo Fisher Scientific	A11001	1:500
568 anti-rabbit	Goat	Thermo Fisher Scientific	A11036	1:500
647 anti-chicken	Goat	Thermo Fisher Scientific	A21450	1:1000

2.3.2.3. Clearing

To clear the hair follicles, they were dehydrated in methanol (Thermo Fisher Scientific) diluted in water. The hair follicles were placed in a series of methanol/ water of 20%, 40%, 60%, 80%, 100%, 100% for 1 hour each at room temperature. The samples were left in 100% methanol overnight at room temperature. The next day, the hair follicles were incubated in 66% dichloromethane (DCM, Sigma-Aldrich) and 33% methanol at room temperature with shaking. Then, the hair follicles were incubated in 100% DCM for 15 minutes twice with shaking. Finally, the hair follicles were placed in dibenzyl ether (DBE, Sigma-Aldrich) with no shaking until imaging.

2.3.3. Whole-mount imaging of hair follicles

Cleared hair follicles were mounted onto a slide in a drop of DBE. A coverslip was placed on top of the sample with Blu Tack (Bostik) placed at the corners to secure the coverslip to the slide. The size of the Blu Tack ensured that the follicles were close to the coverslip but did not get squashed during imaging. The hair follicles were imaged using SP8 Lightning Confocal Microscope (Leica) using 488, 561 and 633 nm lasers with PMT and HyD GaAsP detectors. 10x [HC Plan APO, numerical aperture = 0.40, working distance = 2740 µm] objective lenses were used to image the hair follicles. For hair follicles stained with NFH, each z-stack was taken at every 2 µm. For hair follicles stained with CD31 and LYVE-1, each z-stack was taken at every 2-3 µm.

2.3.4. Immunofluorescence quantification

Fiji was used to perform maximum intensity projections of the z-stacks and to measure the fluorescence intensity using the measure tool in the ‘Analyze’ tab in a region of interest. For NFH, the region of interest was drawn outside the hair follicle, up to the epidermis (if this could

be seen) or up to the highest point to where the upper follicle could be seen and was not masked by the dermis. For CD31 and LYVE-1, due to presence of dermis in the upper portion of the hair follicles in some samples, the hair follicle was divided into equal two parts. Then, the region of interest was drawn outside the hair follicle on the bottom half of the hair follicle. Hair follicles from all three patients were used and at least 2 hair follicles were quantified from each patient.

2.3.5. Statistical analysis

Statistical analysis was carried out in GraphPad Prism V9.3.1. The data was checked for normal distribution using the D'Agostino & Pearson test. For normally distributed data, an unpaired t-test was used for statistical analysis. P-values of <0.05 were considered to be significant.

2.4. Results

2.4.1. Innervation around the hair follicle macroenvironment

To characterise the nerve network of the hair follicle in and around the follicular macroenvironment, whole-mount immunolabelling with neurofilament (NF) heavy (NFH) was used to detect neurons. K15 was used as co-stain to localise bulge region of follicle and to help with orientation of the follicle. Neurofilaments are 10-nm-diameter intermediate filaments and are found in dendrites but have the highest expression in myelinated axons where they are required for the growth of axons and for transmission of electrical impulses along the axon. Neurofilaments consist of 3 polypeptides- NFH, neurofilament medium (NFM) and neurofilament light (NFL) (Yuan *et al.*, 2012). NF-positive nerves have been detected in human skin where they are present in the epidermis as free nerve endings and also around hair follicles (Yuan *et al.*, 2012). Thus, NFH is used in this study as a marker to investigate the

innervation of human hair follicles. As mentioned in section 2.1.2, whole-mount immunolabelling requires tissue clearing. The iDISCO protocol was chosen to immunolabel hair follicles as the dermis associated with hair follicles contain connective tissue which is cleared well with this protocol. For iDISCO, DBE was used to clear the hair follicles. Clearing with DBE made the dermis and the follicle transparent but not the hair shaft and the epidermis (Figure 2.1A and B).

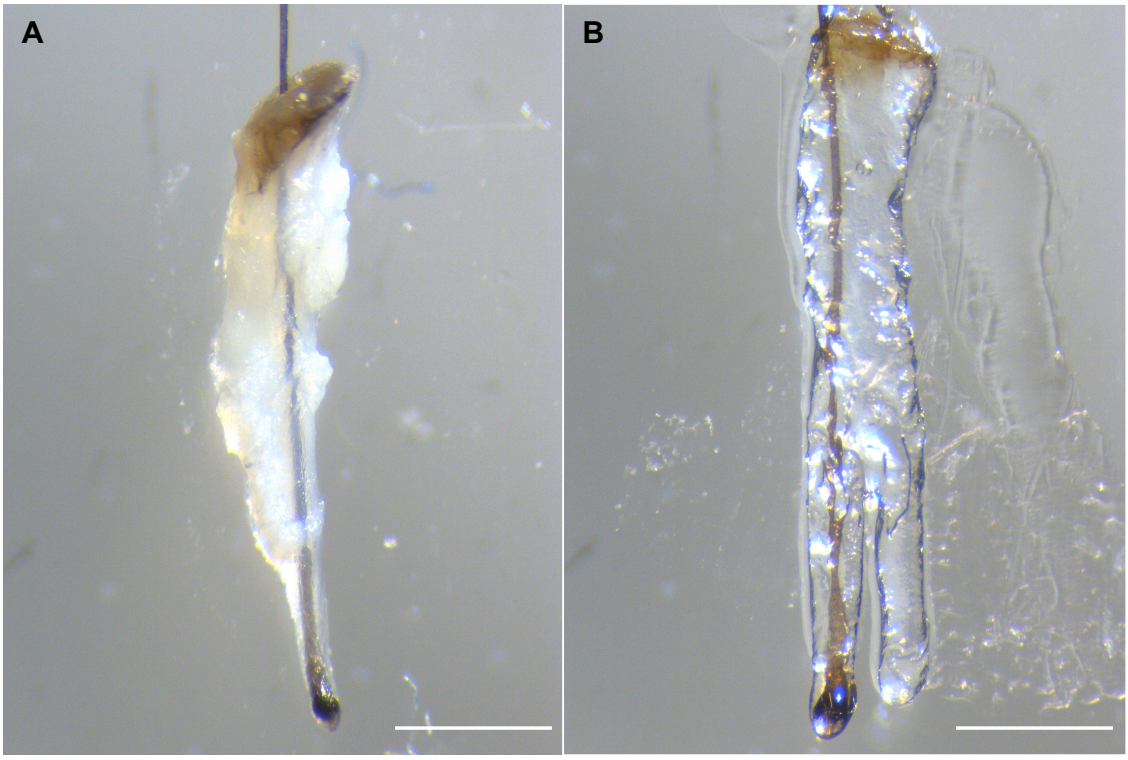


Figure 2.1: Hair follicles before and after tissue clearing.

(A) Brightfield image of a hair follicle before tissue clearing which shows opaque dermis and translucent appearance of the hair follicle. (B) Brightfield image of a hair follicle after clearing with DBE which has made the dermis and the hair follicle transparent. The epidermis and the hair shaft remain pigmented. (Scale bar = 1 cm)

As previously reported in the literature, hair follicles and hairy skin are highly innervated. NFH^+ fibres were present in and around the hair follicle macroenvironment (Figure 2.2A). Large nerve fibres are found in the vicinity of a hair follicle which innervates the follicle and branches

off to innervate the epidermis too (Figure 2.2B). Nerve fibre from the dermis around the hair follicle divides and forms a network of finer fibres to innervate a large area of the epidermis where the fibres terminate as free nerve endings (Figure 2.2C). Nerve fibre originating from the dermis can also branch and innervate a telogen hair follicle (Figure 2.2D) and are present in dWAT (Figure 2.2E).

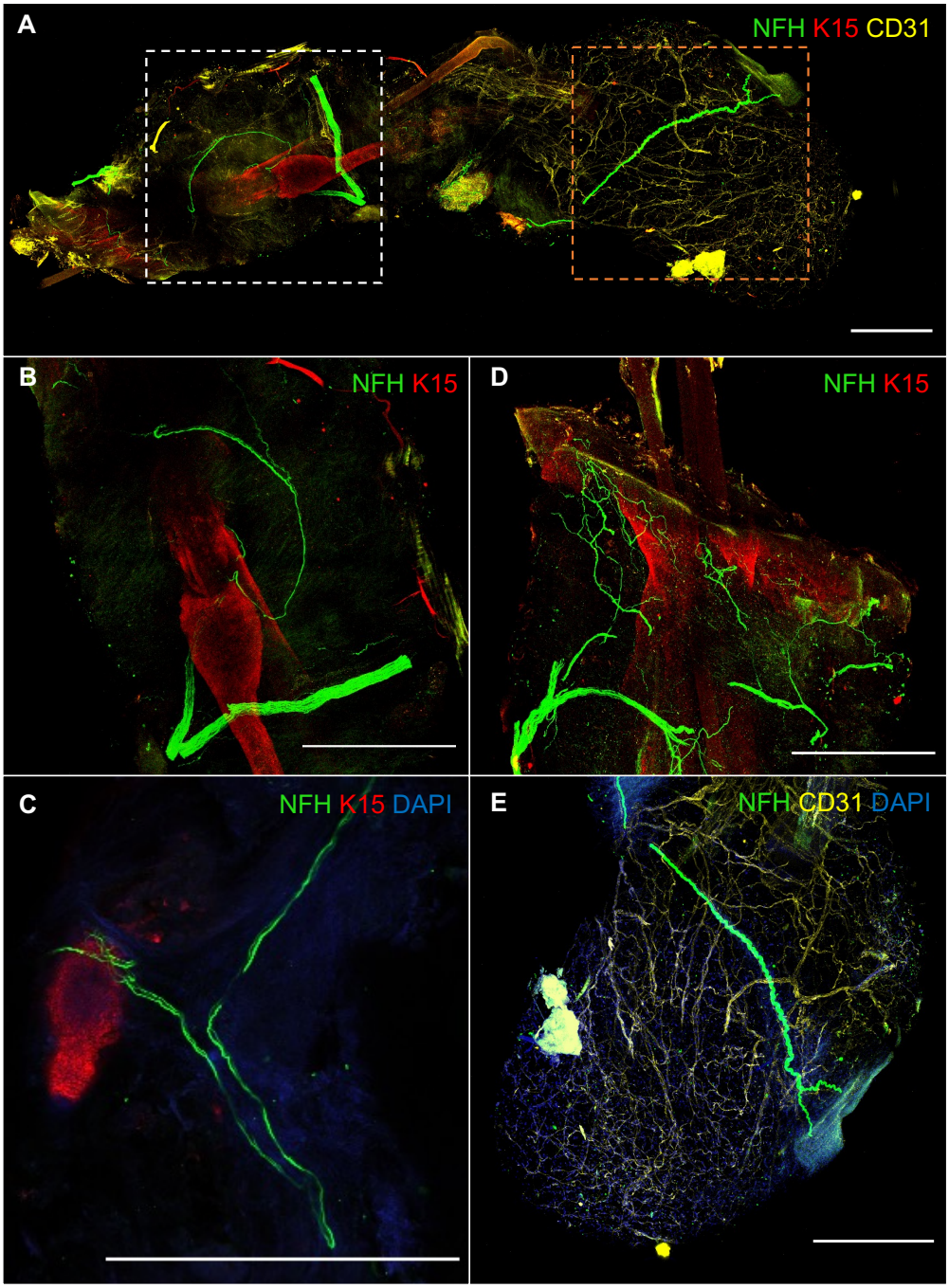


Figure 2.2: Innervation around the hair follicle macroenvironment.

A) NFH (green) labels nerves which are present in the dermis, epidermis, and dermal white adipose tissue (CD31, yellow) around the anagen hair follicle. B) Close up of image A (white dotted box) shows same nerve innervates the hair follicle around the bulge region (K15, red) and branches off to innervate the epidermis. C) Nerves from the dermis innervates a telogen hair follicle (labelled with K15, red). D) Nerve fibre from the dermis branches off multiple times to innervate large area of the epidermis where the basal layer is labelled with K15 (red). E) Close of up image A (orange dotted box) shows presence of nerve fibre in dWAT. (Scale bar = 500 μm)

In addition, NFH^+ nerve fibres were observed to innervate different components associated with the hair follicle. A large nerve fibre in close proximity to the hair follicle branches off into thinner fibres to innervate an eccrine gland (Figure 2.3A) while sebaceous glands are surrounded by thicker bundles of nerve fibres (Figure 2.3B). A nerve plexus was also seen around the bulge region of hair follicle which divided multiple times and was seen to innervate a vessel or gland close to the follicle (Figure 2.3C).

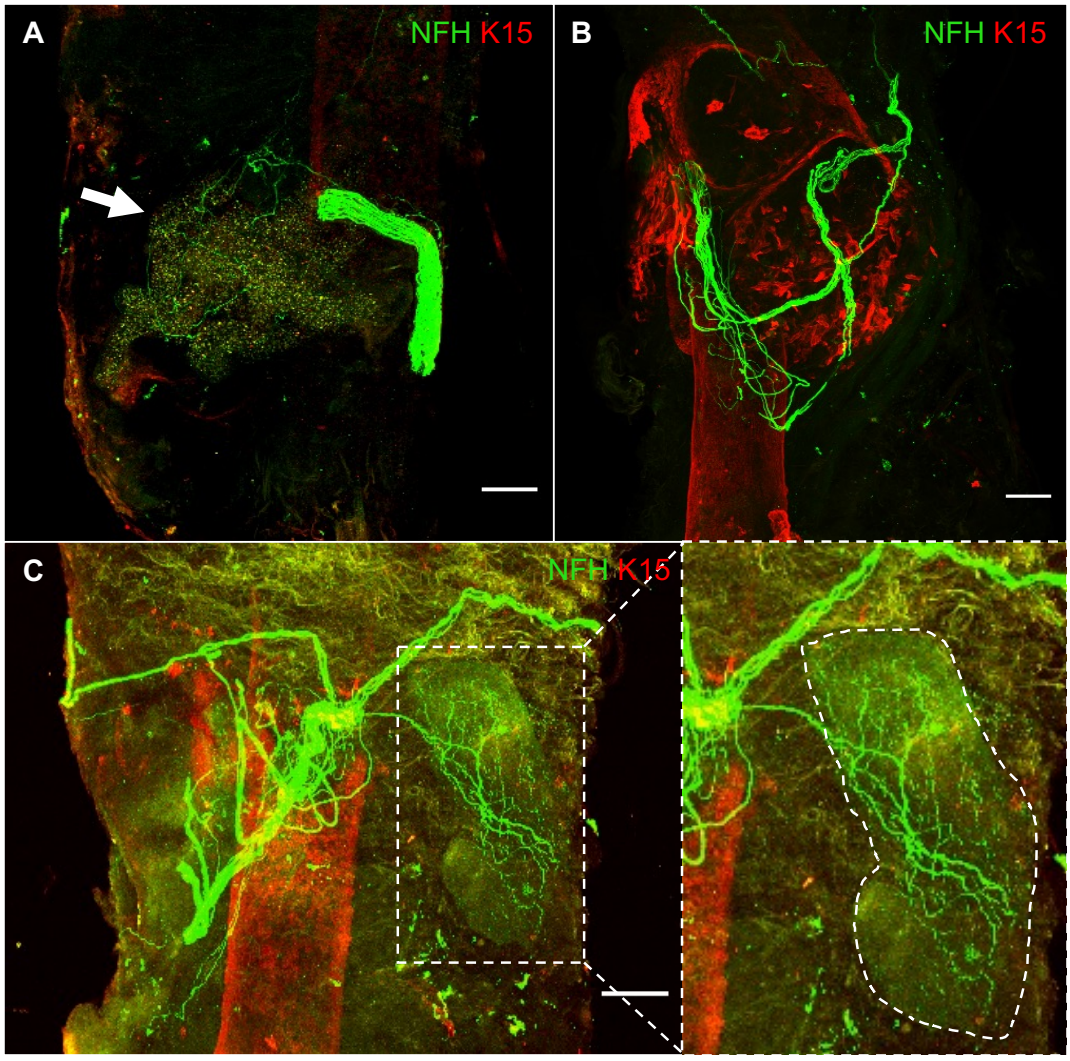


Figure 2.3: Innervation of eccrine gland, sebaceous gland and vessel/gland.

A) Large nerve fibre (NFH, green) which is in close contact to the anagen hair follicle (K15, red) branches off to innervate the eccrine gland (white arrow). B) Multiple nerve fibres innervate the sebaceous gland labelled with K15 (red). C) A nerve fibre innervates a hair follicle and branches off to innervate a vessel or gland (close up in dashed white box, scale bars = 100 μm)

As mentioned in section 1.4.4.3, mice have four different types of hairs and they are surrounded by low threshold mechanoreceptors (LTMRs) which sense mechanical stimuli such as vibration or movement of hair follicles (Dalsgaard *et al.*, 1984). LTMRs are divided into Aß, Aδ and C depending on their conduction velocity (Olson *et al.*, 2016). Guard hairs are innervated by Aß-fibres, awl/auchene have Aß, Aδ and C-LTMR fibres and zigzag hairs are innervated by Aδ and C-LTMR fibres (Olson *et al.*, 2016). These different nerve fibres form specialised nerve endings around the hair follicle and are organised as longitudinal lanceolate endings which run parallel to the hair shaft or as circumferential endings which wrap around the hair follicle. (Lechner and Lewin, 2013) showed the presence of longitudinal and outer circular fibres in human hair follicles using electron microscopy. Similarly, NFH staining here revealed the presence of longitudinal lanceolate and circumferential nerve endings in human hair follicles in anagen (Figure 2.4.4A) while a telogen hair follicle showed longitudinal lanceolate nerve endings (Figure 2.4B).

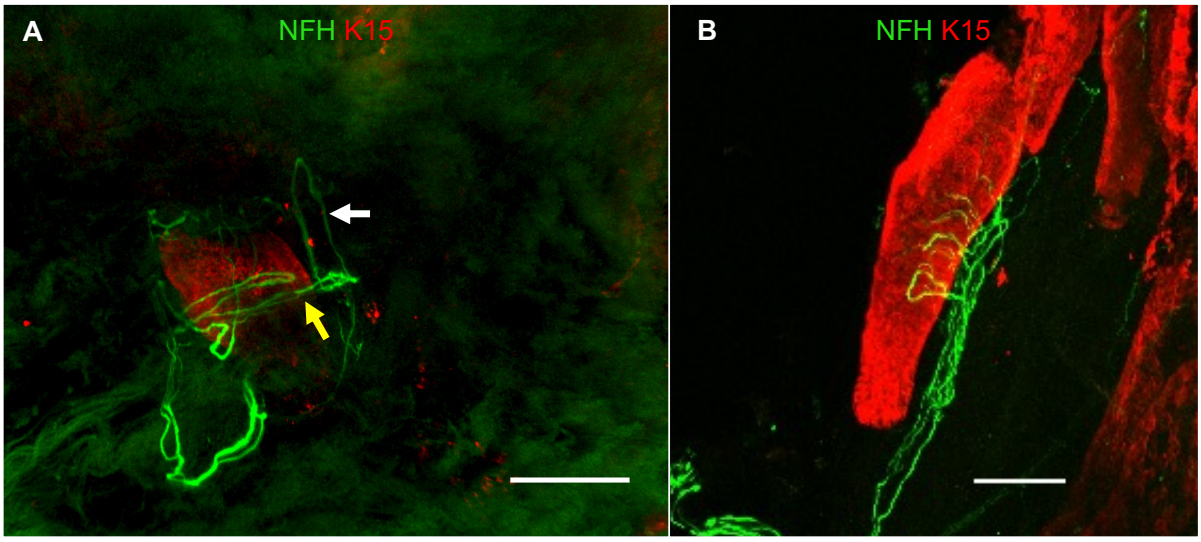


Figure 2.4: Specialised nerve endings in human hair follicles.

A) NFH (green) staining exhibit longitudinal lanceolate (white arrow) and circumferential (yellow) nerve endings. B) A telogen hair follicle is innervated by longitudinal lanceolate nerve ending. (Scale bars = 100 µm)

Furthermore, an NFH^+ nerve fibre from the dermis was observed to branch off multiple times to innervate all the hair follicles in a FU and to innervate the epidermis (Figure 2.5A and B). The same nerve fibre can innervate a telogen hair follicle then divide to innervate a sebaceous gland suggesting a complex nerve network is formed within a FU where the hair follicle is connected to its macroenvironment through the nerve network (Figure 2.5C).

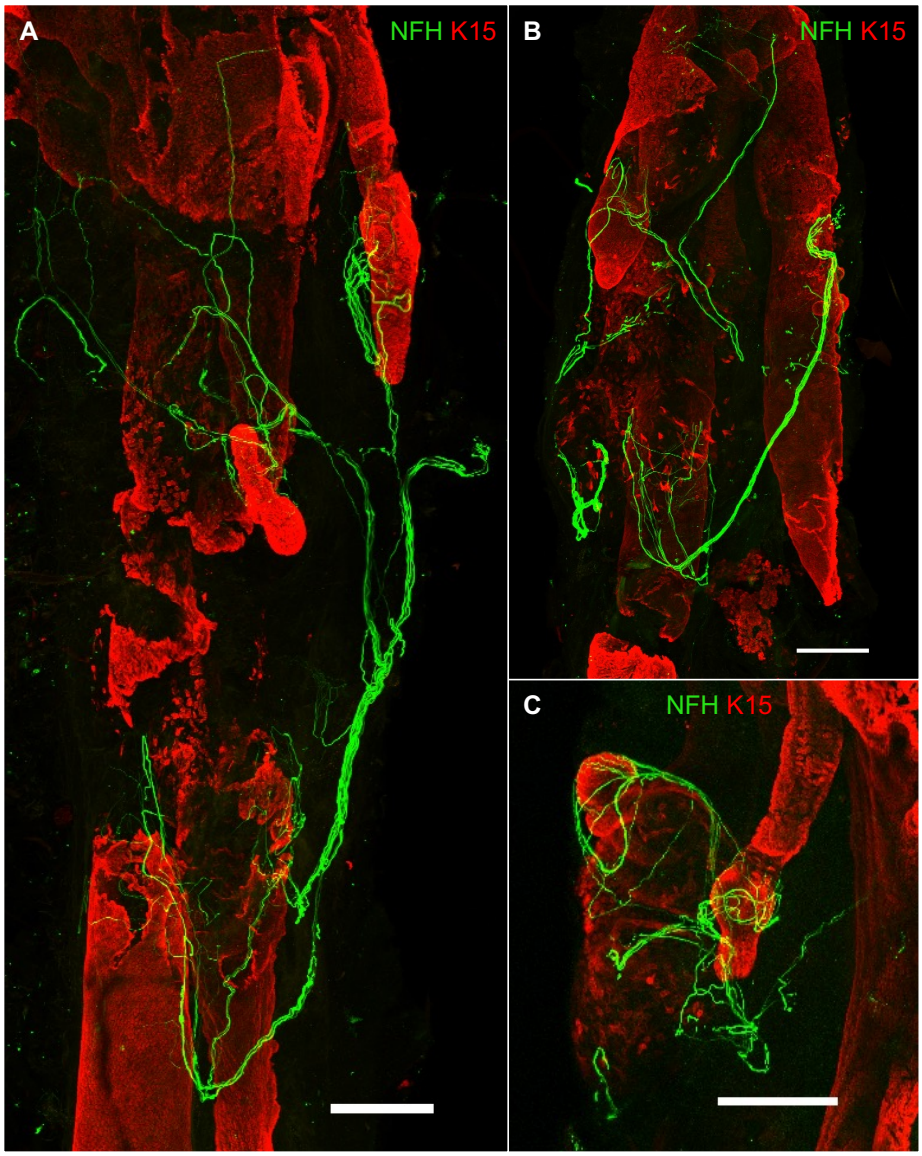


Figure 2.5: Same nerve branches off to innervate multiple hair follicles in a follicular unit.

A) Same nerve fibre (NFH, green) branches off to innervate an anagen hair follicle, a telogen hair follicle and the epidermis (K15, red). B) Same nerve fibre branches off to innervate two follicles in anagen and one in telogen phase. C) Same nerve fibre innervates a telogen hair follicle and sebaceous gland. (White arrow = anagen follicle, yellow arrow = telogen follicle, orange arrow = sebaceous gland. Scale bars = 200 µm)

In some hair follicles, large nerve fibres running along or across the hair follicle were observed which seemed to make a physical contact with the epithelial cells of the ORS. 3D reconstructions of the nerves and hair follicles revealed that there is a close contact between the larger nerve fibres that run along or across the hair follicle and the epithelial cells of the ORS (Figure 2.6A). Lanceolate endings that formed in telogen hair follicles also seemed to physically contact the epithelial cells (Figure 2.6B). 3D reconstructions also showed that large nerve fibres which branch off to innervate multiple hairs can traverse in between hair follicles remaining close to the hair follicle (Figure 2.6C). Whilst the 3D reconstructions indicated that the nerves and epithelial cells could be in physical contact with each other, electron microscopy studies have shown that in human hair follicles, there is a basal lamina separating the smaller longitudinal fibres and epithelial cells of the ORS (Hashimoto, Ito and Suzuki, 1990). Also, immunofluorescent staining in humans by (Hashimoto, Ito and Suzuki, 1990) showed that the large nerve trunks are in close proximity to the hair follicle but do not make physical contact; however, localisation of nerve fibre between hair follicles was not been described.

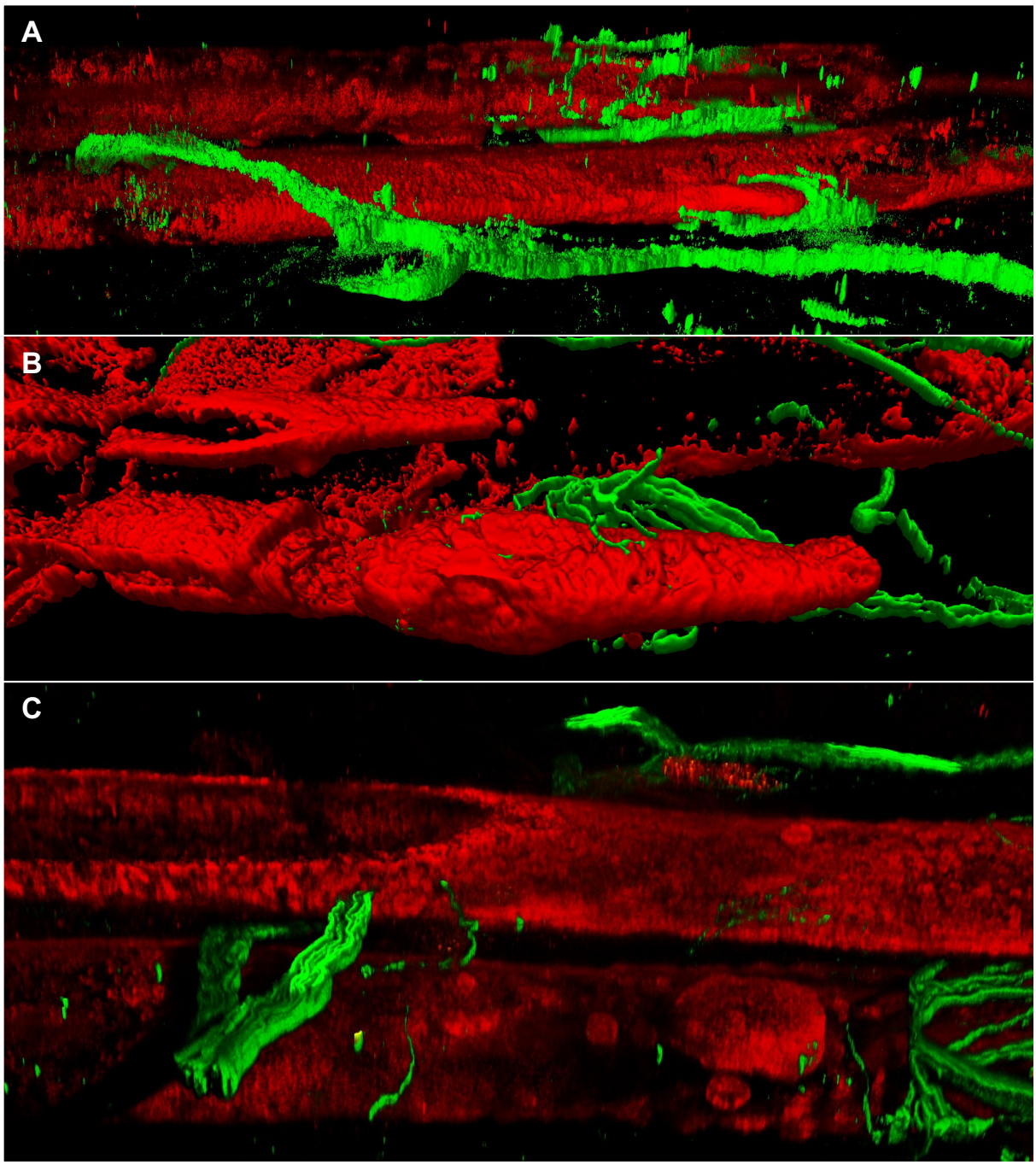


Figure 2.6: Close interactions between nerves and epithelial cells.

A) Large nerve fibre wraps around hair follicles. B) Nerves are in close contact with telogen epithelial cells. C) Large nerve fibre traverses between two anagen hair follicles (white arrow). 3D reconstructions of hair follicle (K15, red) and nerves (NFH, green) were made using 3D viewer software on Leica SP8 confocal microscope.

2.4.2. Innervation of hair follicles is decreased in frontal hair follicles

To verify whether the innervation between frontal and occipital hair follicles is different, fluorescence intensity of NFH present within the hair follicle was quantified (Figure 2.7A and B). The intensity throughout the entire hair follicle was measured as nerves present along the hair follicle contribute to innervation of hair follicles as shown in figure 2.5. Quantification of fluorescence intensity showed 53% decrease in NFH intensity (p-value = 0.0173) in frontal follicles compared to occipital follicles suggesting decreased innervation of frontal hair follicles.

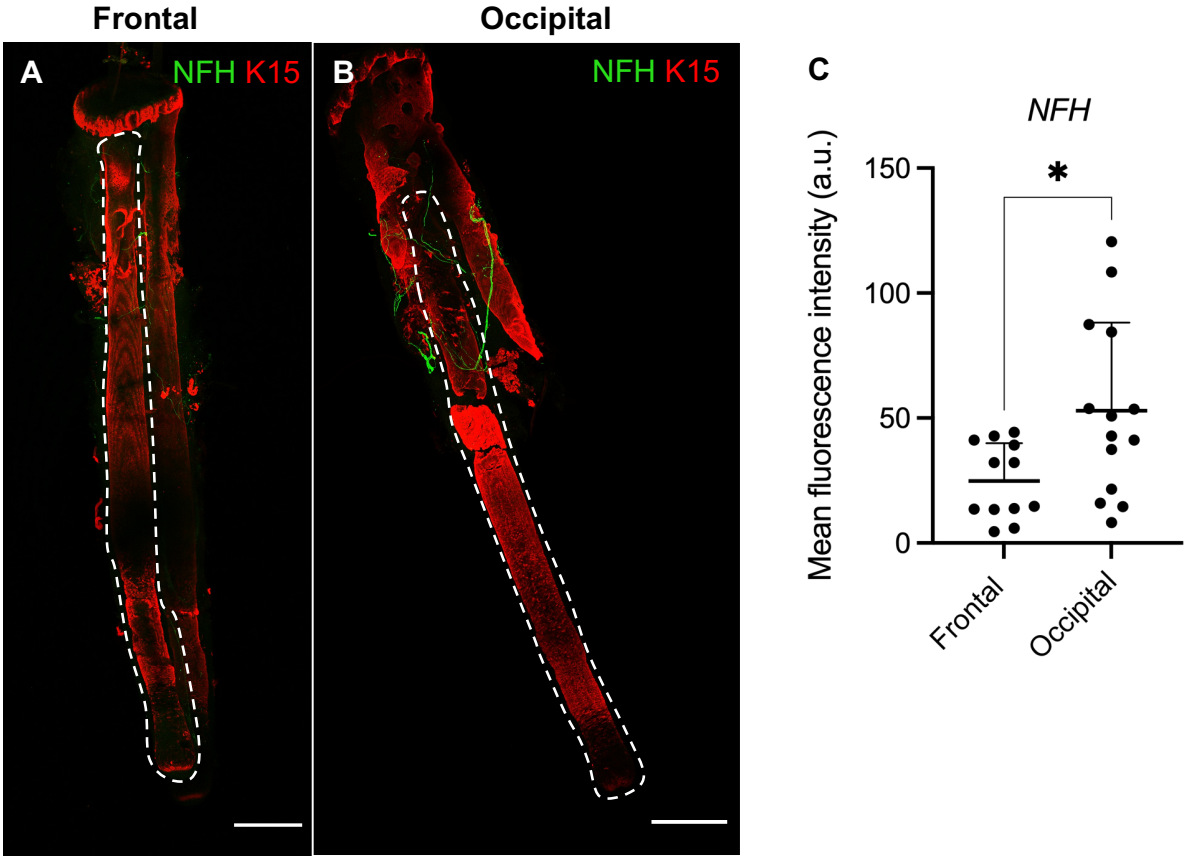


Figure 2.7: Comparison of mean fluorescence intensity of NFH in frontal and occipital hair follicles.

Fluorescence intensity within the dashed lines were measured in frontal (A) and occipital (B) hair follicles. C) There is a decrease in NFH expression in frontal hair follicles compared to occipital hair follicles. (N=3 patients, n= minimum 2 hair follicles per patient. Data were analysed using an unpaired t-test and error bars represent standard deviation, * P = 0.0173, scale bars = 500 μm)

2.4.3. Characterisation of blood vessels in hair follicles

Cluster of differentiation 31 (CD31), also known as platelet endothelial cell adhesion molecule 1 (PECAM-1), is a transmembrane glycoprotein which is expressed in endothelial cells of blood vessels and lymphatic vessels but present at higher levels in blood vessel endothelial cells. CD31 is used as a marker of blood vessels and has been shown to have a role in migration of endothelial cells and angiogenesis (Baluk and McDonald, 2008; Lertkiatmongkol *et al.*, 2016). (Baluk and McDonald, 2008; Lertkiatmongkol *et al.*, 2016) used azo-dye for alkaline phosphatase to detect terminal capillaries present in human hair follicles. They showed the DP contains capillaries connected to the vessels of the hair follicle. The end bulb contains a network of blood vessels that run parallel to the hair follicle and are linked together by cross-shunts. As the blood vessels progress up the hair follicle, the cross-shunts decrease and become surrounded by “palisade of parallel longitudinal vessels”. In the upper part of the follicle, the blood vessels envelop the sebaceous glands and form loose network which “extends to the surface of the skin”. Azo-dye detects terminal capillaries strongly while the endothelium of arteries and veins are weakly reactive. Whole-mount imaging of human hair follicles with CD31 has also revealed a rich network of blood vessels in the bulb regions of the hair follicle (Yoshida, Soma and Kishimoto, 2019) indicating CD31 can be used to study the vasculature of the hair follicle and its macroenvironment.

Whole-mount immunolabelling of hair follicles with CD31 showed complex network of blood vessels spanning the entire hair follicle from the end bulb to the top of the hair follicle. Similar to (Yoshida, Soma and Kishimoto, 2019), I observed dense network of blood vessels present in the end bulb with cross-shunts connecting the vessels that run parallel to the hair follicle. The size of the blood vessels increased as the vessels travelled towards the upper portion of the hair follicle. Less cross-shunts were seen in the upper portion of the hair follicle with a dense disorganised network being present parallel to the hair follicle. The blood vessels eventually reach the epidermis where they vascularise the rete ridges of the epidermis (Figure

2.8A). CD31 also labelled small capillaries present within the DP (Figure 2.8B) and revealed that hair follicles in a FU could have overlap of blood vessels (Figure 2.8C).

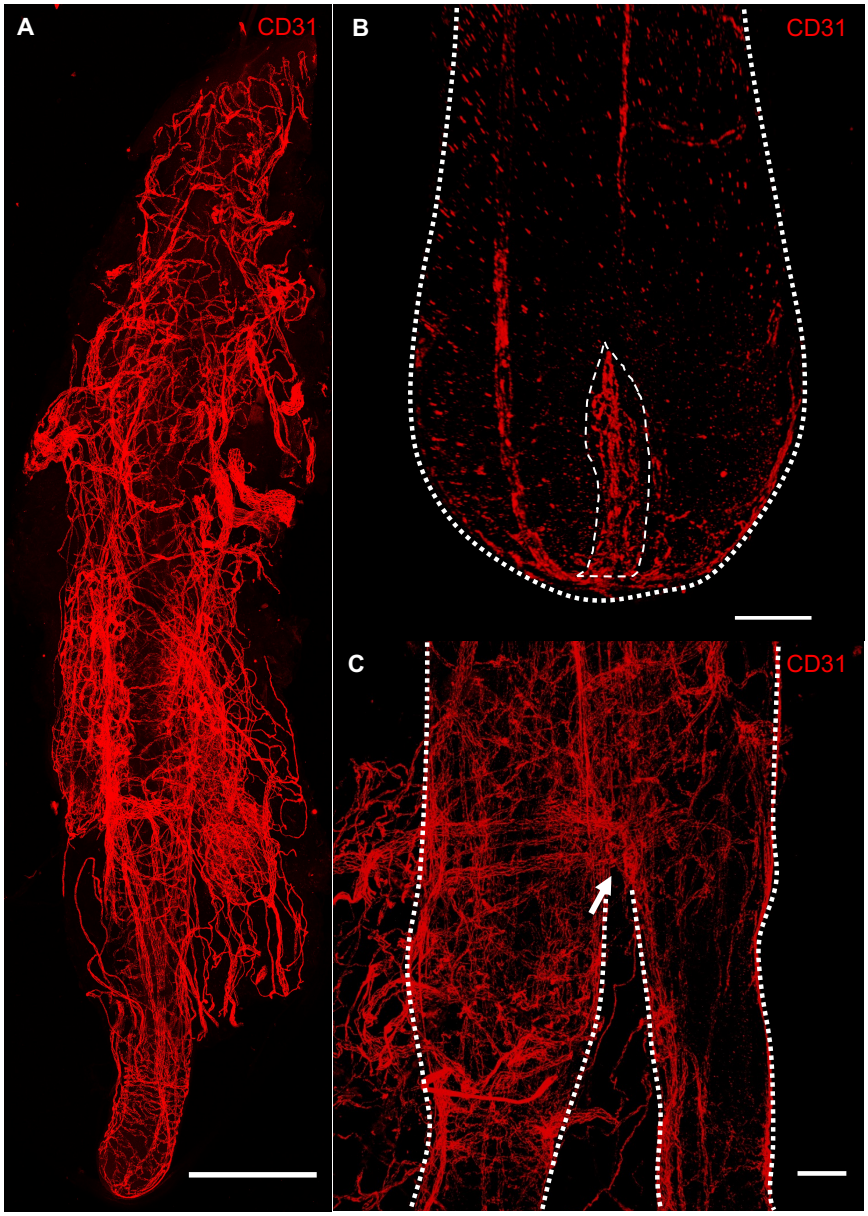


Figure 2.8: Hair follicles are highly vascularised.

A) Hair follicle stained with CD31. B) CD31 staining shows the presence of capillaries in the DP. The dotted lines mark the outside of the follicle while the dashed line outlines the DP. C) Two hair follicles in a follicular unit could have overlapped blood vessels (white arrow). The dotted lines mark the edges of the hair follicle. (A- scale bar = 500 μm. B and C- scale bar = 100 μm)

Moreover, as previously described by Montagna & Ellis, (1957), blood vessels vascularise the sebaceous gland (Figure 2.9A and B) and eccrine gland (Figure 2.9D). Hair follicles are also vascularised by blood vessels that arise from both the dermis and the dWAT (Figure 2.9C). Eccrine and sebaceous glands are also vascularised by the blood vessels that are present near the hair follicle (Figure 2.9D).

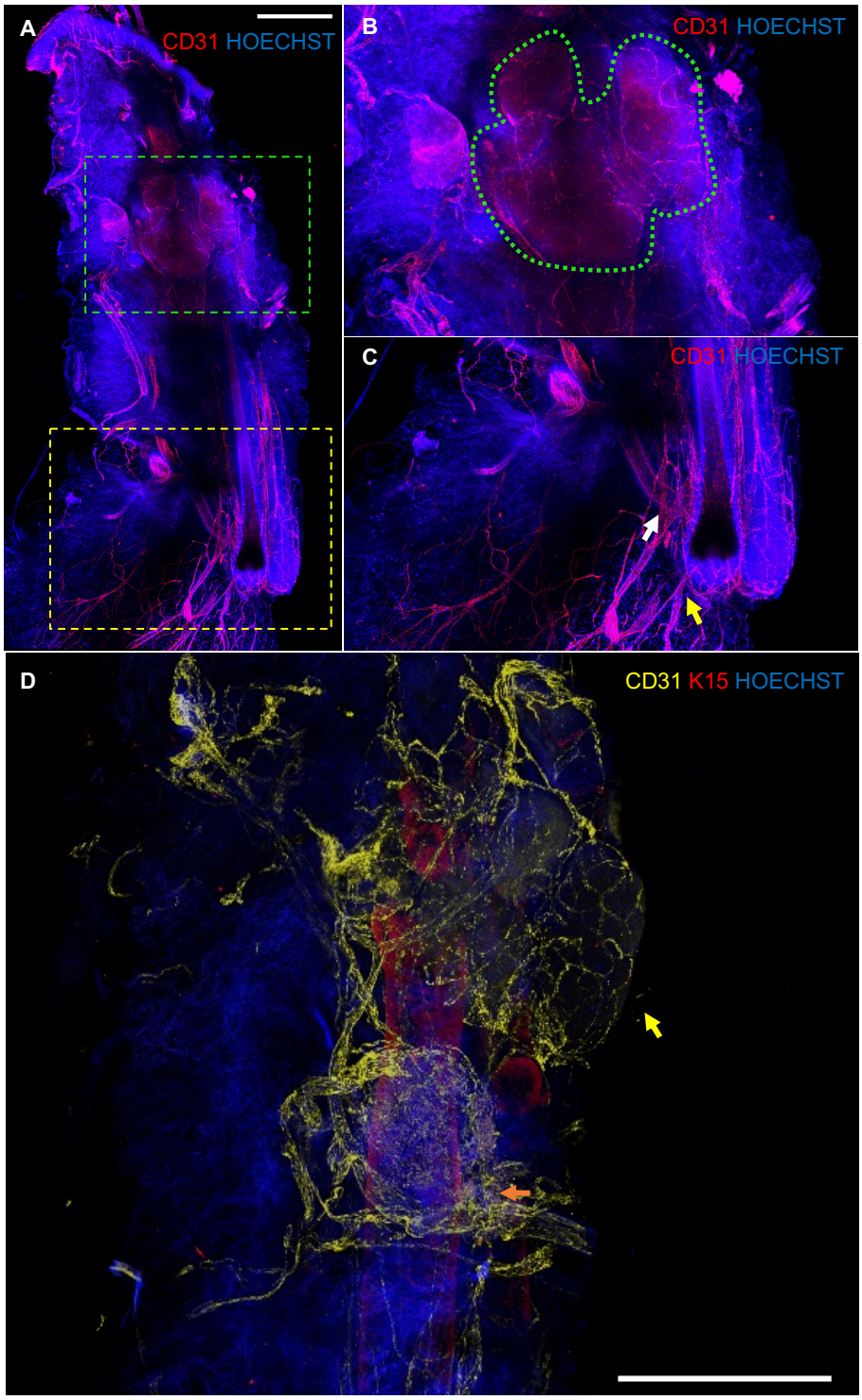


Figure 2.9: Blood vessels around the hair follicle.

A) CD31 (red) staining to show presence of blood vessels within and around the hair follicle. B) Close up of green box in A to show the blood vessels present in sebaceous gland (drawn around in green dots). C) Close up of yellow box in A which shows blood vessels originating from the dermis (white arrow) and the dWAT (yellow arrow) vascularising the hair follicle. D) Eccrine (orange arrow) and sebaceous glands (yellow arrow) have rich supply of blood vessels around them. (Scale bars = 500 μm)

2.4.4. Frontal hair follicles contain less blood vessels

Occipital hair follicles were taken from patients undergoing FUT or FUE surgery which resulted in variable amount of dermis present in the upper portion of the hair follicle. Frontal follicles on the other hand are always removed by FUE. As the lower portion of the hair follicle regenerates at every hair cycle and blood vessels in the lower region degrade during catagen and reform during anagen, it is assumed that the blood vessels in the upper region of the hair follicles are permanent. Thus, fluorescence intensity was measured in the lower portion of the hair follicle only. Variable levels of CD31 intensity were found in frontal and occipital hair follicles and follicles with low CD31 intensity were observed to have less well-connected cross shunts in the end bulb (Figure 2.10A). Quantification of CD31 intensity revealed that the frontal hair follicles had 33% decrease in CD31 intensity (p-value = 0.0029) suggesting a decrease in blood vessels present in the lower portion of the frontal hair follicles compared to occipital hair follicles (Figure 2.10B).

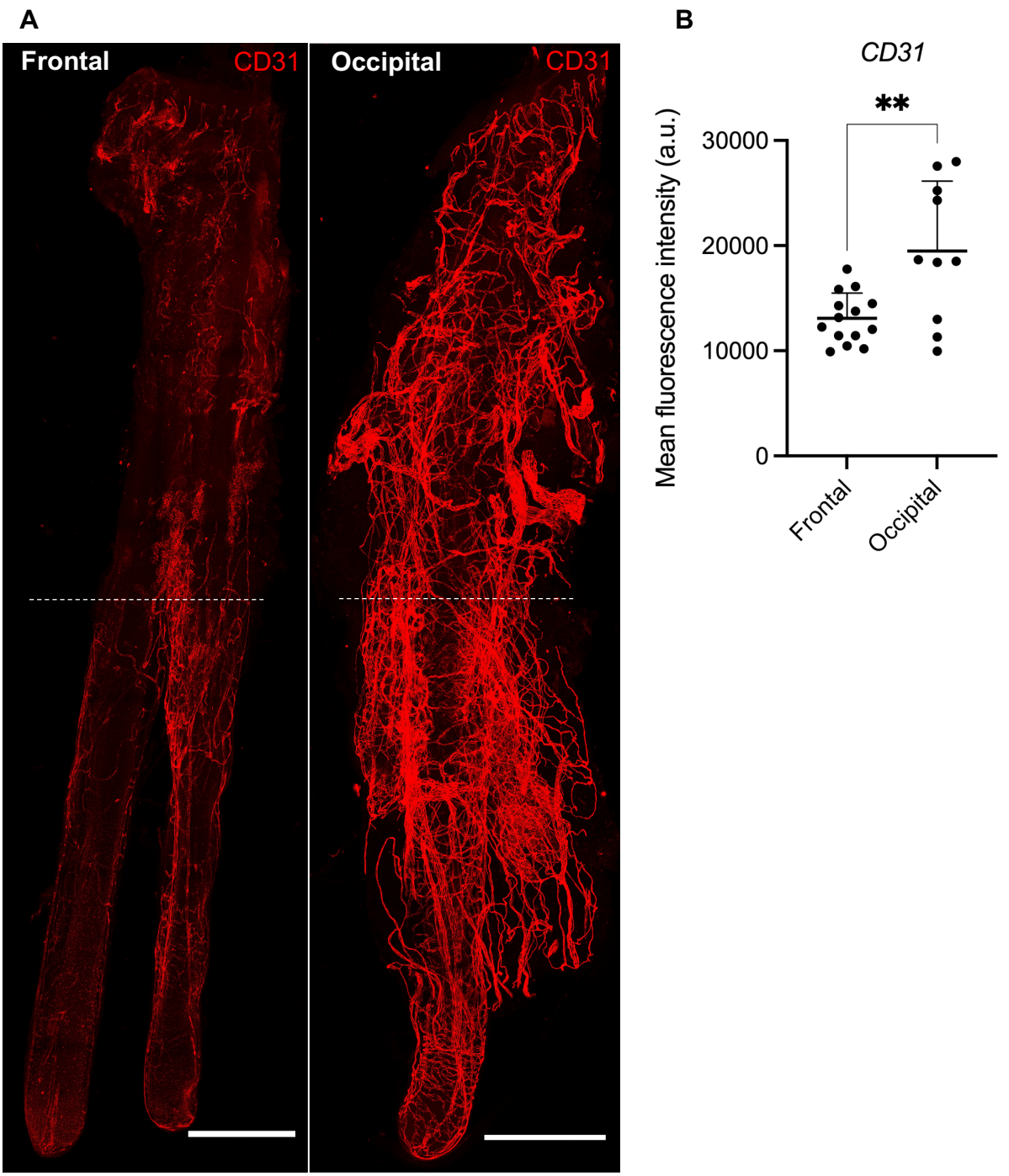


Figure 2.10: Comparison of mean fluorescence intensity of CD31 in frontal and occipital hair follicles.

A) Representative images to show the levels of intensity of CD31 staining seen in lower half of the hair follicle macroenvironment**.** Dotted line to show how the hair follicle was divided into two equal parts. B) There is a decrease in CD31 expression in frontal hair follicles. (N=3 patients, n= minimum 2 hair follicles per patient. Data was analysed using an unpaired t-test and error bars represent standard deviation, ** P = 0.0029. Scale bars = 500 μm)

2.4.5. Characterisation of lymphatic vessels in hair follicles

Lymphatic vessel endothelial hyaluronan receptor 1 (LYVE-1) is a receptor for ECM hyaluronan and is expressed on lymphatic endothelial cells. In mice, lymphatic vessels are present on the anterior side of the hair follicle, opposite to the APM and are found to be closely localised to the bulge region. Lymphatic vessels connect three hair follicles at the bulge region and these triads share a common lymphatic capillary (Peña-Jimenez *et al.*, 2019). Lymphatic vessels were also shown to be in close proximity to the end bulbs in anagen hair follicles in mice which were stained with another lymphatic vessel marker Prox1 (Peña-Jimenez *et al.*, 2019). LYVE-1 mainly seems to mark lymphatic vessels near the bulge region of the hair follicles in mice.

In human hair follicles, LYVE-1^{+} lymphatic vessels were present in upper portion of the hair follicle (Figure 2.11 A and B). LYVE-1 also stained lymphatic capillaries that ran parallel to the hair follicle and formed a sparse network around the end bulb which has not been described before (Figure 2.11C). The presence of large lymphatic vessels in the upper region of the hair follicle were rare and was only observed in only 3 out of 17 follicles. The fine meshwork of lymphatic capillaries around the end bulb was present in 15 out of 17 follicles examined, however they differed in their intensities, amount, and the level of interconnectedness. The lymphatic capillaries which ran parallel to the hair follicles in the lower portion of the hair follicles were common and found in all the hair follicles examined, albeit at different intensities and lengths along the hair follicle.

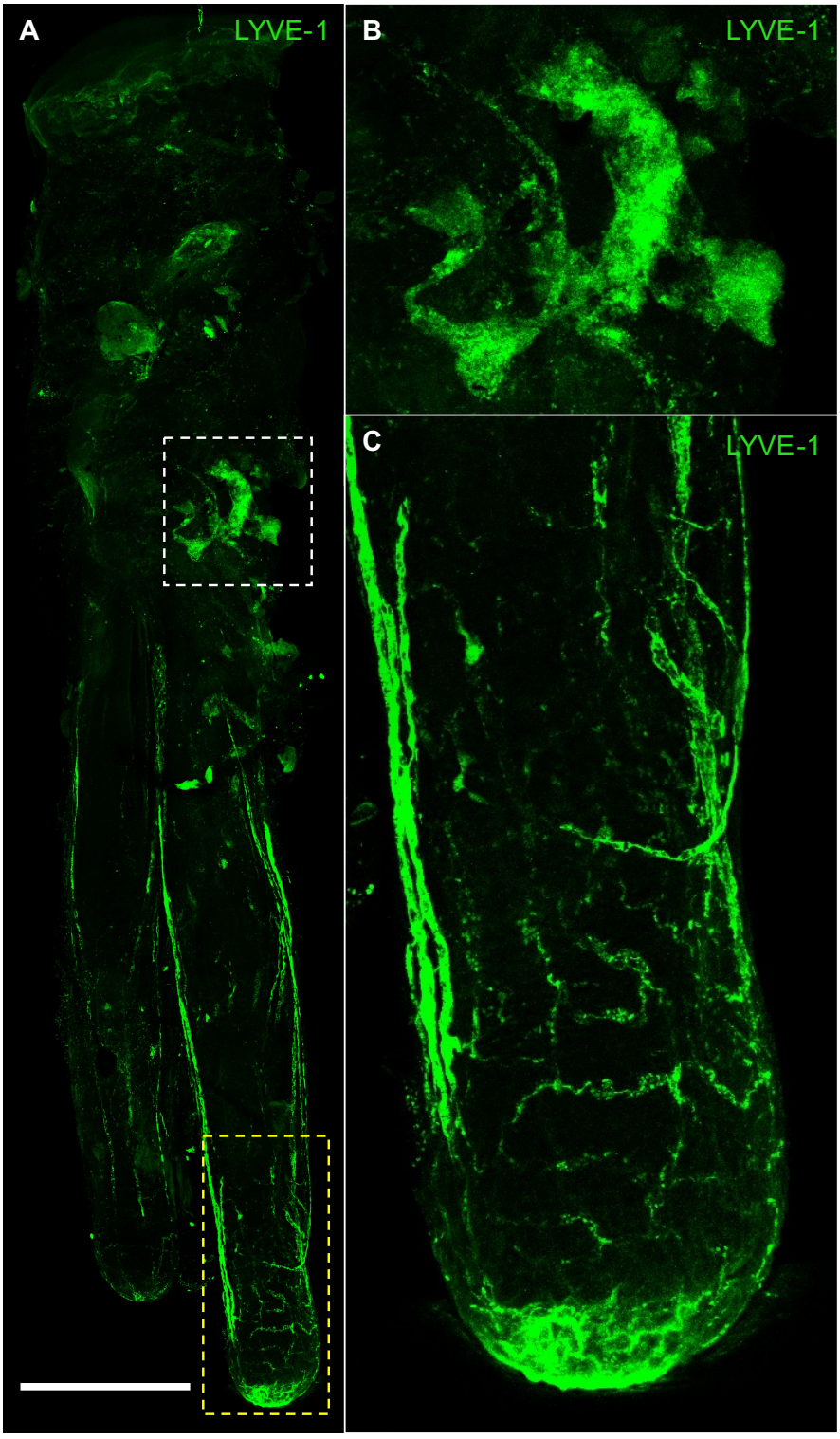


Figure 2.11: Lymphatic vessels of a hair follicle.

A) Smaller lymphatic vessels are present in the lower portion of the hair follicle and bigger vessels are present in the upper region of the hair follicle. B) Close up of white box in A which shows the presence of large lymphatic vessel. C) Close up of yellow box in A which shows the presence of smaller, finer network of lymphatic capillaries surrounding the end bulb. (Scale bar = 500 μm)

As mentioned above, the presence of large lymphatic vessels in the upper portion of the hair follicle was rare. In one occipital follicle, a large lymphatic vessel was observed which measured 70.77 µm in diameter at its largest and 23.19 µm in diameter at its smallest (Figure 2.12A and B).

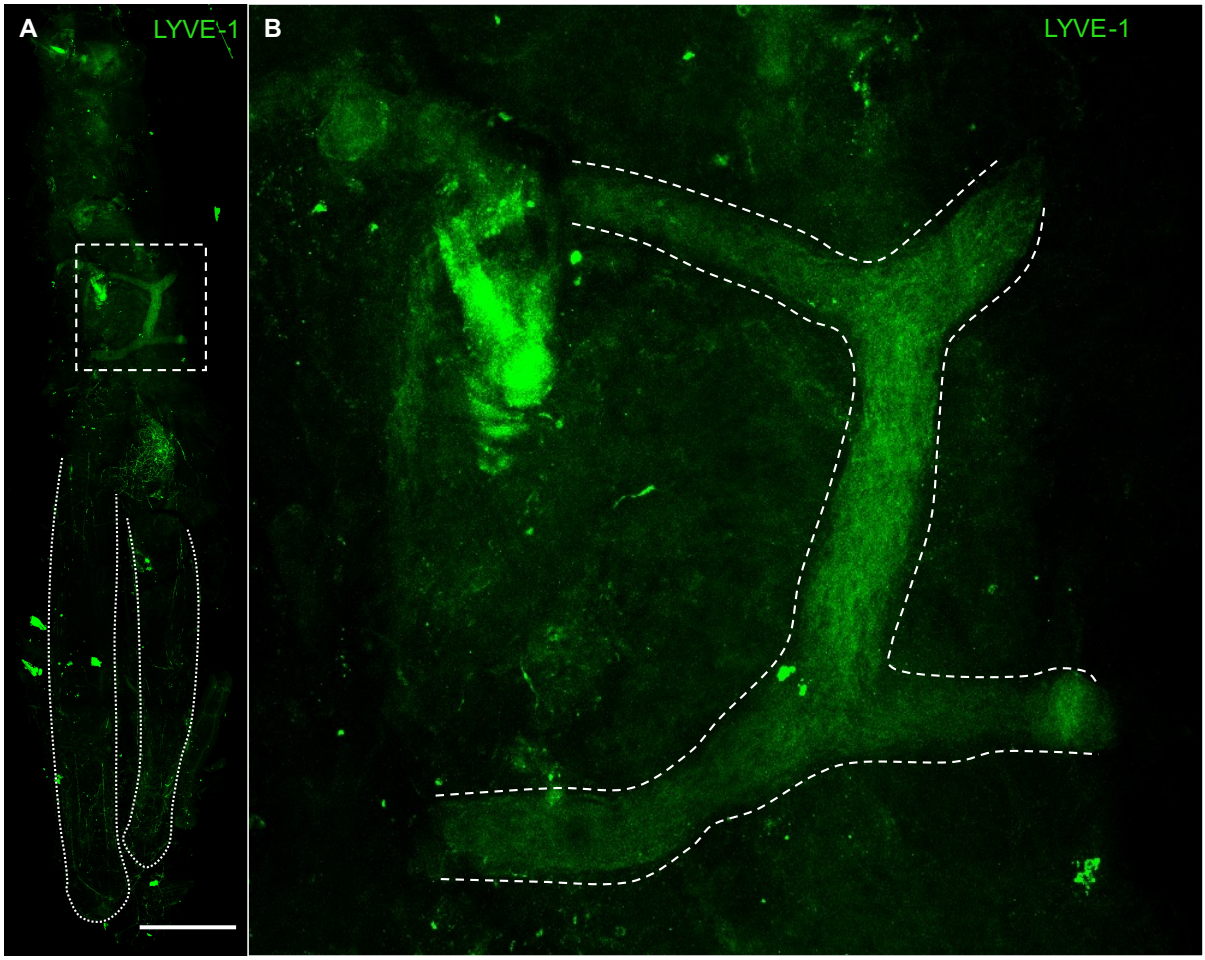


Figure 2.12: LYVE-1 staining of the hair follicle.

A) LYVE-1 (green) staining showed presence of large branched lymphatic vessel in the dermis. Dotted lines are outlines of the lower portion of the hair follicle. B) Close up of white box in A to show the branched lymphatic vessel. Dashed lines are outlines of the lymphatic vessel. (Scale bar = 500 µm)

The main function of lymphatic capillaries is to carry interstitial fluid away from the tissues and back to the blood. Lymphatic capillaries are found close to the blood capillaries, arteries, and veins of the cardiovascular system. In human hair follicles, some lymphatic capillaries that ran

parallel to the hair follicle were found to overlap with blood vessels (Figure 2.13A). This was also the case for the finer lymphatic capillaries that surrounded the end bulbs (Figure 2.13B). Moreover, the large lymphatic vessel was found to be interlaced in a network of blood vessels forming close connection with the blood vessels (Figure 2.13C and D).

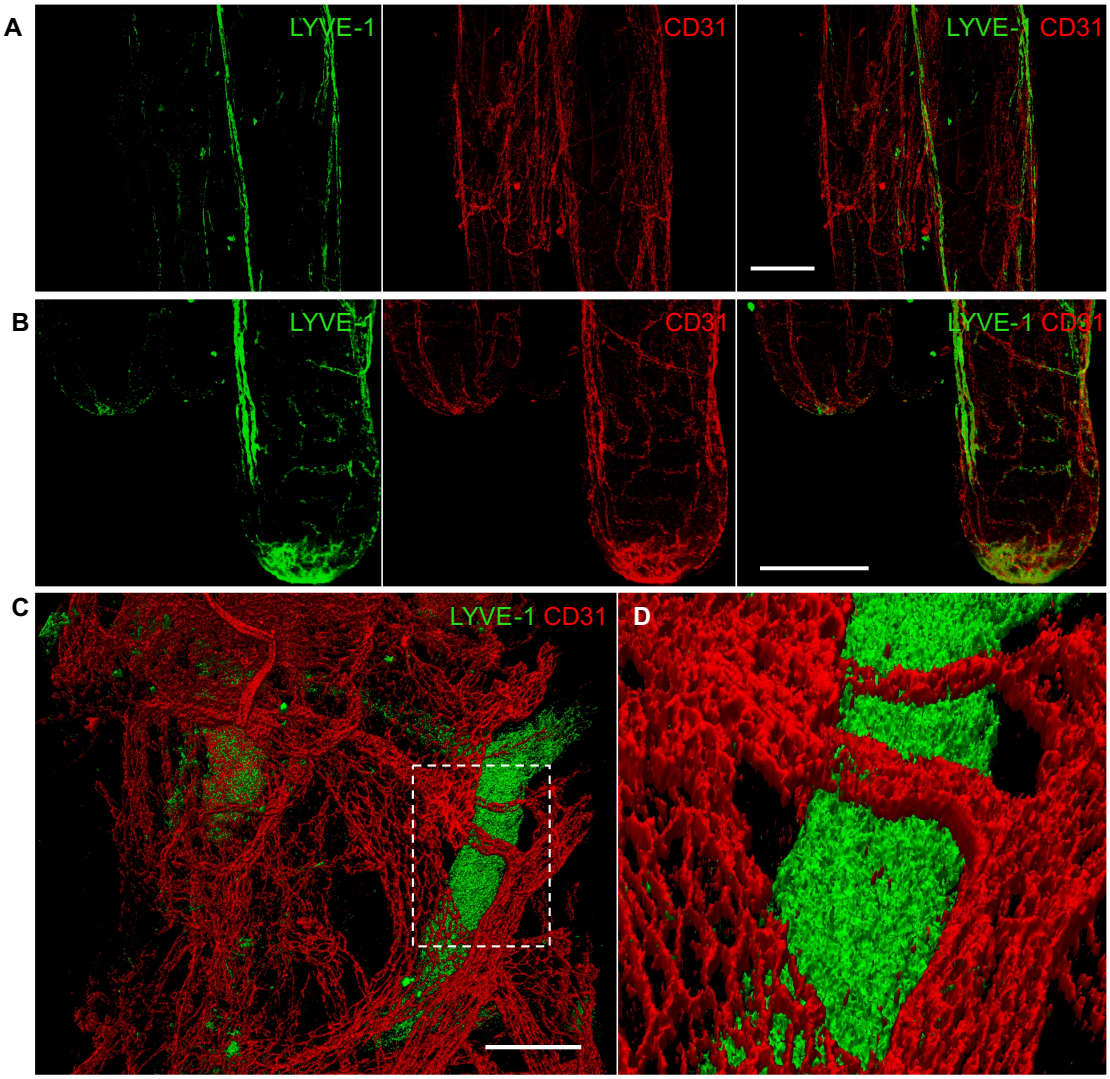


Figure 2.13: Lymphatic vessels and blood vessels are in close association with each other. Lymphatic capillaries (LYVE-1, green) running along the hair follicles (A) and surrounding the end bulb (B) overlap with blood vessels (CD31, red). C) 3D reconstructions of blood vessels and lymphatic vessels show lymphatic vessels are interlaced in the blood vessel network. D) Close up of white dotted box in C showing close association of blood vessels to a lymphatic vessel (A and B- scale bars = 200 µm, C- scale bar = 100 µm)

2.4.6. There is an increase in lymphatic vessels in frontal hair follicles

As mentioned above, the most prominent lymphatic vessels which were stained by LYVE-1 were found in the lower portion of the hair follicle and varied in their intensities. To verify whether the lymphatic vessels are different in frontal and occipital hair follicles, fluorescence intensity was measured in the lower half of hair follicles (Figure 2.14A). Quantification of LYVE-1 intensities revealed a 28% increase in LYVE-1 intensity (p-value = 0.0288) in frontal hair follicles compared to occipital hair follicles suggesting presence of higher amount of LYVE-1^{+} lymphatic vessels in frontal hair follicles (Figure 2.14B).

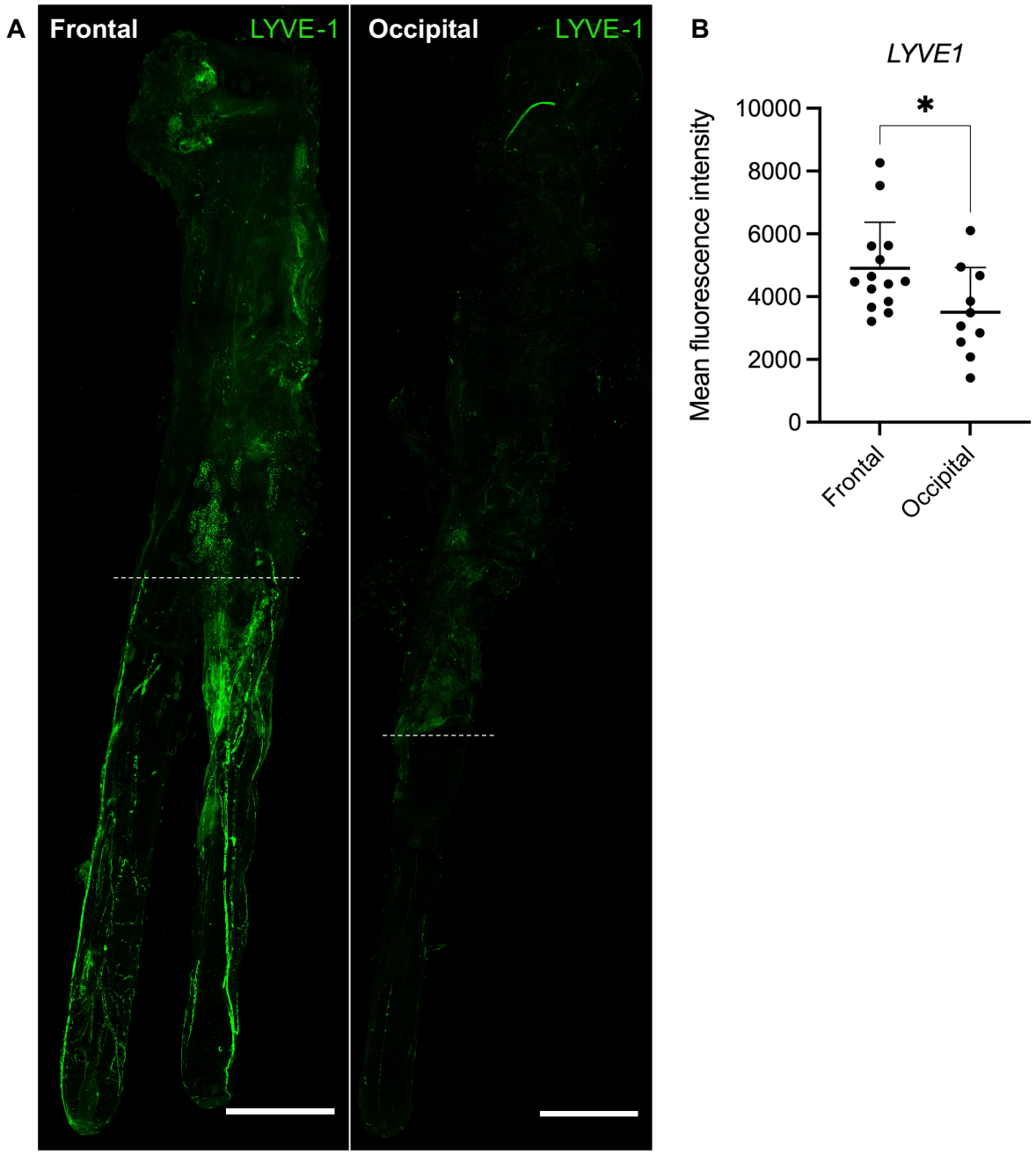


Figure 2.14: Comparison of mean fluorescence intensity of LYVE-1 in frontal and occipital hair follicles.

A) Representative images of frontal and occipital hair follicles with LYVE-1 staining. The dotted line shows the lower half of the follicle from which intensities were measured. B) There is a decrease in LYVE-1 expression in occipital hair follicles. (N=3 patients, n= minimum 2 hair follicles per patient. Data was analysed using an unpaired t-test and the error bars represent standard deviation, * P = 0.0288. Scale bars = 500 μm)

2.5. Summary

The follicular macroenvironment consists of a vast network of blood vessels, lymphatic vessels, neurons, dWAT and immune cells. Changes to the epidermis, dermis, dWAT, blood vessels and nerves have been observed as the hair follicle cycles (Yoon *et al.*, 2019). In addition, the macroenvironment around the hair follicle can influence the cycling and regeneration of the follicle. Angiogenesis occurs during anagen and is important for anagen initiation (Chase, Montagna and Malone, 1953; Botchkarev *et al.*, 1997) and influences follicle size (Mecklenburg *et al.*, 2000). Lymphatic vessels, which are mainly associated with the bulge region of the hair follicles, also influence anagen initiation (Yano, Brown and Detmar, 2001) and maintenance (Gur-Cohen *et al.*, 2019). In mice, increase in number of nerve fibres around hair follicles have been described in anagen (Yoon *et al.*, 2019). Substance P, a neuropeptide released by sensory fibres which innervate hair follicles, have been shown to promote anagen in murine skin organ culture (Botchkarev *et al.*, 1997). However, denervation of mice hair follicle had no effect on anagen induction (Peters *et al.*, 2001) .

In AGA, changes to the follicular macroenvironment have been observed. There is miniaturisation of primary and secondary follicles in a FU with loss of APM attachment and enlarged sebaceous glands. Miniaturised follicles have been described to have smaller capillaries and changes to the nerve plexus have also been observed (Maurer *et al.*, 1998). However, these changes have not been quantified and it is unknown the degree to which there is reduction in vasculature and innervation of hair follicles. Moreover, changes in lymphatic vessels in AGA have not been previously described.

In this chapter, I aimed to characterise and quantify the density of neurons, blood vessels and lymphatic vessels present in frontal and occipital hair follicles using whole-mount immunolabelling and volumetric imaging.

The presence of nerves in and around the hair follicles were observed using an antibody against NFH which is present in myelinated axons of neurons. Large NFH^+ fibre originating from the dermis were observed to branch off multiple times to innervate all the follicles in a FU along with the epidermis, eccrine and sebaceous glands. Longitudinal lanceolate and circumferential nerve endings around the bulge region of the hair follicles were also observed. The type of mechanoreceptors present in human hair follicles is unknown and will require further investigation. Moreover, quantification of NFH fluorescence intensity revealed a significant decrease in frontal hair follicles compared to occipital hair follicles. This suggested that there were less nerves present innervating the frontal hair follicles.

In addition, the network of blood vessels was characterised in frontal and occipital hair follicles using CD31. $CD31^+$ capillaries were observed in the DP which joined the blood vessels that ran parallel to the hair follicle and formed cross-shunts across the end bulbs. There was an increase in blood vessel length towards the upper portion of the hair follicle. The blood vessels also vascularised neighbouring hair follicles in a FU along with eccrine and sebaceous glands. Same blood vessel network vascularised the epidermis. Quantification of CD31 fluorescence intensity revealed a significant decrease in frontal hair follicles compared to occipital hair follicles suggesting loss of blood vessels in the lower portion of frontal hair follicles.

Finally, characterisation of lymphatic vessels through immunolabelling with LYVE-1 revealed presence of LYVE-1^+ lymphatic capillaries in the end bulbs with larger lymphatic capillaries present parallel to the hair follicles. Smaller lymphatic capillaries were present in lower portion of the hair follicles examined in this study while the larger lymphatic vessels were observed in upper portion of the hair follicle. Quantification of LYVE-1 fluorescence intensity revealed a significant increase in frontal hair follicles indicating presence of more lymphatic vessels in frontal hair follicles.

Collectively, these results demonstrate that the macroenvironment around frontal, and thus miniaturising follicles is different from occipital follicles. I postulate that these differences contribute to the pathogenesis observed in AGA. Differences in innervation and blood and lymphatic vascularisation were seen in frontal hair follicles that had not miniaturised. This suggests that these differences could be used as markers to indicate whether frontal hair follicles could undergo miniaturisation. This could help to detect AGA in younger patients and how far along they could recede in the future leading to early treatment.

Chapter 3: Transcriptomic analysis to elucidate the protective nature of occipital hair follicles

3.1. Introduction

Hair follicles in the balding scalp miniaturise in response to androgens such as DHT which leads to production of paracrine factors that promote catagen and stimulate apoptosis of epithelial cells. This shortens anagen phase and results in miniaturised hair follicles. The balding scalp can be defined as the frontal, temples, and vertex as this is where miniaturisation occurs. Hairs from the balding scalp are not lost as miniaturised hair follicles produce small hair fibres but they do not reach the surface of the skin which gives the bald appearance (Lattanand and Johnson, 1975). In contrast, hairs on the occipital scalp are spared and are unaffected by DHT when transplanted into the balding scalp. They retain their large size and resume normal cycling suggesting occipital hair follicles are inherently different from frontal hair follicles. This is the donor dominance theory which was discussed in section 1.5.4. Furthermore, one of the characteristics of a miniaturised hair follicle is its tendency to stay in telogen (or kenogen) longer as discussed in section 1.5.1 and there is also a lack of conversion of BC into progenitor cells. It has been hypothesised that this deficiency in progenitor population could be due to "lack of activation of parent KRT15^{hi} cells in AGA" (Cranwell and Sinclair, 2016). As discussed in section 1.4.3., the DP is the main activator of BC at late telogen. This led me to hypothesise that signalling from the androgen-sensitive frontal DP (FDP) is modified resulting in less activation of BC and reduced differentiation of BC into follicular keratinocytes (KC). I believe it is differences in the hair follicle mesenchyme between the balding and non-balding areas of the scalp which lead to the specific pattern of alopecia seen in AGA.

In this chapter, I will elucidate the differences between androgen-sensitive frontal and androgen-insensitive occipital DP (ODP) in order to determine whether expression of specific genes in ODP offers protection against miniaturisation.

3.1.1. Differences between balding and non-balding dermal papilla

As briefly discussed in section 1.5.1., there are several differences between balding and non-balding DP cells. We know that FDP cells release paracrine factors including DKK-1, IL-6, TGF-ß in response to DHT which contribute to miniaturisation of the hair follicle (Garza *et al.*, 2011). Transcriptomic profiling of cultured DP from balding and non-balding sites have revealed differential gene expression in DP from these sites. In the first study in this research area, a DNA macroarray was used to assess the expression of 1,185 genes in cultured balding and non-balding DP cells (Midorikawa *et al.*, 2004). They found upregulation of 38 genes while 69 genes were downregulated in balding DP cells compared to non-balding DP cells. However, as discussed in section 1.3.1., 2D culture of DP cells induces changes to their gene expression. There were still some differences between balding and non-balding DP suggesting that balding and non-balding DP cells retain some of the characteristics of their original position; however, this study used unmatched balding and non-balding DP cells, so we don't know how much of the differential gene expression is due to patient variation.

Another study which looked into the transcriptomic profiling of balding and non-balding cells was by (Midorikawa *et al.*, 2004). The researchers used immortalised 2D human balding and non-balding DP cells. They showed immortalised DP cells expressed 69 out of 117 human DP signature genes as established by Ohyama et al., (2012) suggesting balding and non-balding DP cells in culture retain DP identity even though they lose their inductive ability in culture. The immortalised balding and non-balding DP cells were treated with DHT at 1 nM and 10 nM which resulted in large changes in the gene expression in response to DHT. There were 1,482 genes upregulated and 1,508 genes downregulated in balding DP cells compared to non-balding DP cells. However, like the previous study, this study also used immortalised balding and non-balding DP cells from non-matched patient samples. Therefore, to understand why hair follicles from the frontal scalp miniaturise but the occipital hair follicles do not, it is important to undertake transcriptomic profiling of intact DP from the same patient as

it would allow us to find differences due to their location and sensitivity to androgens and would remove the effects of patient variation and culture conditions.

3.1.2. *In vitro* co-culture systems

2D cell cultures have been used extensively to understand molecular and cellular mechanisms of normal tissues and to model disease. They are useful in interrogating rate of proliferation, migration, and differentiation of cells. Human 2D DP cell cultures have been used to understand how androgens affect hair growth through identification of DHT-induced factors such as DHT, IL6 and TGF-ß2 (Madaan *et al.*, 2018). Moreover, the effect of minoxidil on human DP cells has allowed researchers to elucidate how it promotes hair growth (Madaan *et al.*, 2018) . Simple co-culture systems with DP and KC have been used to interrogate the hair-inducing ability of DP and understand how androgen affects this ability. Roh et al., (2005) cultured BC with DP cells on a transwell membrane to mimic mesenchymal-epithelial interactions and identify changes in BC upon activation by DP. In a transwell co-culture system, cells are not in contact with each other; thus, the changes seen are due to paracrine effects. They discovered that K6hf (also known as keratin 75, K75) was specifically expressed in BC when co-cultured with DP. K75 has since been used as a hair differentiation marker as it is expressed in the companion layer of hair follicles and is not expressed by epidermal KC. In addition, Leirõs et al., (2012) used a transwell co-culture system with BC and DP cells to study the effect of androgens on stem cell differentiation. They found that DHT decreased the expression of K75 in BC showing androgens decrease stem cell differentiation ability of DP cells.

Even though 2D human DP cell cultures have revealed a myriad of fascinating results, 2D cell culture is an artificial environment for DP cells. *In vivo*, DP cells are present in a 3D flame shaped structure while embedded in an ECM composed of collagen type I, collagen type 4, laminin, perlecan and versican (Malgouries et al., 2008; Messenger et al., 1991). 3D co-culture

systems would be better than simple 2D co-culture systems as they would closely mimic the cell-cell interactions that takes place both between DP cells themselves and between DP and BC in human hair follicles.

Several 3D co-culture systems have been developed which combine human DP cells and KC. Havlickova et al., (2009) used human DP and ORS cells to develop “folliculoid microspheres” as an *in vitro* assay to test the effect of hair growth inhibitors and stimulators. Lindner et al., (2011) also used human DP, ORS cells and melanocytes to form “microfollicle” that produced hair shafts. This method would be used to produce new hair follicles *in vitro* before transplanting it into patients. Furthermore, Kalabusheva et al., (2017) developed an *in vitro* 3D co-culture model to study cell-cell interactions where human DP cells and skin KC were mixed in a hanging drop which they called mixed aggregates. The DP cells and KC self-organised with DP forming spheroids spontaneously with KC forming trabeculae around the spheres. DP-KC mixed aggregates expressed P-cadherin, LEF1 and EpCAM; however, KC did not express these markers when mixed with lung fibroblasts (LF) showing DP-specific induction of these markers. They also showed mixed aggregates induced expression of K75 suggesting skin KC were directed towards follicular KC lineage, but they did not compare the K75 expression between DP-KC and LF-KC. Therefore, it is unknown if KC in a 3D environment or cell contact with another fibroblast has an influence on K75 expression.

In addition, Yen et al., (2010) co-cultured rat DP cells and rat KC from footpads on poly (ethylene-co-vinyl alcohol) (EVAL) substrate where the DP cells aggregated together first and then KC attach to aggregated DP cells to form “hybrid aggregates”. The aggregates form a core of DP cell core surrounded by KC outside. They show that DP cells in aggregates induce differentiation of skin KC towards follicular KC through increased expression of K75.

Co-culture systems are useful as they are easy to produce, reproducible, can be used to test effect of various drugs, genes or growth factors and are cheaper compared to using animals.

However, to my knowledge, there has not been any *in vitro* 3D models that have used FDP cells along with ODP cells to directly compare their hair-inducing abilities.

3.2. Specific aims in Chapter 3

Organ-cultured human hair follicles have been used to study anagen-catagen transition and the effect of various genes and drugs to promote or inhibit hair growth; however, there are not any *in vitro* models currently that can be used to study catagen-telogen or telogen-anagen phases of the human hair cycle. When hair follicles transition from telogen into anagen, the DP signals to the BC instructing new hair growth which is similar to the mesenchymal-epithelial signalling required to induce new hair follicle during embryogenesis. An *in vitro* model which could recapitulate the basic mesenchymal-epithelial signalling between DP cells and BC that takes place during telogen-anagen transition could be helpful in trying to understand the roles of different genes for this transition. Thus, the first aim of this chapter is to develop an *in vitro* miniaturisation model that allows mesenchymal-epithelial interactions to take place between DP cells and BC to mimic telogen-anagen transition. Given what we know about the pathogenesis of AGA, I hypothesise that the ability of FDP to initiate anagen is impaired. By using FDP cells, I aim to determine whether miniaturisation can be modelled *in vitro*.

The second aim of this chapter is to elucidate the differences between frontal and occipital follicular mesenchyme to determine the protective nature of occipital DP. To do this, I carried out transcriptomic profiling of intact DP and DS from frontal and occipital hair follicles. After identifying signature genes of hair follicle mesenchyme from frontal and occipital hair follicles, I decided to focus on the role of TRPS1 in AGA.

3.3. Materials and Methods

3.3.1. Collection of human tissue

Hair follicles from the frontal and occipital scalp were collected from patients undergoing hair transplantation surgery at the Farjo Hair Institute at Manchester, U.K. Consent was taken from patients using IC-REC approved consent forms. Fifteen frontal and fifteen occipital hair follicles were extracted from each patient. If follicles were to be used for isolation of DP and DS cells, they were placed in William's E medium (Thermo Fisher Scientific) supplemented with 2 mM L-Glutamine (Thermo Fisher Scientific), 10 ng/mL hydrocortisone (Sigma-Aldrich), 10 µg/mL insulin (Sigma-Aldrich) and 100 U/mL and 100 µg/mL of penicillin-streptomycin (Sigma-Aldrich) during transportation. If follicles were to be used to extract RNA, they were placed in RNALater (Thermo Fisher Scientific) during transportation. All hair follicles were kept at 4°C until microdissection.

Breast skin was collected from patients undergoing mastectomies at Charring Cross Hospital, using NHS REC approved consent forms. Tissue was kept in saline at 4°C until microdissection.

3.3.2. Isolation and culture of dermal papilla and dermal sheath cells

Hair follicles were microdissected to obtain DP and DS cells using previously published methods (Topouzi *et al.*, 2017). First, the hair follicles were transferred into wash media consisting of 2% antibiotic-antimycotic (ABAM, Thermo Fisher Scientific) in Dulbecco's minimal essential medium (DMEM) with Glutamax (Thermo Fisher Scientific). After 30 minutes, they were transferred into 1% ABAM/DMEM media. The end bulbs were cut using spring scissors and placed into drops of media on a lid of a 10 cm dish. The DP was inverted out of the end bulbs using 27G needles, placed into a larger drop and this process was

repeated with the rest of the end bulbs. The DP was separated from the DS. For isolation of cells, the DP and DS were transferred into separate 35 mm dishes with 20% foetal bovine serum (FBS, Thermo Fisher Scientific), 1% ABAM in DMEM. The DP and DS were stuck onto the bottom of the dish by scratching them using needles. The dishes were placed in an incubator for 10 days at 37°C and 5% CO_2. After 10 days, media was changed with 20% FBS/ 1% ABAM/ DMEM media every 2-3 days and passaged when confluent.

3.3.3. Isolation and culture of papillary and reticular fibroblasts

To isolate papillary and reticular fibroblasts from scalp skin, the skin was cut close to the epidermis and separated into two parts. The top part close to the epidermis was used to isolate papillary fibroblasts (PFI) and the rest was used to isolate reticular fibroblasts (RFI). After separation, the papillary and reticular dermis were placed in separate 35mm dishes containing 1% ABAM/DMEM media. The papillary and reticular dermis were chopped up using spring scissors and spread onto the bottom of an empty 35 mm dish. The dermis was left to dry for 5 minutes, then 2.5 mL of 20% FBS/ 1% ABAM/ DMEM media was added onto the dish gently. The dishes were incubated for 10 days at 37°C and 5% CO_2. After 10 days, media was changed with 20% FBS/ 1% ABAM/ DMEM media every 2-3 days and passaged when confluent.

3.3.4. Isolation and culture of human bulge cells

Human BC were isolated from hair follicles from the occipital scalp using previously published method (Topouzi *et al.*, 2017). Briefly, the hair follicles were placed in 5 U/mL dispase (Sigma-Aldrich) for 10 minutes at 37°C. After 10 minutes, the hair shaft was gently pulled out using forceps and placed in 0.025% trypsin-EDTA (Thermo Fisher Scientific) for 10 minutes at 37°C. The hair shafts were vortexed and filtered through 70 µM cell strainer (Starlab). The cells were centrifuged at 200 rcf for 5 minutes. The supernatant was removed, and cells were

resuspended in keratinocyte serum-free medium (KSFM, Thermo Fisher Scientific) with 10 μM Y-27632 dihydrochloride (ROCK inhibitor, Bio-Techne). Cells were seeded in one well of a 6 well plate coated with 10 μg/mL of fibronectin (Corning) and incubated for 15 minutes at 37°C and 5% CO_2. Cells that did not attach after 15 minutes were transferred onto another well of a 6 well plate. Media was changed every 2-3 days with KSFM + 10 μM Y-27632 and passaged when confluent.

3.3.5. Isolation and culture of skin keratinocytes

KC were isolated from skin from occipital scalp and breast. For the occipital scalp skin, the hair shafts were removed from the skin strip using forceps. The skin strip was cut into smaller pieces using a scalpel and transferred into 15 mL falcon tube containing 5 U/mL dispase overnight at 4°C. The next day, epidermis was separated from the dermis, transferred into 0.025% trypsin-EDTA at 37°C and shaken every 5 minutes for 30 minutes. After 30 minutes, defined trypsin inhibitor (Thermo Fisher Scientific) was added, and cells were filtered through 70 μM cell strainer. Cells were centrifuged at 300 rcf for 10 minutes. For feeder-free culture, cells were resuspended in Epilife supplemented with Epilife Defined Growth Supplement (EDGS, Thermo Fisher Scientific) and seeded onto flasks coated with Coating Matrix (Thermo Fisher Scientific). For feeder-dependent culture, cells were resuspended in FAD media (components listed in table 3.1) and seeded onto feeders of mouse embryonic fibroblasts (MEFs) which were already treated with 10 μg/mL of Mitomycin C (Sigma-Aldrich) for 2 hours. The flasks were incubated at 37°C and 5% CO_2. Media was changed every 2-3 days and passaged when confluent.

Table 3.1: FAD media components.

Reagent	Stock concentration	Final concentration	Supplier
DMEM	-	45%	Thermo Fisher Scientific
DMEM/F12	-	45%	Thermo Fisher Scientific
FBS	-	10%	Thermo Fisher Scientific
Penicillin-Streptomycin	10000 U/ 10 mg/mL	100 U/ 0.1 mg/mL	Sigma-Aldrich
Transferrin	25 mg/mL	5 µg/mL	Sigma-Aldrich
Hydrocortisone	2 mg/mL	0.4 µg/mL	Sigma-Aldrich
Cholera toxin	10^{-6} M	10^{-10} M	Sigma-Aldrich
EGF	10 µg/mL	10 ng/mL	Sigma-Aldrich
Insulin	10 mg/mL	5 µg/mL	Sigma-Aldrich
Liothyronine	2 µM	2 nM	Sigma-Aldrich
Adenine	37 mM	0.18 mM	Sigma-Aldrich

3.3.6. Transcriptomic analysis of intact dermal papilla and dermal sheath

For transcriptomic analysis, 5 frontal and 5 occipital follicles from 4 patients were used. End bulbs of hair follicles placed in RNALater were transferred into drops of media on a lid of a 10 cm dish. Intact DP and DS were microdissected using the protocol described in section 3.3.2. After microdissection, DP and DS were placed in separate 2 mL Eppendorf tubes with 350 µL RLT lysis buffer (QIAGEN) containing 1% 2-ß-mercaptoethanol (Sigma-Aldrich). Intact DP and DS were snap frozen on dry ice and placed in -80°C freezer until RNA extraction. To extract RNA, DP and DS were homogenised using T10 basic ULTRA-TURRAX (IKA) for 15 seconds on ice. RNA from DP and DS were extracted using RNeasy Plus Micro kit (QIAGEN) following the company's protocol. RNA from DP and DS were sent to UK Bioinformatics Ltd at Kings College London. GeneChip WT Pico Reagent kit was used to convert mRNA into cDNA using reverse transcriptase. In vitro transcription reaction was used to amplify cDNA into cRNA. cRNA was then amplified into single strand-cDNA which was fragmented and labelled with biotin. Finally, the labelled cDNA was placed into GeneChip Human Genome U133 Plus 2.0

array (Affymetrix) from which the signals were recorded using a confocal laser scanner. The microarray data was analysed using GeneSpring GX 14.9 (Agilent Technologies). Entities were filtered based on signal intensity with values between 20-100%, p-value ≤ 0.05 and fold change of ≥ 1.5 or ≤ -1.5 was used as the threshold value. A one-way ANOVA test was used as the statistical test to identify significantly upregulated or downregulated genes. For biological processes analysis of the gene lists, genes were uploaded onto www.pantherdb.org and compared against the entire Homo sapiens genes in the database. Fisher's Exact test was used as the statistical test to identify biological processes which were statistically overrepresented in the gene lists. A p-value of <0.05 was considered to be statistically significant. To identify pathways regulated by the genes in different cell types, Ingenuity Pathway Analysis software (IPA, QIAGEN) was used.

3.3.7. Establishment of frontal and occipital dermal papilla cells as spheres

To establish spheres, FDP and ODP cells were washed with 1X PBS once and 0.025% trypsin-EDTA was added for 5 mins at 37°C. 10% FBS-DMEM media was added, and cells were centrifuged at 1400 rpm for 4 minutes. Cells were resuspended in 10% FBS-DMEM media. 300,000 cells were transferred into a 15 mL falcon tube and centrifuged. Cells were resuspended in 10 mL 10% FBS-DMEM media and 100 µL of cells were transferred into one well of a 96-well ultra low attachment microplates (Corning) and incubated at 37°C and 5% CO_2 for 2 days. Spheres were placed in 350 µL RLT lysis buffer, snap frozen on dry ice and kept in -80°C freezer until RNA extraction. Some spheres were embedded in OCT, snap frozen on dry ice, and kept in -80°C freezer until sectioning.

3.3.8. *In vitro* inductivity model

For the *in vitro* inductivity model, 3000 ODP, PFI or RFI cells were combined with 3000 KC per well to create double spheres. Mixture of cells were combined in 10% FBS-DMEM and

FAD media in 1:1 ratio with 10 μM Y-27632. 100 μL of ODP/ PFI/RFI and BC were plated in 96-well ultra low attachment microplates and incubated at 37°C and 5% CO_2 for 3 days. For 3D-KC, 3000 cells per well were seeded in 10% FBS-DMEM and FAD media in 1:1 ratio with 10 μM Y-27632. After 3 days, spheres were placed in 350 μL RLT lysis buffer, snap frozen on dry ice and kept in -80°C freezer until RNA extraction. Some spheres were embedded in OCT, snap frozen on dry ice, and kept in -80°C freezer until sectioning.

3.3.9. Collection of 3D dermal papilla conditioned media

For conditioned media, 8000 ODP cells suspended in 10% FBS-DMEM were established as spheroids in 96-well ultra low attachment microplates and cultured as spheroids for 3 days. For unconditioned control media, 10% FBS-DMEM in a flask without any cells were incubated for 3 days. The control and conditioned media were transferred into a 15 mL falcon tube and centrifuged at 1400 rpm for 4 minutes. The control and conditioned media were then filtered through 0.22 μm pore sized filter, aliquoted and stored at -20 °C. For controls, ODP or PFI cells and KC were mixed with control media and FAD with 10 μM Y-27632 in 1:1 ratio. For the conditioned media, PFI cells and KC were mixed in conditioned media and FAD with 10 μM Y-27632 in 1:1 ratio and cultured for 3 days.

3.3.10. *In vitro* miniaturisation model

For the *in vitro* miniaturisation model, 3000 FDP or ODP cells were mixed with 1000 BC per well to create double spheres. FDP or ODP cells and BC were combined in 10% FBS-DMEM and KSFM media in 1:1 ratio with 10 μM Y-27632. 100 μL of FDP or ODP and BC were plated in 96-well ultra low attachment microplates and incubated for 3 or 5 days at 37°C and 5% CO_2. After 3 and 5 days, spheres were placed in 350 μL RLT lysis buffer, snap frozen on dry ice and kept in -80°C freezer until RNA extraction. Some spheres were embedded in OCT, snap frozen on dry ice, and kept in -80°C freezer until sectioning.

3.3.11. siRNA transfection

To knockdown expression of TRPS1, 15,000 ODP cells per well were seeded onto a 24 well plate to ensure 70-80% confluency the next day. 24 hours later, cells were transfected with siCONTROL (Silencer™ Select Negative Control No. 1 siRNA, Thermo Fisher Scientific) or siTRPS1 (s531872, Thermo Fisher Scientific) following the manufacturer's instructions. For the *in vitro* miniaturisation model, ODP cells were used 24 hours after transfection and mixed with BC to make double spheres. For other experiments, ODP cells were collected 72 hours after transfection for RNA extraction.

3.3.12. Compounds

CI-4AS-1 (Bio-Techne) and bicalutamide (Sigma-Aldrich) were reconstituted in DMSO. 15,000 cells per well were seeded onto a 24 well plate. 24 hours later, the media was changed to 10% charcoal stripped FBS (CSFBS)-DMEM (Thermo Fisher Scientific). 24 hours after the media change, 100 μM CI-4AS-1 and 1 μM bicalutamide was diluted in 10% CSFBS-DMEM and added to the cells. For control, cells were treated with DMSO in 10% CSFBS-DMEM. Cells were collected for RNA extraction 24 hours later.

3.3.13. RNA extraction, reverse transcription, and quantitative RT-PCR

For double spheres, they were collected in a 15 mL falcon tube and left to settle at the bottom of the tube. Most of the media was removed except for 1 mL of media which was used to resuspend the spheres and transfer into a 1.5 mL Eppendorf tubes. The spheres were centrifuged at 300 rcf for 1 minute. The remaining media was removed, and 1 mL of PBS was added. Spheres were centrifuged at 300 rcf for 1 minute and PBS was removed. 350 μL of RLT lysis buffer was added to the spheres, vortexed for 1 minute at full speed and placed on ice or in -80°C freezer until RNA extraction was carried out. For cells, media was removed and washed with PBS once. Then, 350 μL of RLT lysis buffer was added and cell scraper was

used to scrape the cells off the plate. The lysed cells were transferred into a 1.5 mL Eppendorf tube, snap frozen on dry ice, and placed in -80°C freezer until RNA extraction was carried out. RNA was extracted from spheres and cells using RNeasy Plus Micro kit following the manufacturer's instructions. Reverse transcription was carried out using SuperScript IV Reverse Transcriptase (Thermo Fisher Scientific) according to the manufacturer's protocol. For the quantitative RT-PCR, PowerUP™ SYBR Green Master Mix (2X, Thermo Fisher Scientific) was used. RT-PCRs were run on an ABI 7500 Fast Real-Time PCR or QuantStudio™ 3 Real-Time PCR System with cycles as follows: 2 minutes at 50°C and 2 minutes at 95°C followed by 40 cycles of 15 seconds at 95°C and 1 minute at 60°C. The primers used in this chapter are listed in table 3.2. Primers were designed using sequences on the UCSC genome browser and human GRCh38/hg38 assembly was used. The Ct values for each sample was normalised against the housekeeping gene, GAPDH, and fold changes were calculated using the delta-delta CT algorithm. An unpaired t-test or one-way ANOVA with multiple comparison's test was used to determine whether the differences in gene expression between samples were significant with p-value of <0.05 regarded to be statistically significant.

Table 3.2: Primer sequences used for quantitative RT-PCR.

Gene	Sequence (5' to 3')	Product size
GAPDH	F- CGGGAAGCTTGTCATCAATGG R- ATGACGAACATGGGGGCATC	207
KRT75	F- AAGGTGAGGTTCTTGGAGCAGC R- CCTCTCGGTGGTGATGCTTT	159
KRT15	F- AGATCGCTACTTACCGCAGCC R- CCTGTCCATCCACTGACTCTTC	138
COCH	F- AGAGGCTTGGACATCAGGAAAG R- TGCCAGTTTTCTTCTCGGGT	367
BLCAP	F- GATTGCAGAGTGACCAGCAC R- GGCCAGGAGAAAGTCTCGTT	211

TRIM2	F- TAGTCACCAGGTTTGGTAGCCG R- GAGTGGGTCAGCAGATGTGT	317
FNDC5	F- TCGTGGTCCTGTTCATGTGG R- TACCAGAGCATGAGGCACAG	211
FBXW11	F- CACCACAATGAGGCTGTATTGC R- AGTGATGTCGGTCGCAGAAG	111
HNRNPM	F- GTGGAGCTCTTAATGGACGCT R- CATACCCATCCCACCAGTCG	207
ARF4	F- GCTGCAGAAAATGCTTCTGGT R- GTTGCACAAGTGGCTTGAAC	165
RSPO4	F- GAATTTGGGGGTCACTTGAGG R- GTCACAGCGAAGCACAGATG	271
TRPS1	F- GCTAGGGCAGAAGTATGTCAAG R- GAGGAACCTGAGGCACAAAAAG	326
CXXC5	F- TCCACAGAGATGCTGAAGCG R- GCAGCGGAAGGCTTCTTTTT	416
LAMB2	F- TGAGCTCTGCAGGTGAAAGG R- CCTCATCCCGCAGTTGTTCT	255
ZHX1	F- TTTGGGGACACCCGTTATGC R- TCTGACCTGCTCATAGCCCA	324
EGR1	F- CCCCTTCCCCAATTACTATTCCC R- CGAAATCCATGGCACAGACAC	243

3.3.14. Immunofluorescence

For immunofluorescence staining, double spheres were placed in Optimal Cutting Temperature (OCT, Agar Scientific) compound and frozen on dry ice. Double spheres were sectioned at 7 µM on a cryostat. Sections were fixed with 4% PFA for 10 minutes or in 100% ice-cold methanol for 7 minutes. Slides were washed with PBS 3 times for 3 minutes each. Then, the sections were permeabilised and blocked for 40 minutes in blocking solution made up of 10% NGS in 0.3% triton X-100 in PBS. Primary antibodies (listed in table 3.3) were made up in blocking solution and sections were incubated in primary antibodies overnight at 4°C. The next day, slides were washed with 0.1% triton X-100 in PBS 3 times for 3 minutes each.

Secondary antibodies (listed in table 3.3) were diluted in PBS and slides were incubated in secondary antibodies for 1 hour at room temperature. Then, the slides were washed with 0.1% triton X-100 in PBS 3 times for 3 minutes each. Mounting media with DAPI (Vector Laboratories) was added to sections and coverslips were sealed onto samples using nail varnish.

Table 3.3: List of primary and secondary antibodies used for immunofluorescence staining.

Name	Host species	Supplier	Catalogue number	Dilution
Keratin 14	Chicken	Biolegend	SIG-3476	1:1000
Collagen 4	Mouse	Abcam	ab6311	1:200
Keratin 75	Guinea pig	Progen	GP-K6hf	1:200
Keratin 74	Guinea pig	Progen	GP-K6irs4	1:200
Keratin 85	Guinea pig	Progen	GP-hHb5	1:200
Keratin 17	Mouse	Santa Crux Biotechnology	sc-101461	1:400
TRPS1	Rabbit	antibodies.com	A12162	1:200
488 anti-mouse	Goat	Thermo Fisher Scientific	A11001	1:200
568 anti-rabbit	Goat	Thermo Fisher Scientific	A11036	1:200
647 anti-chicken	Goat	Thermo Fisher Scientific	A21450	1:1000
546 anti-guinea pig	Goat	Thermo Fisher Scientific	A11074	1:200

3.3.15. Bisulfite sequencing

To analyse the methylation status of ELOVL2, genomic DNA (gDNA) was isolated from ODP cells transfected with siCONTROL or siTRPS1 3 days after transfection. gDNA was extracted using Quick-DNA Microprep Plus kit (Zymo) following the manufacturer's instructions. 40 ng

of gDNA was used for bisulfite conversion using EZ DNA Methylation-Gold kit (Zymo) following the manufacturer's instructions. Bisulfite PCR was performed using ELOVL2 primers from Bekaert et al., (2015). Primer sequences are in table 3.4. 2 µL of bisulfite converted DNA was used with 0.8 µM of forward and reverse ELOVL2 primers. The following thermocyclic conditions were used for bisulfite PCR: 95°C for 15 minutes, 40 cycles of 95°C for 30 seconds, 60°C for 30 seconds and 72°C for 30 seconds and a final hold stage of 72°C for 6 minutes. PCR products were ligated into TOPO 4 vector (Thermo Fisher Scientific) for 10 minutes at room temperature. The ligated vectors were transformed into TOP10 cells by incubating for 10 minutes on ice followed by a heat shock at 42°C for 30 seconds. SOC medium was added to the TOP10 cells/vector mix and incubated at 37°C for 1 hour with shaking at 200 rpm. After 1 hour, TOP10 cells were spread onto LB-agar plates containing 50 µg/mL ampicillin (Thermo Fisher Scientific) and 40 µg/mL X-gal (Promega) and incubated at 37°C overnight. The next day, 10 individual white colonies were picked and transferred into LB broth containing 50 µg/mL ampicillin. The picked colonies were shaken at 200 rpm at 37 °C overnight. The following day, 150 µL of broth containing the sample were sent to Source Bioscience to be sequenced using the Colony PCR service. Sequences were analysed using Codon Code Aligner V.9.0.2.

Table 3.4: Primer sequences and the sequence to analyse for ELOVL2.

Primer	**Primer sequence**
ELOVL2-for	AGGGGYGTAGGGTAAGTGAG
ELOVL2-rev	AAACCCAACTATAAACAAAACCAA
Sequence to analyse	RTAAACRTTAAACCRCCRCRCRAAACCRACRCCRACTAAACCTA

3.4. Results

3.4.1. Dermal papilla cells reprogramme skin keratinocytes towards a follicular fate

To first establish whether 3D *in vitro* co-cultures can be a useful alternative to the test hair-inducing ability of DP, a mixed aggregate method by (Wen *et al.*, 2021) was used with skin keratinocytes and DP cells. Cells were mixed in ultra low-attachment 96 well plates instead of hanging drops (Figure 3.1A). Skin KC cultured feeder-free or on feeder-dependent MEFs were mixed with DP cells from the occipital scalp and cultured for 3 days. The KC and DP cells spontaneously self-organised to form a core sphere of DP cells with a layer of KC surrounding the DP sphere (Figure 3.1B). With feeder-free KC, the KC did not form a complete layer outside the DP cells as can be seen through staining of collagen 4 (COL4) for DP cells and keratin 14 (K14) for KC (Figure 3.1C). On the other hand, the feeder-dependent KC formed a complete layer outside the DP spheres which will be referred to as “double spheres” from here on in (Figure 3.1D). KC cultured on feeders were chosen for the subsequent experiments.

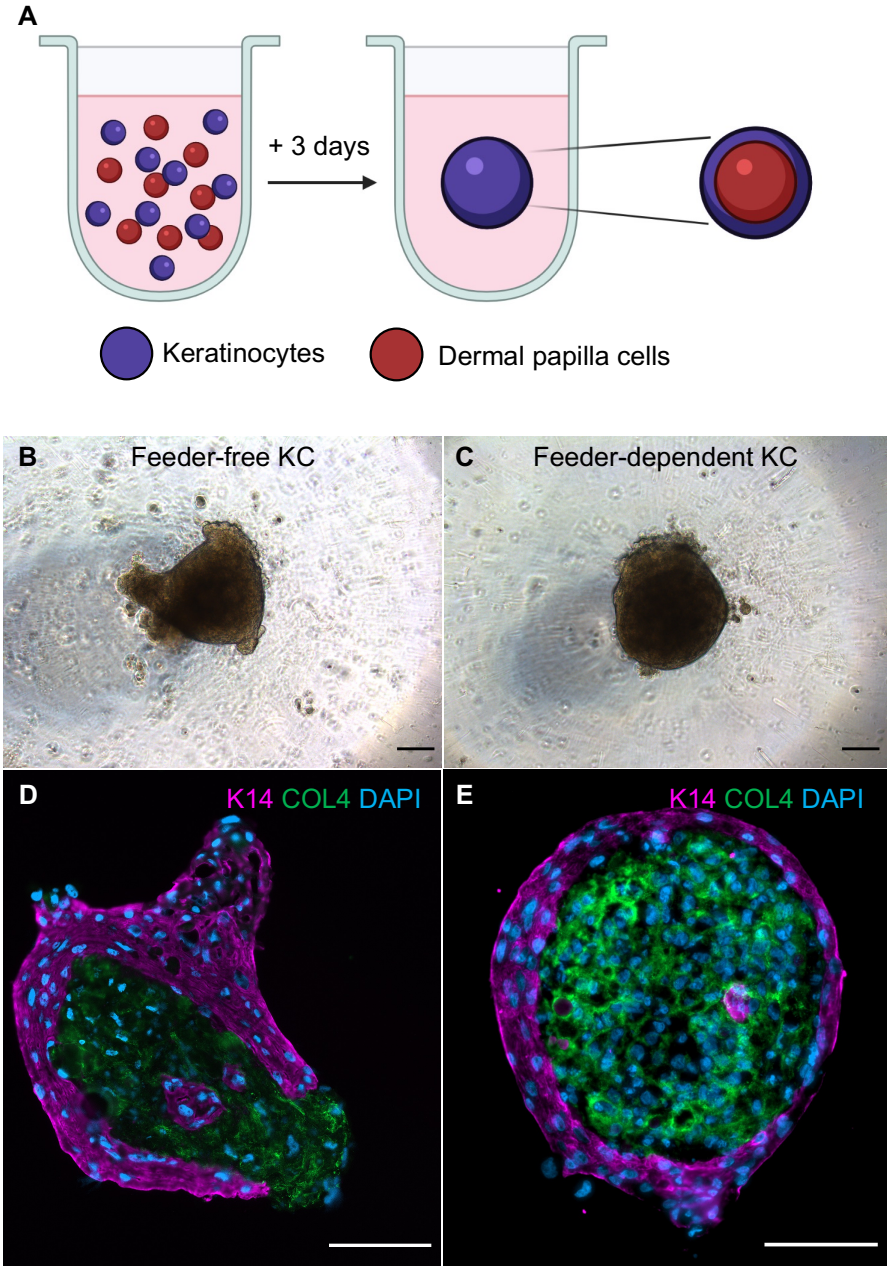


Figure 3.1: DP-KC spheres formed using KC grown under feeder-free and feeder-dependent culture conditions.

A) Schematic diagram to illustrate the process of forming double spheres with KC and DP cells. B) Brightfield images of DP-KC spheres formed with KC grown feeder-free on coating matrix and with Epilife media. C) Brightfield images of DP-KC formed using KC grown on feeders and with FAD media. Immunofluorescence staining of DP-KC using feeder-free KC (D) and feeder-dependent KC showing DP sphere in the middle (COL4, green) and layer of KC outside surrounding the DP sphere (K14, magenta). (Brightfield images taken at x10 magnification. B and C- scale bars = 0.1 cm, D and E scale bars = 100 μm)

As mentioned in section 3.1.2, DP spheres can direct reprogramming of skin KC into follicular KC. To determine whether DP spheres in double spheres can do this, immunofluorescence staining was used to detect expression of follicular keratins. The expression of hair keratins such as keratin 74 (K74), keratin 85 (K85), keratin 75 (K75) and keratin 17 (K17) were present in double spheres (Figure 3.2A). Also, RT-PCR of double spheres showed significantly higher expression of K75 in DP-KC double spheres compared to KC alone suggesting directed reprogramming of skin KC into follicular KC by DP spheres (Figure 3.2B).

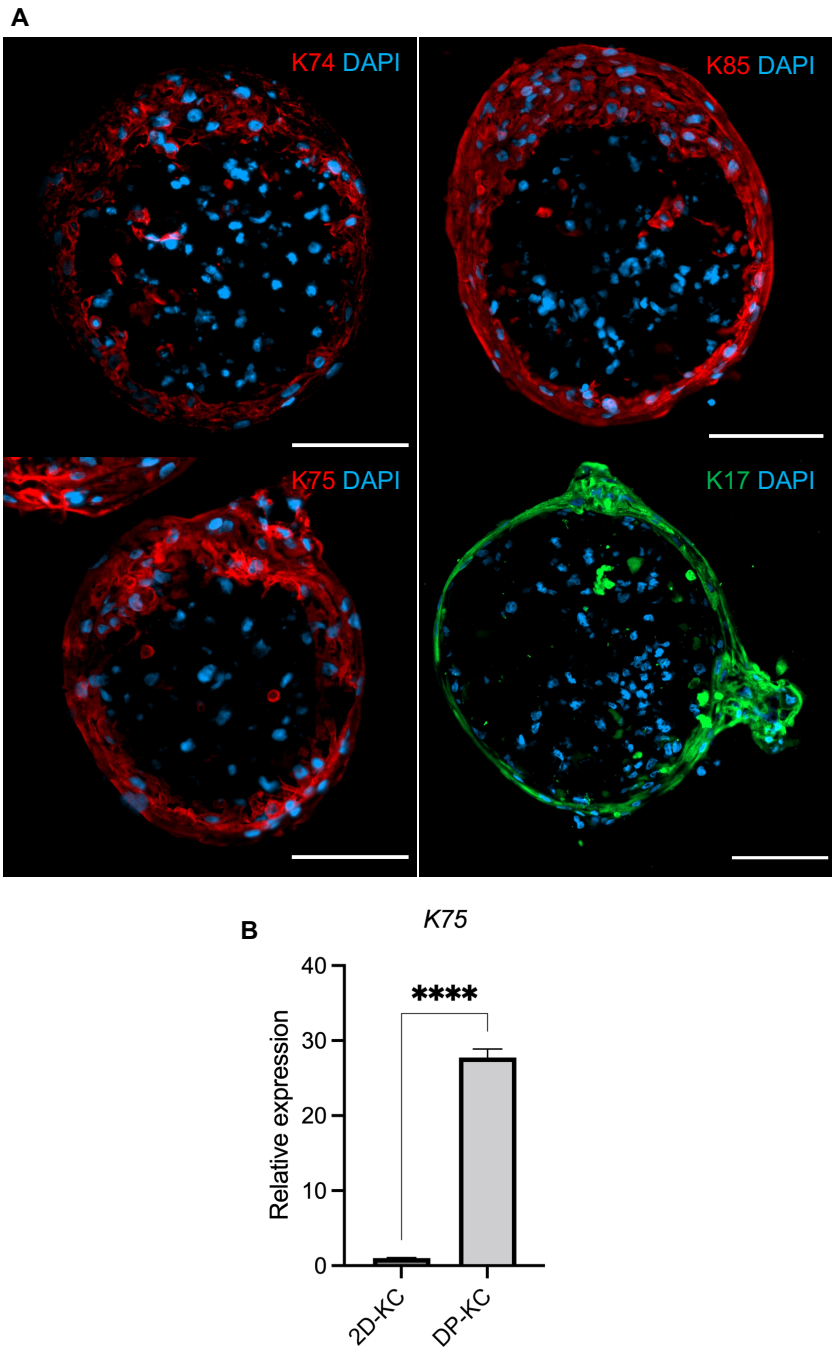


Figure 3.2: DP reprogrammes skin KC into follicular KC.

A) DP-KC spheres express follicular keratins K74 (red), K85 (red), K75 (red) and K17 (green). B) RT-PCR shows DP induces expression of K75 in KC 3 days after plating. (Data were analysed using an unpaired t-test and the error bars represent standard deviation. **** $P \leq 0.0001$, n=4. Scale bar = 100 µm)

3.4.2. Dermal papilla induces highest expression of keratin 75 compared to papillary and reticular fibroblasts

In order to verify whether K75 expression is induced specifically by DP cells, KC were co-cultured with DP, PFI or RFI as double spheres and KC were also cultured by themselves as single spheres for 3 days (Figure 3.3A). DP and PFI originate from the same progenitor during development (Driskell *et al.*, 2013), but PFI cells are not inductive. RFI cells are also present in the dermis but do not have a role in hair follicle morphogenesis. KC were cultured as single spheres to assess the effect of 3D culturing on KC. The expression of K75 was 1.16X, 1.35X and 4.01X more in DP-KC compared to PFI-KC, RFI-KC, and 3D-KC respectively. Culturing KC as 3D spheres led to induction of K75 expression suggesting that 3D environment may alter gene expression in KC causing KC to increase expression of all keratins or 3D environment by itself could reprogramme skin KC towards a follicular fate. In addition, PFI and RFI cells also increase the expression of K75, more than 3D-KC suggesting cell-cell contact also induces expression of K75 in KC. However, DP cells induced the highest expression of K75 compared to other cell types and 3D-KC. This suggests that specific contact with DP cells and/or release of specific paracrine factors by DP cells is required to reprogramme skin KC into follicular KC (Figure 3.3B).

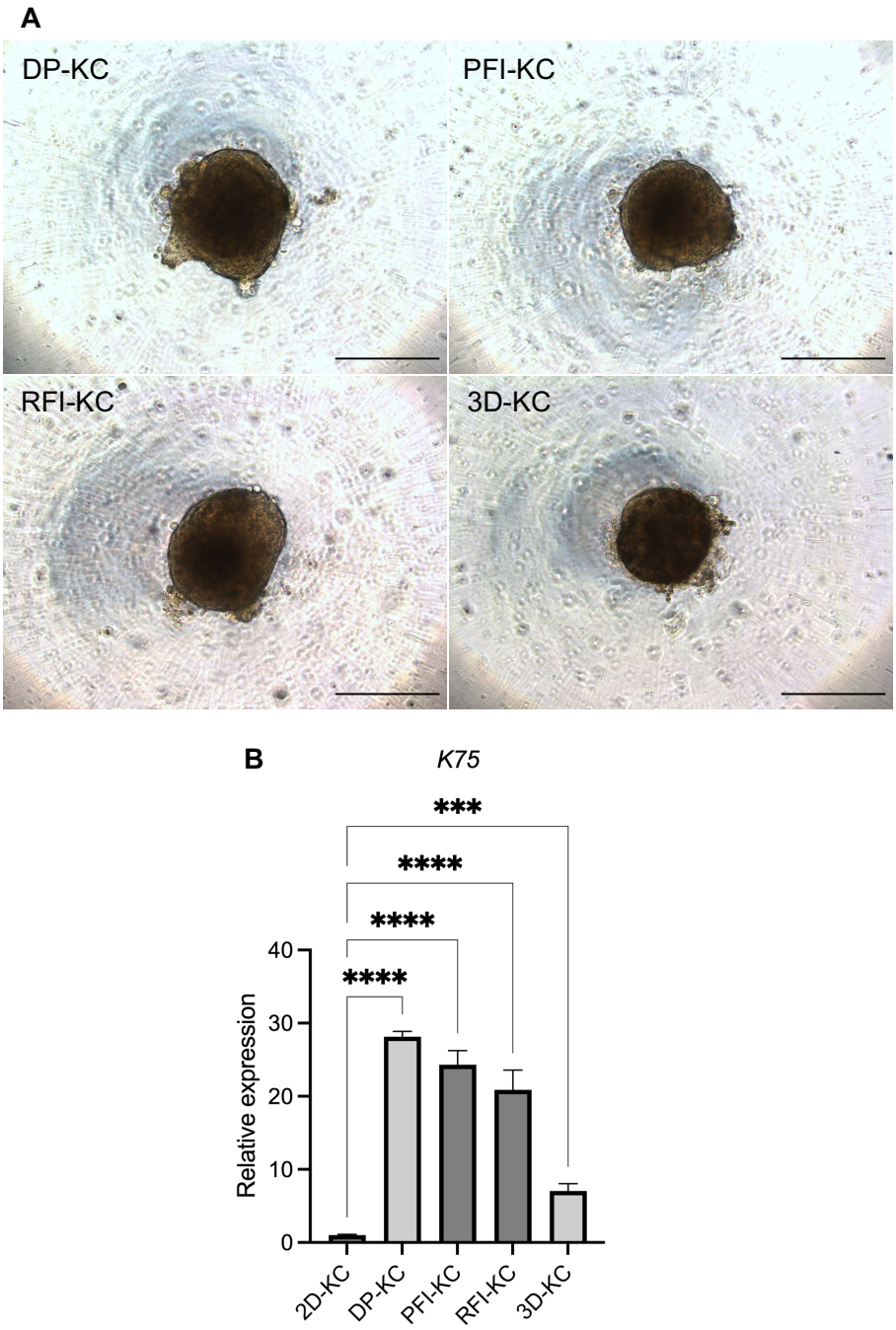


Figure 3.3: Comparison of K75 induction across different dermal fibroblast cell types.

A) Brightfield images of DP-KC, PFI-KC, RFI-KC, and 3D-KC spheres. (Scale bar = 100 μm). B) DP induces highest expression of K75 compared to PFI, RFI and with KC by itself. (Data were analysed using Ordinary one-way ANOVA with Tukey's multiple comparisons test and the error bars represent standard deviation. *** $P \leq 0.001$, **** $P \leq 0.0001$, n=4).

To determine if specific contact with DP cells or paracrine factors from the DP is more important for inductivity, DP cells were replaced with PFI cells and conditioned media (CM) from 3D cultured DP cells were added to PFI-KC double spheres (Figure 3.4A). The expression of K75 with 3D-DP CM was similar to DP-KC (Figure 3.4B). This suggests that specific cell contact with DP cells is not required for inductivity and contact with another fibroblast cell type with DP paracrine factors is enough to induce follicular fate in skin KC.

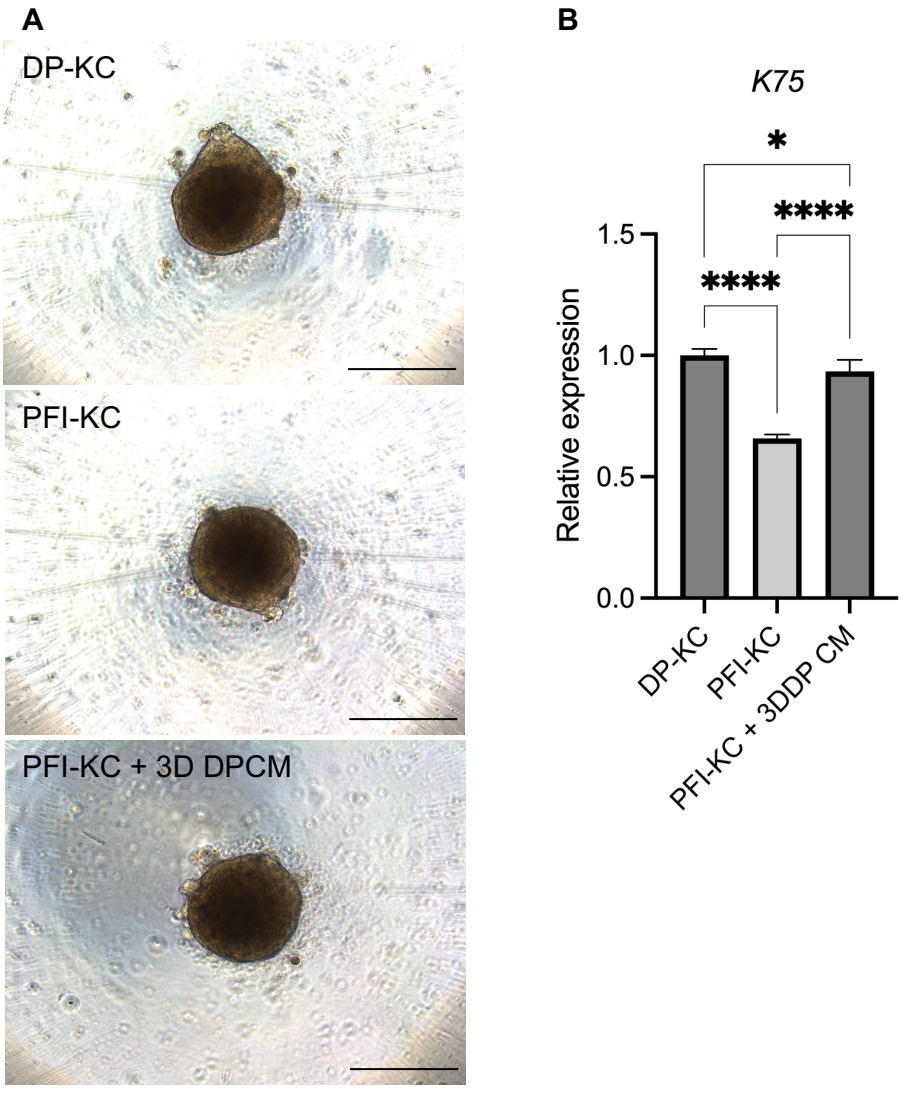


Figure 3.4: Assessment of DP cell contact and paracrine factors for inductivity.

A) Brightfield images of DP-KC, PFI-KC, PFI-KC with 3D-DP conditioned media. (Scale bar = 100 μm)

B) Conditioned media from DP spheres and cell contact with PFI together induces similar level of K75 expression to DP-KC. (Data were analysed using Ordinary one-way ANOVA with Tukey's multiple comparisons test and the error bars represent standard deviation. *P ≤ 0.05, **** P ≤ 0.0001, n=4).

3.4.3. Frontal and occipital dermal papilla cells have different hair inducing ability

The *in vitro* double sphere model shows that it can be a useful method to test the hair inducing ability of DP cells. To recapitulate mesenchymal-epithelial interactions that take place during telogen-anagen transition in miniaturised hair follicles, a similar *in vitro* organoid model was developed. In this miniaturisation model, BC grown on fibronectin with KSFM were used instead of KC (Figure 3.5A). The BC were mixed with DP cells in ultra low-adherent 96 well plates and co-cultured for 3 and 5 days (Figure 3.5B). In this model, BC and DP cells were co-cultured for extra 2 days to assess whether a longer co-culturing time increases DP-induced differentiation of BC. In miniaturised hair follicles, BC are present but there is a lack of progenitor cells suggesting FDP may not be able to effectively induce differentiation of BC. To test this, patient-matched FDP or ODP cells were mixed with BC and co-cultured for 3 and 5 days (Figure 3.5C).

Similarly to the *in vitro* double spheres model, FDP and ODP cells formed spheres in the middle and BC formed a layer outside the FDP and ODP spheres spontaneously as seen through the presence of COL4 at the core of the double spheres with K14 expression on the outside (Figure 3.5D). Keratin 15 (K15), a marker of BC, decreased significantly by 12.1X in FDP-BC and 6.4X in ODP-BC compared to 2D-BC at day 3. At day 5, K15 expression significantly decreased by 2.4X in FDP-BC and 4.6X in ODP-BC compared to 2D-BC (Figure 3.5E). This indicated that both FDP and ODP cells induced differentiation of BC in double spheres, but the differentiation of BC decreases by day 5 when the expression of K15 goes up. This could be due to longer culturing time which could increase BC proliferation. At day 3, K75 expression significantly increased by 8.6X in FDP-BC and 10.6X in ODP-BC compared to 2D-BC. At day 5, K75 expression increased by 7.7X in FDP-BC while in ODP-BC, it increased by 10.3X in ODP-BC. ODP cells induced significantly higher expression of K75

expression both at day 3 and 5 compared to FDP cells which suggests that ODP cells have higher ability to induce differentiation of BC compared to FDP cells (Figure 3.5F).

Both FDP and ODP cells induced expression of K75 in BC; however, FDP cells induced it at a lower level. As the BC were from occipital hair follicles, they may be primed to respond to signals from the DP and thus FDP cells could induce K75 expression. Using a combination of both DP and BC from miniaturised follicles may show the biggest difference in K75 induction as miniaturised DP may not be able to signal well to the BC and the BC from miniaturised follicles may not be able to respond to DP signals. By combining DP and BC from different sites (for example- ODP with occipital BC, ODP with frontal BC, FDP with occipital BC and FDP with frontal BC), we might be able to see stronger differences in K75 expression with the lowest K75 expression expected in the combination of FDP with frontal BC.

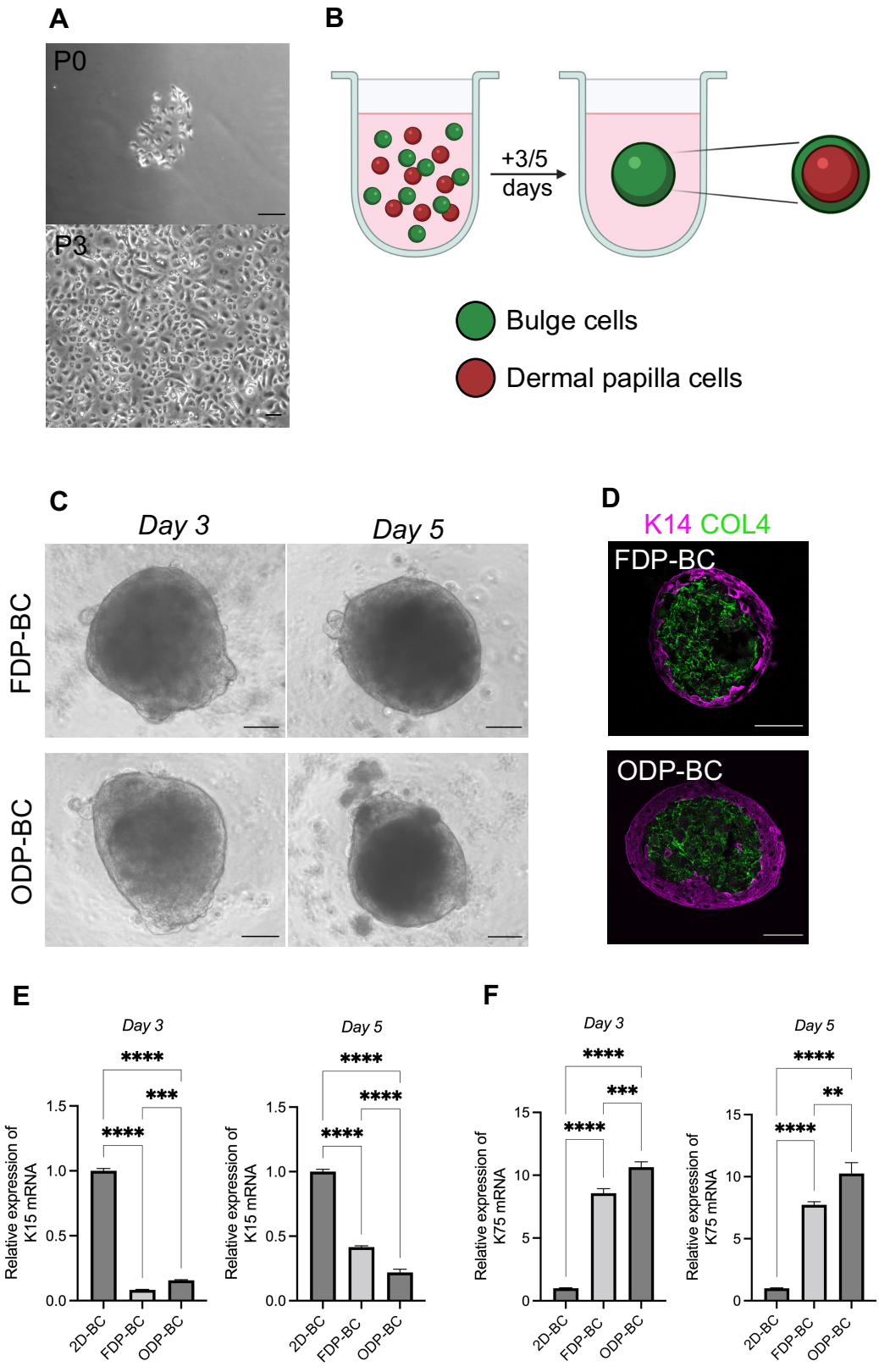


Figure 3.5: Development of an *in vitro* miniaturisation model.

A) Brightfield images of BC at P0 and P3. B) Schematic diagram of *in vitro* miniaturisation model. C) DP and BC self-aggregate with dense DP core with a layer of BC outside. Brightfield images show FDP-BC and ODP-BC spheres 3 and 5 days after plating. D) Immunofluorescence staining of K14 (magenta) and COL4 (green) in FDP-BC and ODP-BC spheres. E) Expression of K15 in FDP-BC and ODP-BC spheres decreases after 3 and 5 days of co-culture. F) Expression of K75 in FDP-BC and ODP-BC spheres increases 3 and 5 days after co-culture. (Data were analysed using Ordinary one-way ANOVA with Tukey's multiple comparisons test and error bars represent standard deviation. ** $P \leq 0.01$, *** $P \leq 0.001$, **** $P \leq 0.0001$, n=3. Scale bar = 100 μm)

3.4.4. Frontal and occipital follicular mesenchyme have inherently different gene expression

To elucidate the difference in the ability of FDP and ODP cells to induce BC differentiation, unbiased microarray profiling was performed on intact patient-matched DP and DS from the frontal and occipital scalp. The transcriptomic profiling of frontal DS (FDS) and occipital DS (ODS) was conducted too as HFDSCs replenish the DP at the start of anagen in mice; thus, defect in self-renewal or differentiation capability of FDS cells might affect the hair differentiation ability of FDP cells. The frontal hair follicles were taken from haired sites on the edge of the miniaturised area and are therefore of similar size to occipital hair follicles (Figure 3.6A). The microdissected FDP and FDS were of similar size to ODP and ODS as well (Figure 3.6B). Principal component analysis showed stronger correlation by cell type rather than location. While FDP and ODP were clustered on both the 1st and 2nd principal components, FDS and ODS were only clustered on the 1st principal component (Figure 3.6C). Analysis comparing FDP and ODP showed upregulation of 83 genes and downregulation of 68 genes in FDP compared to ODP (Figure 3.6D). Comparing FDS with ODS, there were 126 genes upregulated and 102 genes downregulated in FDS (Figure 3.6E).

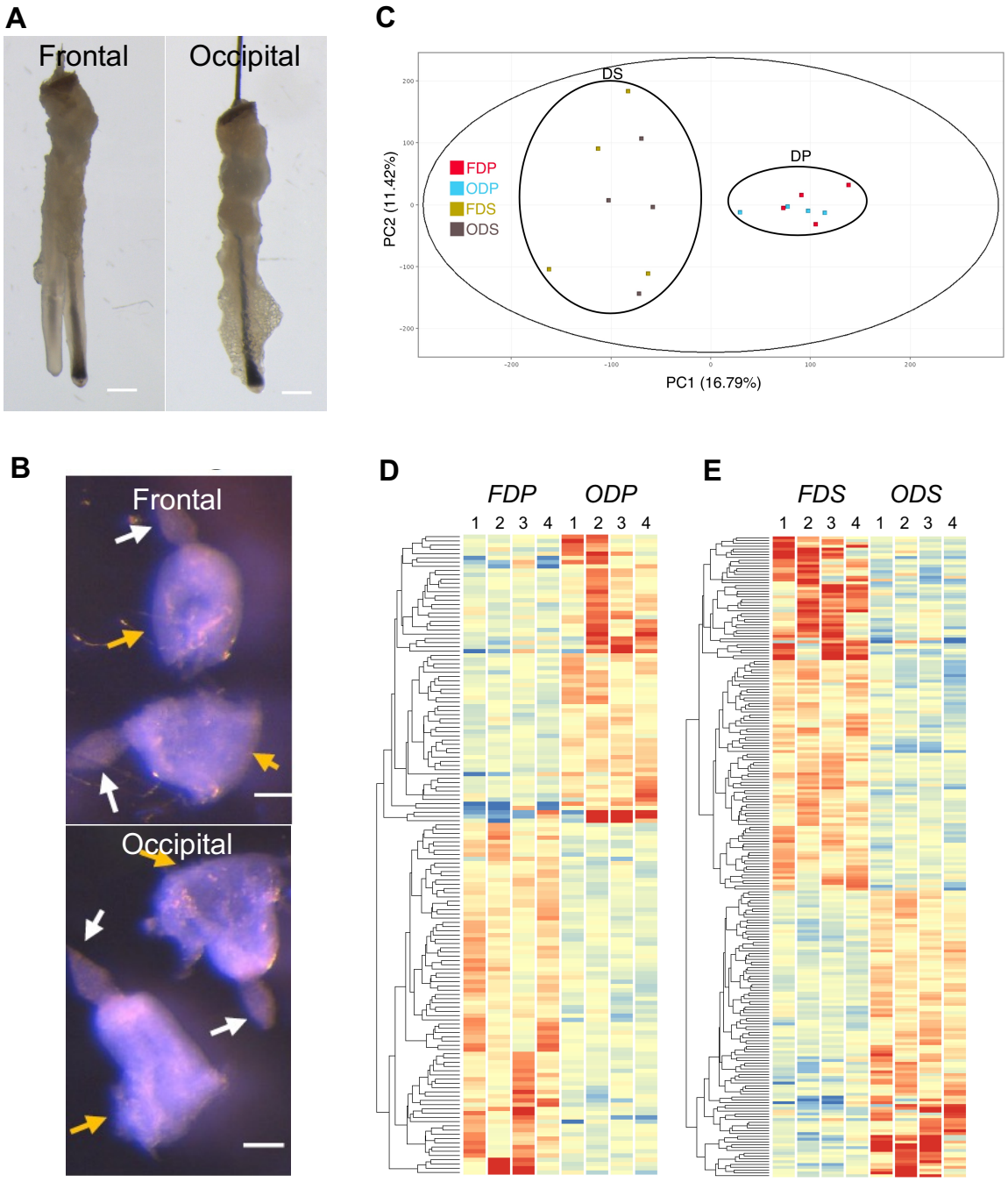


Figure 3.6: Differential gene expression in frontal and occipital follicular mesenchyme.

A) Brightfield images of frontal and occipital hair follicles. B) Brightfield images of microdissected frontal and occipital DP (white arrow) and DS (yellow arrow). C) Principal component analysis plot shows stronger correlation between cell type rather than location. D) Heatmap to show differential gene expression between frontal and occipital DP across 4 patients. E) Heatmap to show differential gene expression between frontal and occipital DS across 4 patients. (A- scale bar = 5 mm, B- scale bar = 0.1 mm).

Gene ontology analysis of these lists showed biological processes involving ribosomal assembly, biogenesis, and localisation as highly enriched in FDP along with processes involved in protein modifications (Figure 3.7A). Increased ribosomal function could indicate increased protein synthesis in FDP. This suggests that FDP cells could be undergoing proliferation which is not seen normally in the DP. In addition, there was downregulation of processes involved in intra- and post-Golgi vesicle-mediated transport in FDP suggesting disruptions in post-translational modifications and localisation of proteins in FDP (Figure 3.7B). “WNT signalling pathway” and “cell-cell signalling by wnt” are also both downregulated in FDP. This is interesting as WNT signalling is crucial for hair follicle induction in undifferentiated epidermis as discussed in section 1.3.

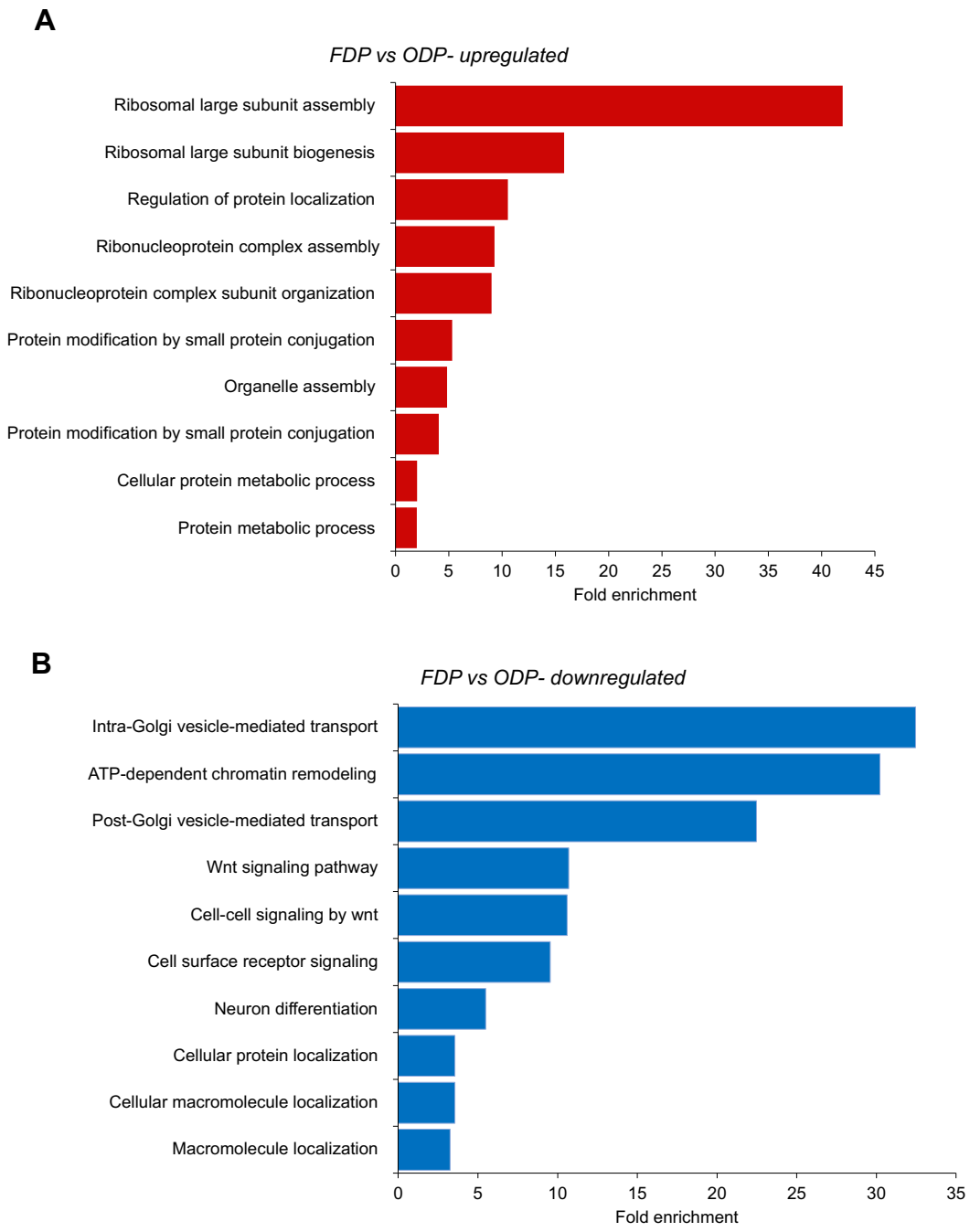


Figure 3.7: Fold enrichment of biological processes upregulated (A) and downregulated (B) in FDP compared to ODP.

Moreover, gene ontology analysis in FDS revealed similar processes to FDP such as ribosomal biogenesis and protein modifications as highly enriched showing the close relationship between the two cell types. Interestingly, processes involved in cell cycle such as mitotic G2/M transition checkpoint, DNA replication checkpoint, mitotic checkpoint and the

negative regulation of cell cycle were downregulated in FDS versus ODS. This indicates that there could be increased proliferation and cell cycling in FDS similar to FDP cells.

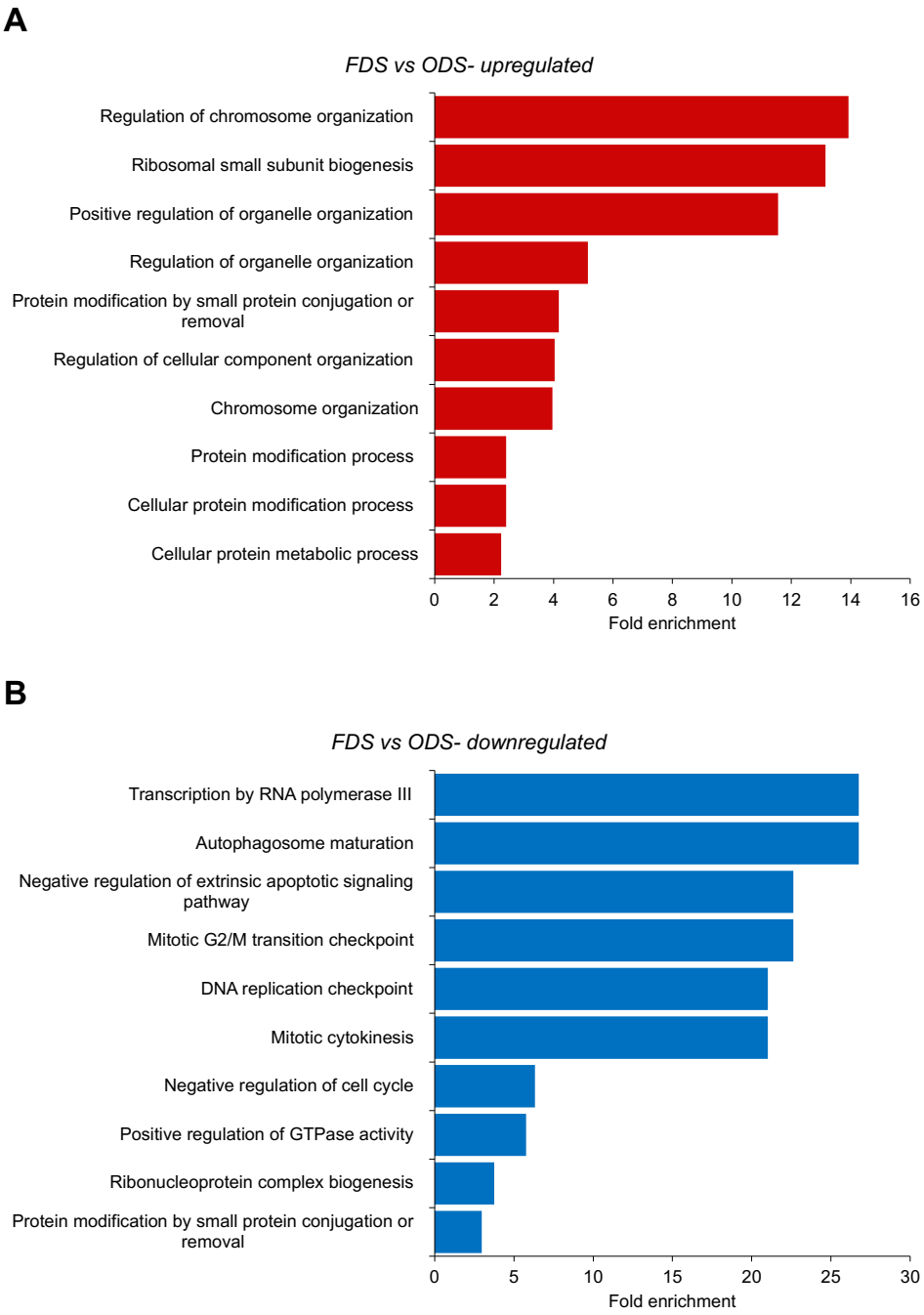


Figure 3.8: Fold enrichment of biological processes upregulated (A) and downregulated (B) in FDS compared to ODS.

3.4.5. Identification of signature genes of follicular mesenchyme

To identify genes that are uniquely upregulated in each cell type, a venn analysis was carried out which revealed signature genes for the four cell types analysed (Figure 3.9A). In FDP, 60 genes are expressed while in ODP only 16 genes were unique. In FDS, 181 genes were expressed and ODS had 84 unique signature genes. Heatmap analysis of the signature genes for each cell type showed a strong upregulation in the corresponding cell type confirming expression specifically in one of the 4 cell types analysed (Figure 3.9B).

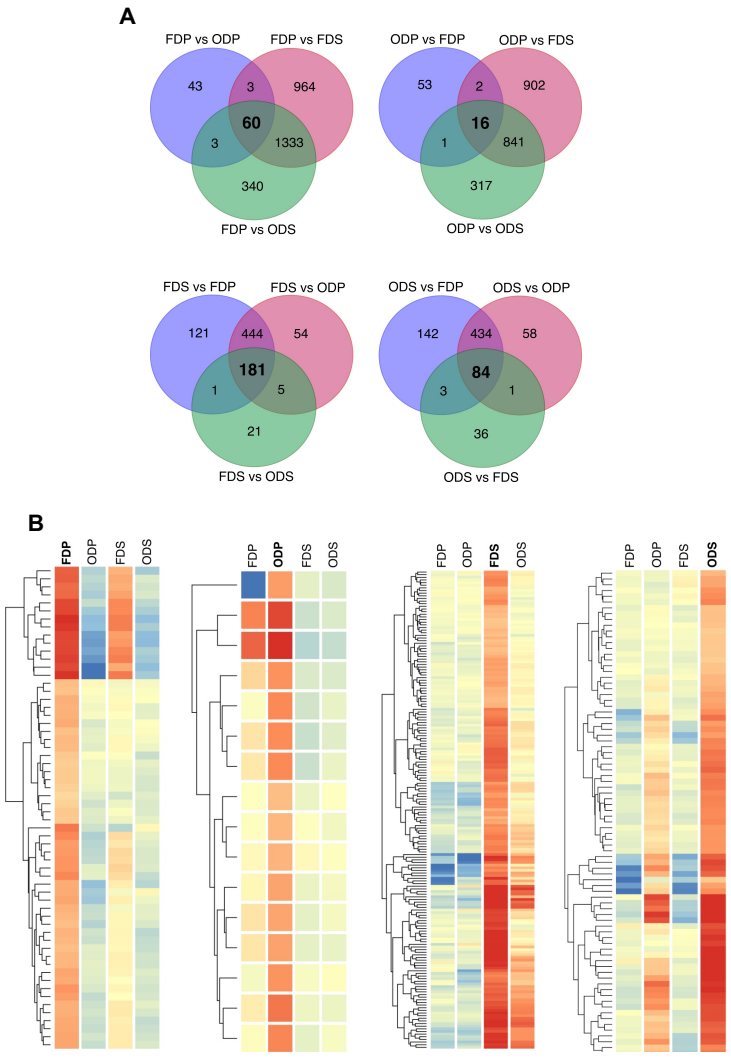


Figure 3.9: Identifying unique cell type signatures.

A) Venn diagram to identify signature genes of FDP, ODP, FDS and ODS. B) Heatmap shows the expression of signature genes of each cell type compared to other cell types.

Pathway analysis of FDP signature genes revealed upregulation of androgen signalling which is consistent with the literature research about aberrant androgen signalling in the FDP leading to miniaturisation of frontal hair follicles (Figure 3.10A). In addition, glucocorticoid (GC) receptor signalling was upregulated in FDP. GC is a steroid hormone which is released in response to stress. Human hair follicles have been shown to release GC and addition of GC to human DP cells inhibits proliferation of DP cells and also decreases expression of VEGF and HGF (Driskell *et al.*, 2013). GC has been shown to upregulate DKK-1 expression in human DP cells which is a well-known DHT-regulated catagen inducer (Choi *et al.*, 2013). This suggests that contributions from other hormones may also play a part in AGA pathogenesis.

Pathway analysis of ODP signature genes revealed upregulation of sonic hedgehog (SHH) and BMP pathways (Figure 3.10B). SHH signalling regulates expression of DP-specific genes and dysregulation of this pathway leads to decreased hair growth (Woo, Zhen and Oro, 2012). Likewise, BMP signalling has been shown to maintain DP signature genes and is required for hair induction (Woo, Zhen and Oro, 2012). Upregulation of these pathways in ODP signature genes may help to maintain ODP identity and inductivity and could help to protect against miniaturisation through maintenance of DP identity.

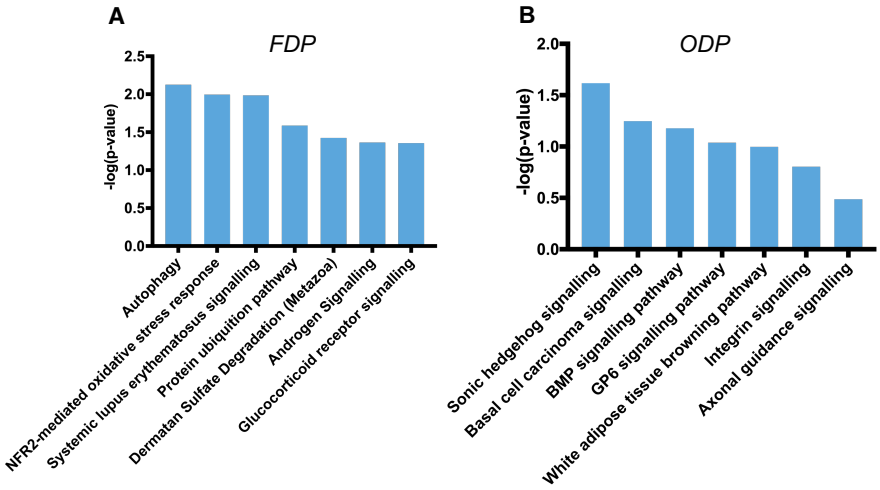


Figure 3.10: Gene ontology analysis of signature FDP and ODP signature genes.

Graphs to show pathways upregulated in FDP (A) and ODP (B).

I hypothesise that these 16 ODP signature genes identified through the microarray has a role in protection of follicles against miniaturisation. These 16 genes were classified according to their protein classes to further understand their biological roles (Figure 3.11A). Two of the genes did not have any annotations, thus they were classified as unknown. The protein classes which were most enriched were transcription factor (CXXC5, ZHX1, TRPS1) and protein binding (BLCAP, FNDC5, HHIP). The second most enriched protein classes were ubiquitin-protein ligase (TRIM2, FBXW11) and extracellular matrix structural protein (COCH, LAMB2). The protein classes with only one gene were G-protein (ARF4), RNA splicing factor (HNRNPM), secreted protein (RSPO4) and intercellular signal molecule (SOSTDC1).

The ODP signature genes were validated in patient-matched FDP and ODP spheres from a 5th patient using RT-PCR. Since it is known that there are differences between ODP and FDP in culture with regards to the K75 induction, I wanted to know which of the 16 genes maintained differential expression *in vitro*. Out of the 14 annotated genes, 12 genes could be detected via RT-PCR. Two of the genes (HHIP and SOSTDC1) had high Ct values (>35 cycles); thus, they were excluded from the analysis. Seven genes (BLCAP, FNDC5, FBXW11, ARF4, RSPO4, TRPS1, LAMB2, ZHX1) followed the same trend as the microarray but only 6 genes (BLCAP, FNDC5, FBXW11, RSPO4, TRPS1, ZHX1) were found to be both significantly and differentially expressed between FDP and ODP spheres (Figure 3.11B). COCH, TRIM2 and HNRNPM were found to be downregulated in ODP spheres compared to FDP spheres, however, this difference was not significant.

BLCAP

The microarray revealed a 2.3X fold increase in BLCAP in ODP vs FDP, and a 1.1X fold change in ODP spheres vs FDP spheres. BLCAP is located in chromosome 20 in humans. It was originally identified to have a role in invasive bladder cancer where its expression is strongly decreased. BLCAP has been shown to act as a tumour suppressor in multiple cancers such as tongue carcinoma (Rendl, Polak and Fuchs, 2008), Ewing's carcinoma (Yao *et al.*,

2006) and cervical carcinoma (Fan *et al.*, 2011) where it inhibits growth of cancer cells by inducing apoptosis. BLCAP expression is not present in the vibrissae of E14.5 (Appendix Figure A.1A) suggesting it might not be involved in hair follicle formation. Currently, there is no research in the role of BLCAP and hair follicle formation or regeneration.

FNDC5

The microarray revealed a 1.9X fold increase in BLCAP in ODP vs FDP, and a 1.9X fold change in ODP spheres vs FDP spheres. FNDC5 is found in chromosome 1 in humans. It is a transmembrane protein expressed in skeletal muscles which is cleaved by an unknown protease in response to exercise to produce a hormone called irisin in mice. Irisin has been shown to convert white adipose tissue into brown adipose tissue decreasing body weight and insulin resistance; thus it could have an important role in preventing obesity (Zuo *et al.*, 2006). FNDC5 is not expressed in the vibrissae of E14.5 (Appendix Figure A.1B) and the role of FNDC5 in hair follicle morphogenesis or regeneration is unknown.

FBXW11

The microarray revealed a 2.2X fold increase in BLCAP in ODP vs FDP, and a 1.2X fold change in ODP spheres vs FDP spheres. FBXW11 is located in chromosome 5 in humans. It is also known as β-TrCP2, is a component of the SCF E3 ubiquitin ligase with a role in cell cycle, cell migration and carcinogenesis. $SCF^{\beta\text{-}TrCP}$ has a wide variety of substrates and therefore regulates wide range of signalling pathways such as WNT pathway, PI3K/AKT/mTOR pathway and ErbB pathway (Panati, Suneetha and Narala, 2016). FBXW11 is not expressed in the vibrissae of E14.5 (Appendix Figure A.1C) and there is no link between FBXW11 and hair follicle at the moment.

RSPO4

The microarray revealed a 1.6X fold increase in BLCAP in ODP vs FDP, and a 2.5X fold change in ODP spheres vs FDP spheres. RSPO4 is found in chromosome 20. It belongs to a

family of R-spondin proteins (RSPO1/2/3/4) which are secreted agonists of the WNT signalling pathway. R-spondins enhance WNT signalling in the target cell (Bi *et al.*, 2021). RSPO4 is expressed in the mesenchyme of forelimbs and hindlimbs which develops into nails of mouse embryos at E15.5 suggesting a role in nail development (de Lau, Snel and Clevers, 2012). In humans, mutations in RSPO4 results in anonychia/hyponychia congenita which is the absence of nails on fingers and toes; however, these patients did not present any abnormalities in other ectodermal appendages such as hair and teeth (Blaydon *et al.*, 2006). Recently, it was shown that RSPO2/3 can promote proliferation of human follicular dermal progenitors and addition of RSPO2/3 induces anagen in mice by activating hair follicle stem/ progenitors (Ishii *et al.*, 2008). Whether RSPO4 has a similar role in hair follicle induction and proliferation of HFDSCs is unknown. There is faint expression of RSPO4 on outer vibrissae follicles at E14.5 (Appendix Figure A.1D) suggesting RSPO4 is expressed during hair follicle morphogenesis.

TRPS1

The microarray revealed a 1.7X fold increase in BLCAP in ODP vs FDP, and a 1.2X fold change in ODP spheres vs FDP spheres. TRPS1 is located in chromosome 8 and has been associated as one of the risk loci for AGA (Hagner *et al.*, 2020). It is a transcription factor with a role in hair follicle morphogenesis, chondrocyte and kidney development, and cancer. In humans, mutations in TRPS1 gene leads to Tricho-rhino-phalangeal syndrome (TRPS) type I (MIM 190350), type II (MIM 150230) and type III (MIM 190351). TRPS is characterised by craniofacial and skeletal abnormalities such as pear-shaped nose, short stature, hip dysplasia along with fine, sparse and slow growing hair (Hagenaars *et al.*, 2017; Pirastu *et al.*, 2017). The severity of hair loss has been reported to vary from slight thinning to alopecia in a similar pattern to male pattern baldness (Maas *et al.*, 1993; Gai, Gui and Muragaki, 2011).

In mice, TRPS1 is expressed throughout hair follicle morphogenesis and postnatally. During hair follicle morphogenesis, TRPS1 is expressed diffusely in the dorsal epithelium at E14.0. It

is also expressed strongly in vibrissae follicles at E14.5 (Appendix Figure A.1E). At E15.5, it is expressed in the DC and epidermis. Between E15.6-E17.5, TRPS1 is expressed in the nuclei of DP, mesenchymal cells surrounding hair peg and the underlying epidermis. Postnatally, TRPS1 is expressed in the DP and epithelial cells during all stages of the hair cycle. In anagen human hair follicles, similar expression of TRPS1 is seen in the DP along with Mx cells, ORS, IRS and companion layer (Yanez, Hernandez-Vincente and Armijo, 1992). TRPS1 contains GATA C_4-type domain which is used to bind consensus GATA sequences present in its target genes (Fantauzzo, Bazzi, *et al.*, 2008). Homozygous mice mutants with deletion of the GATA region *(Trps1$^{\Delta}$gt/$^{\Delta}$gt)* have reduced number of vibrissae follicles at E12.5 and have developmentally delayed follicles at E13.5 (Chang *et al.*, 2002). On the other hand, a position effect on TRPS1 gene has been associated with Ambras syndrome in humans, which is a rare form of congenital hypertrichosis resulting in excessive vellus-type hair growth (Fantauzzo and Christiano, 2012). Moreover, in prostate cancer, AR has been shown to repress the expression of TRPS1 (Chang *et al.*, 2000). As there is extensive evidence of TRPS1 having a role in hair follicle morphogenesis and cycling whilst also being regulated by the AR, I decided to focus on TRPS1 to determine whether it could have a role in miniaturisation of hair follicles.

ZHX1

The microarray revealed a 1.6X fold increase in BLCAP in ODP vs FDP, and a 1.1X fold change in ODP spheres vs FDP spheres. ZHX1 is found in chromosome 8 and is a member of the zinc fingers and homeoboxes gene family. It functions as a transcription repressor and has been shown to have a role in various cancers. In gastric cancer and hepatocarcinoma, overexpression of ZHX1 decreases proliferation and migration while in breast cancer and cholangiocarcinoma, it promotes proliferation, migration and invasion suggesting cell type-specific role of ZHX1 (Chang *et al.*, 2000). In addition, ZHX1 has been associated with TRPS type II. Prenatal diagnosis of a 36-year-old woman revealed craniofacial abnormalities in the foetus and cytogenetic analysis of amniocentesis showed deletion of 8q23.2-q24.11 which

encompassed TRPS1, EIF3H, RAD21, SLC30A8, MED30, and EXT1. The foetus also had a further 1.383-Mb deletion of 8q24.13 which encompassed ZHX2, DERL1, ZHX1, and ATAD2 (Kwon *et al.*, 2016). This is the only case of ZHX1 being linked to TRPS type II and whether this deletion involving ZHX1 plays a role in development of TRPS type II or is simply a side-effect of chromosomal rearrangements is unknown. There is also diffuse staining of ZHX1 at E14.5 in vibrissae follicles (Appendix Figure A.1F).

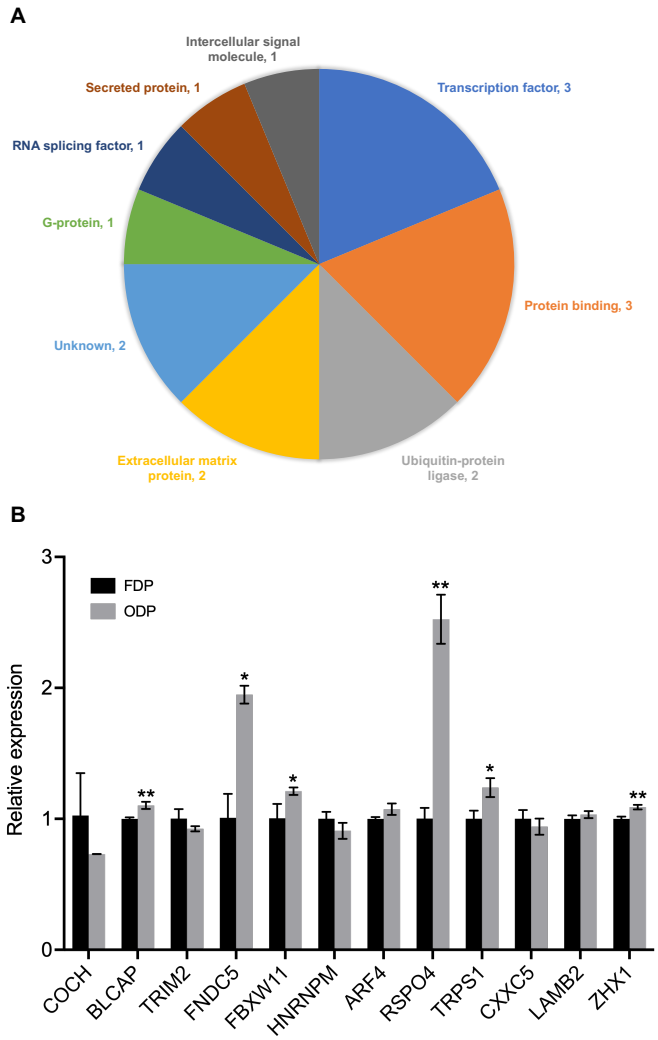


Figure 3.11: Protein class categorisation and RT-PCR validation of ODP signature genes.

A) Pie chart to show different protein classes and the number of genes present in each protein class of ODP signature genes. B) RT-PCR to validate the expression of ODP signature genes in spheres from a 5th patient. (Data were analysed using an unpaired t-test and the error bars represent standard deviation, * $P \leq 0.05$, ** $P \leq 0.01$, n=3).

3.4.6. TRPS1 regulates expression of BLCAP

TRPS1 is a transcription factor which activates and represses expression of multiple genes. The effect of loss of TRPS1 in maintaining ODP identity was examined through knockdown of TRPS1 using small interfering RNA (siRNA) in 2D ODP cells. The knockdown of TRPS1 by siTRPS1 was maintained for 125 hours (Figure 3.12A) and showed efficient gene knockdown ranging from 92.22% to 94.83% (Table 3.4). To assess whether loss of TRPS1 changes ODP identity, the gene expression of the 5 significantly differentially expressed genes were tested using RT-PCR after knockdown of TRPS1 in ODP cells. Out of the 5 significantly expressed ODP signature genes, only BLCAP was downregulated significantly when TRPS1 was knocked down suggesting TRPS1 could regulate the expression of BLCAP and make ODP cells similar to FDP cells (Figure 3.12B). Downregulation of TRPS1 had no effect on the expression of FBXW11 and ZHX1. RSPO4 and FNDC5 had high Ct values (>35 cycles), therefore, they were excluded from the analysis.

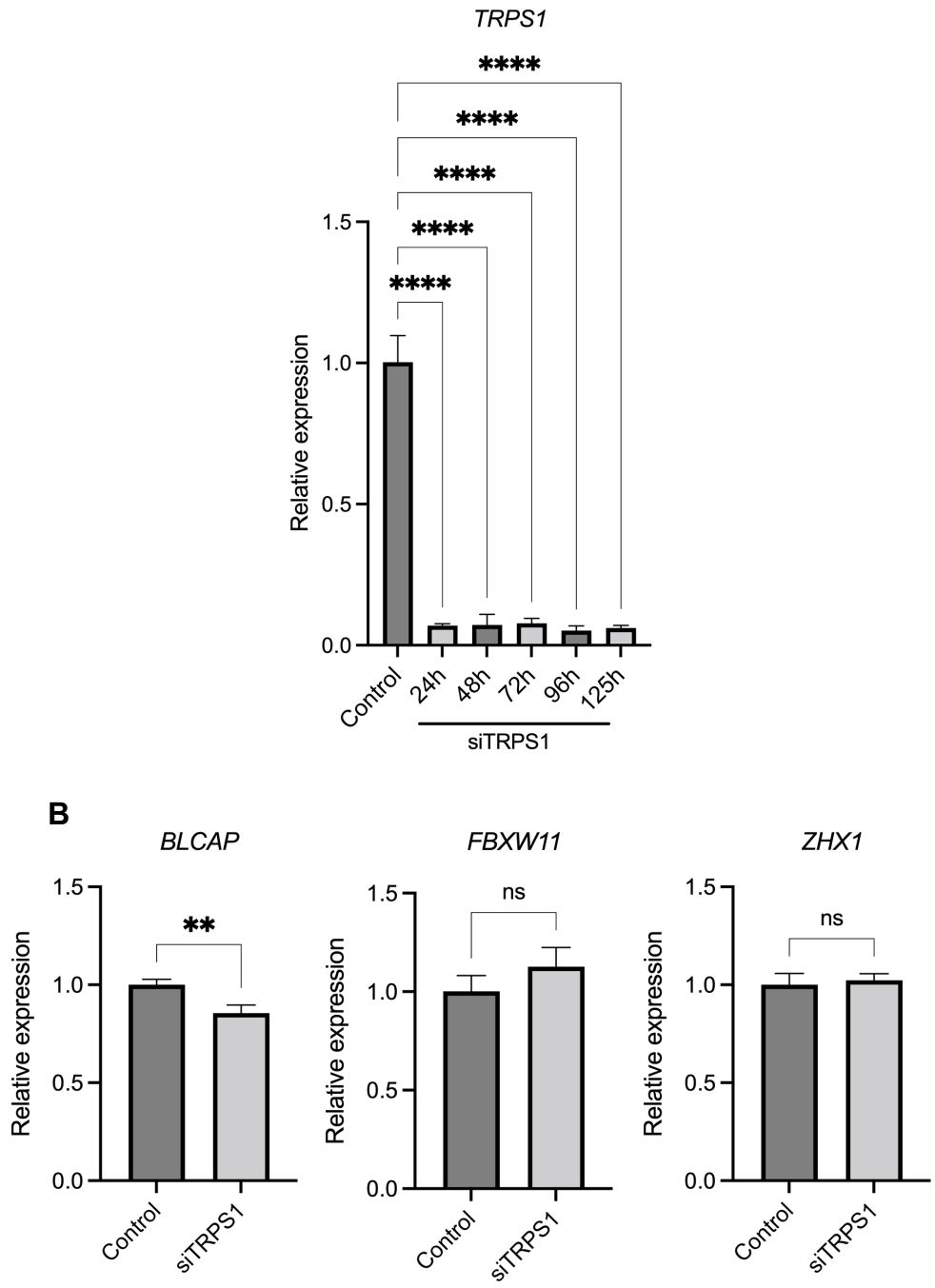


Figure 3.12: Effect of TRPS1 knockdown on ODP signature genes.

A) RT-PCR shows expression of TRPS1 decreases significantly following transfection of ODP cells with siTRPS1 after 24, 48, 72, 96 and 125 hours compared to control siRNA. (Data were analysed using Ordinary one-way ANOVA with Dunnett's multiple comparisons test and the error bars represent standard deviation, **** $P \leq 0.0001$, n=3). B) BLCAP expression decreases after knockdown of TRPS1 while the expression of FBXW11 and ZHX1 are not changed. (Data were analysed using an unpaired t-test and the error bars represent standard deviation, ** $P \leq 0.01$, ns = not significant, n=3).

Table 3.5: Knockdown efficiency of siTRPS1 after 24, 48, 72, 96 and 125 hours of transfection.

Time (hr) after transfection with siTRPS1	Percentage (%) knockdown of TRPS1
24	93.07
48	92.79
72	92.22
96	94.83
125	93.90

3.4.7. TRPS1 knockdown decreases K75 expression

To determine whether TRPS1 has a role in miniaturisation, the *in vitro* double sphere miniaturisation model was used to assess whether TRPS1 knockdown affects the ability of ODP cells to induce BC differentiation. TRPS1 was knocked down in 2D ODP cells which were then mixed with BC 24 hours after transfection. BC and ODP cells were co-cultured for 3 days to create double spheres (Figure 3.13A). Knockdown of TRPS1 did not significantly change the expression of K15 (Figure 3.13B), but it decreased the expression of K75 (Figure 3.13C). Knockdown of TRPS1 in ODP cells led to 1.1X decrease in K75 expression. Even though the difference was small and the knockdown of TRPS1 in ODP cells does not result in the same reduction in K75 as that observed when FDP cells are used (1.24X lower in FDP compared to ODP, Figure 3.5), it was still significant suggesting loss of TRPS1 decreases the ability of ODP cells to differentiate BC into follicular KC. Thus, a decrease in TRPS1 in ODP makes these cells more similar to FDP in terms of their BC differentiation capacity.

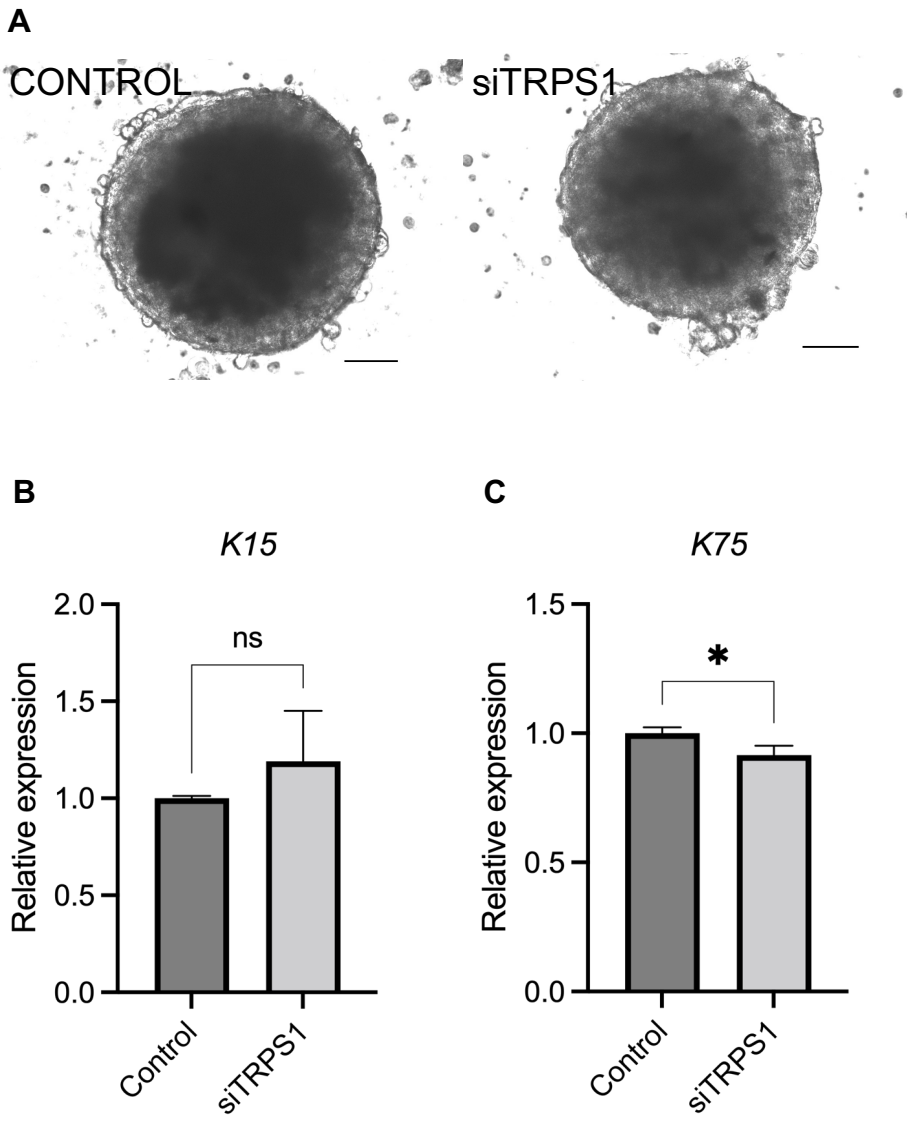


Figure 3.13: Effect of TRPS1 knockdown on K15 and K75 expression.

A) Brightfield images of ODP-BC spheres containing ODP cells transfected with siCONTROL or siTRPS1. B) Knockdown of TRPS1 does not change the expression of K15. C) TRPS1 knockdown leads to decreased induction of K75. (Data were analysed using an unpaired t-test and the error bars represent standard deviation, * $P \leq 0.05$, ns = not significant, n=3. Scale bar = 100 µm).

3.4.8. TRPS1 does not affect the age of dermal papilla cells

To determine how the loss of TRPS1 could decrease the hair induction capability of DP cells, the presence of genes regulated by TRPS1 were explored in the microarray analysis. Genes upregulated and downregulated by TRPS1 published by Fantauzzo & Christiano (2012) were compared with the various gene lists from my microarray analysis (Appendix Figure B.2A-F). This revealed two genes which overlapped in both FDP vs ODP upregulated and downregulated gene lists. TRPS1 was the gene that is present in FDP vs ODP downregulated list and was present in the downregulated list of Fantauzzo & Christiano (2012) suggesting TRPS1 controls its own expression through negative feedback loop. The gene that was present in FDP vs ODP upregulated list and overlapped with Fantauzzo & Christiano (2012) was EGR1 (Figure 3.14A). This gene was present in downregulated list in Fantauzzo & Christiano, (2012) suggesting it's expression is downregulated by TRPS1.

EGR1 is a transcription factor and can be induced by various external stimuli such as growth factors, ultraviolet radiation and hypoxia. It regulates the expression of various genes which have wide variety of roles in biological processes such as apoptosis, differentiation, angiogenesis and proliferation. EGR1 has been shown to have a role in cancer both as an oncogene and tumour suppressor depending on the cancer type. In prostate cancer, EGR1 is overexpressed and its expression correlates with malignancy in prostate cancer (Adamson and Mercola, 2002). EGR1 has also been shown to have a role in synaptic plasticity and neuronal acitivity through regulation of genes involved in vesicular release and endocytosis, proteasome complex and neurotransmitters metabolism (Adamson and Mercola, 2002).

I looked at whether EGR1 expression is regulated by TRPS1 and found that knockdown of TRPS1 in ODP cells increased EGR1 expression by 2.4X (Figure 3.14B). Recently, it was shown that EGR1 is overexpressed in aged mice DP cells (Duclot and Kabbaj, 2017). Aged mice displayed delayed hair growth and a decrease in DP cell number which is similar to the

process of miniaturisation in AGA in humans. This led me to hypothesise that loss of TRPS1 in FDP upregulates EGR1, which could be a marker of ageing of the DP, and thus expression of EGR1 could indicate an aged phenotype. To test this hypothesis, TRPS1 was knocked down in ODP cells and DNA methylation status of ELOVL2 was carried out. Hypermethylation of ELOLV2 has been shown to correlate with increasing age in various tissues such as blood (Shin *et al.*, 2020) and plucked hair (Garagnani *et al.*, 2012; Bekaert *et al.*, 2015; Zbieć-Piekarska *et al.*, 2015); thus ELOLV2 was used to assess whether there is a link between loss of TRPS1 and ageing of DP cells. 9 CpG sites were assessed, although CpG sites 1,6 and 9 have been specifically associated with ageing (Hao *et al.*, 2021; Naue *et al.*, 2021). Methylation analysis of ELOVL2 in control and TRPS1 knocked down ODP cells showed hypomethylation of CpG sites 1, 6 and 9 in both patients of similar age (Figure 3.14C and D). Control ODP cells had hypomethylated CpG 1,6 and 9 which could reflect the young age of the patients (24 and 25 years old) used in these experiments. It would be interesting to see if ODP cells from older patients would have hypermethylated ELOVL2 and if loss of TRPS1 could increase the methylation levels.

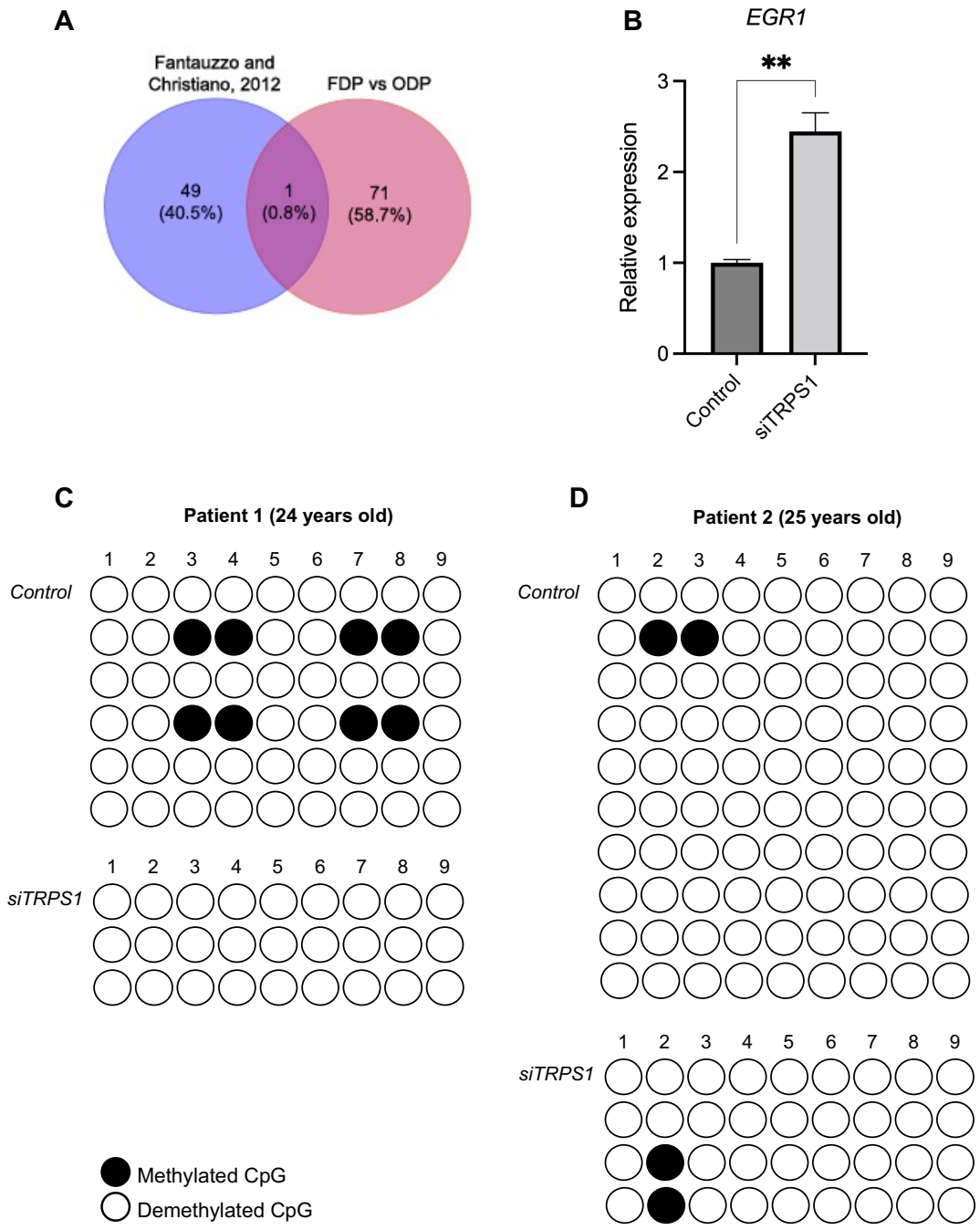


Figure 3.14: Effect of TRPS1 knockdown on ELOVL2 methylation status.

A) Venn diagram comparing genes regulated by TRPS1 published by Fantauzzo & Christiano, (2012) and my FDP vs ODP upregulated gene list. B) Knockdown of TRPS1 leads to an increase in EGR1 expression. DNA methylation status determined by bisulfite conversion of the CpG sites (1-9) of ELOVL2 in patient 1 (C) and patient 2 (D).

3.4.9. Expression of TRPS1 is regulated by the androgen receptor

As discussed in section 1.5.2, AR expression is increased in androgen-sensitive frontal follicles and promote catagen transition and miniaturisation through the release of DHT-mediated factors. Prostate cancer is androgen-dependent and requires the transcriptional activity of AR for growth and survival. The first line of treatment for prostate cancer is androgen deprivation therapies which includes castration and antiandrogens such as bicalutamide (Bekaert *et al.*, 2015). Prostate cancer can transition from androgen-dependent into androgen-independent which is resistant to apoptosis. (Feng and He, 2019) found that TRPS1 is downregulated in an androgen-independent prostate cancer cell line. They showed that activation of AR through the addition of the androgen agonist (R1881) decreases TRPS1 while the addition of an androgen agonist (bicalutamide) reversed the repression of TRPS1 suggesting androgen-mediated regulation of TRPS1 in prostate cancer (Figure 3.15A).

To determine whether TRPS1 expression is regulated by the AR in FDP cells, CI-4AS-1 was used to activate the AR. CI-4AS-1 is a DHT-mimic that binds to the AR resulting in translocation of the AR into the nucleus (Chiu *et al.*, 2016). To confirm the effect of CI-4AS-1 on FDP, I first looked at DKK-1, a well-known DHT induced AR target gene which is also known to be elevated in the frontal scalp. Addition of CI-4AS-1 in FDP cells upregulated the expression of DKK-1 by 1.1X compared to control, while addition of antiandrogen, bicalutamide leads to 1.1X decrease in DKK-1 expression compared to control (Figure 3.15B). This shows that CI-4AS-1 works in a similar way to DHT by activating similar genes. Next, the expression of TRPS1 was checked in patient-matched FDP and ODP cells in response to CI-4AS-1 and bicalutamide. In FDP cells, CI-4AS-1 decreased the expression of TRPS1 by 1.5X; however, the addition of bicalutamide did not relieve the repression induced by CI-4AS-1 (Figure 3.15C). On the other hand, in ODP cells, addition of CI-4AS-1 decreased TRPS1 expression by 1.9X but bicalutamide increased the expression of TRPS1 (Figure 3.15D). This

suggests that the AR responds differently to antiandrogens in FDP cells compared to ODP cells.

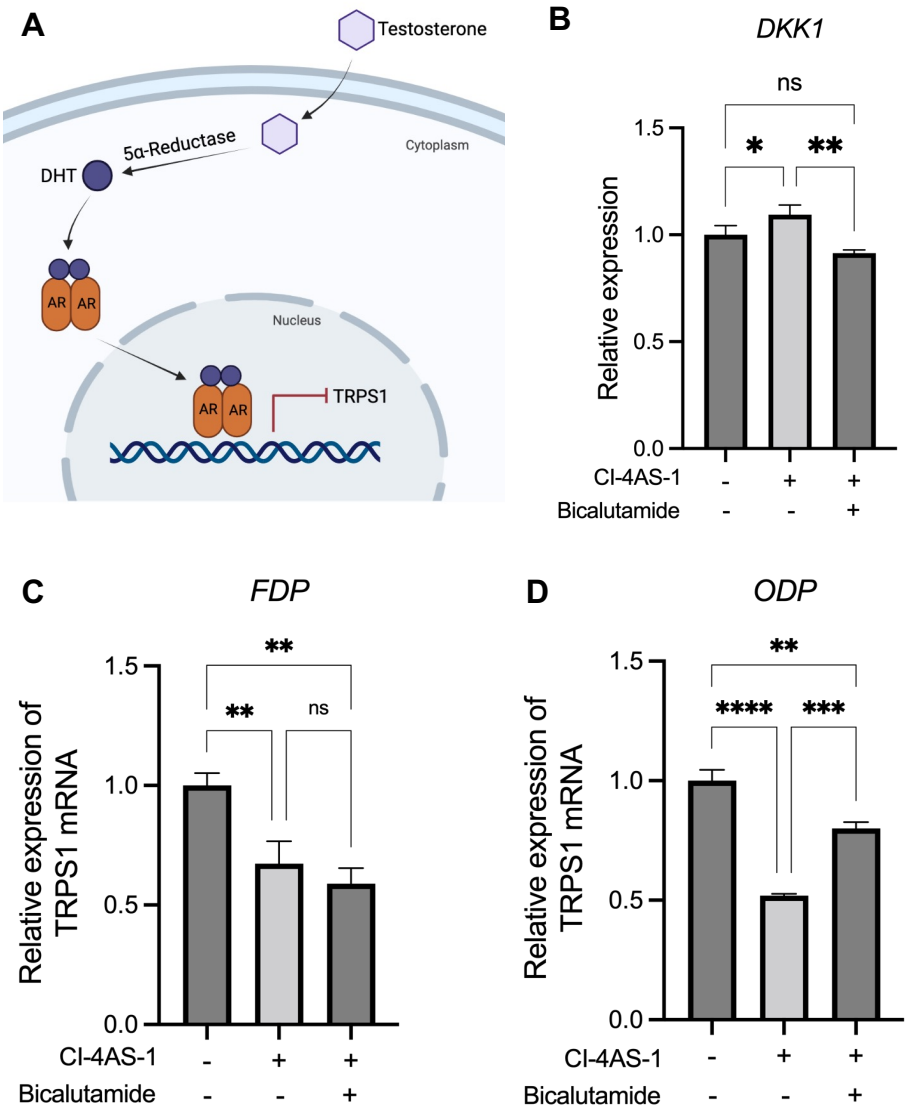


Figure 3.15: Effect of androgen receptor activation and inactivation on DKK-1 and TRPS1 expression.

A) Schematic diagram to illustrate repression of TRPS1 by the AR (Image created in BioRender). B) DKK-1 expression increases with addition of CI-4AS-1 and decreases with addition of bicalutamide. C) In FDP cells, CI-4AS-1 decreases TRPS1 expression while bicalutamide has no effect. D) In ODP cells, addition of CI-4AS-1 increases TRPS1 expression and bicalutamide increases TRPS1 expression. (Data were analysed using Ordinary one-way ANOVA with Tukey's multiple comparisons test and the error bars represent standard deviation, * P ≤ 0.05, ** P ≤ 0.01, *** P ≤ 0.001, **** P ≤ 0.0001, n=3)

3.5. Summary

In AGA, hair follicles undergo miniaturisation which is the transition of terminal follicles into a vellus state. The miniaturised hair follicles have dysregulated hair cycle with shortened anagen, premature catagen onset and longer telogen/ kenogen phase (Chiu *et al.*, 2016). There is also a decrease in the number of progenitors found in miniaturised hair follicles but the number of BC remains similar to occipital hair follicles (Cranwell and Sinclair, 2016). The differentiation of BC to progenitors take place at telogen-anagen phase and the DP has been shown to stimulate the activation and differentiation of BC through release of paracrine factors such as FGF7 (Garza *et al.*, 2011). This indicates that the DP in miniaturised hair follicles from balding scalp (frontal, temples, and vertex) may have impaired ability to initiate anagen through decreased BC differentiation. ODP with their normal hair differentiation capability could promote normal hair cycling and thus protect occipital hair follicles from miniaturisation. Thus, in this chapter, I aimed to elucidate whether FDP and ODP have different BC differentiation capabilities suggesting differences in anagen initiating ability and to determine the differences between FDP and ODP to explain the protective nature of ODP against miniaturisation.

An *in vitro* double spheres model combining FDP or ODP cells with BC revealed decreased ability of FDP cells to differentiate BC compared to ODP cells. This decreased conversion of BC into follicular KC by FDP cells indicate an impairment in FDP to initiate anagen. This also suggested intrinsic differences between FDP and ODP exist that allows ODP cells to promote normal anagen phase transition while inhibiting this ability in FDP cells. To determine the inherent differences between FDP and ODP, an unbiased microarray analysis was undertaken with patient-matched intact FDP and ODP along with FDS and ODS from 4 patients undergoing hair transplantation surgeries. This revealed differential gene expression between frontal and occipital DP and DS. Venn analysis allowed me to dissect unique signature genes in each cell type which were highly expressed in a particular cell type. ODP signature genes

consisted of well-known DP signature genes such as HHIP, SOSTDC1, RSPO4 and TRPS1 (Alonso and Fuchs, 2006; Greco *et al.*, 2009). Pathway analysis of ODP signature genes revealed upregulation of SHH and BMP signalling pathways which help to maintain a DP identity (Rendl, Lewis and Fuchs, 2005; Hagner *et al.*, 2020) suggesting important roles of the 16 unique ODP signature genes for normal DP functioning and loss of these genes in FDP could result in decreased hair inductivity and dysfunction of DP cells.

Out of the 16 ODP signature genes, only TRPS1 has already been identified as a risk loci for AGA in GWAS (Rendl, Polak and Fuchs, 2008; Woo, Zhen and Oro, 2012) indicating a role of TRPS1 in miniaturisation of hair follicles. Mutations in TRPS1 is linked to a hypotrichosis disorder called TRPS (Hagenaars *et al.*, 2017; Pirastu *et al.*, 2017) while position effects on this gene is associated with Ambras syndrome, a form of hypertrichosis (Maas *et al.*, 1993). Loss of TRPS1 in ODP cells led to a decrease in BC differentiation and an increase in EGR1 within DP cells suggesting a potential role of TRPS1 in miniaturisation of hair follicles. In prostate cancer, the AR represses TRPS1 expression. The AR has a key role in AGA pathogenesis. In FDP and ODP cells, AR repressed expression of TRPS1 when an androgen agonist was added. In ODP cells, addition of an antiandrogen reversed this repression while it had no effect in FDP cells suggesting differential response of the AR to antiandrogens in FDP cells.

Chapter 4: Discussion and future directions

4.1. Changes in nerves, blood vessels and lymphatic vessels in AGA

We know that in AGA there is a loss of APM attachment with an increase in eccrine and sebaceous glands size and number (Yazdabadi *et al.*, 2012; Kim *et al.*, 2014; Poblet *et al.*, 2018). In AGA, VEGF expression is also decreased suggesting a decrease in blood vessels (Yazdabadi *et al.*, 2012; Kim *et al.*, 2014; Poblet *et al.*, 2018). Lattanand & Johnson, (1975) have described decrease in capillaries and changes in the nerve plexus in vellus hair follicles. However, these changes were not quantified. The data presented in chapter 2 shows that there is a decrease in nerves (Figure 2.7B) and blood vessels (Figure 2.10B) in frontal hair follicles. An increase in lymphatic vessels (Figure 2.14B) were observed in frontal follicles in this study.

A possible explanation for loss of nerves in follicular macroenvironment may involve the APM. In AGA, loss of APM attachment to miniaturised hair follicles have been observed. APM, attached to the hair follicle at the bulge region, is highly innervated by sympathetic nerves which when activated by stimuli such as cold or danger causes the APM to contract promoting piloerection of hair follicles (Goldman *et al.*, 1995). The sympathetic nerves also innervate the upper bulge region of hair follicles, and this innervation requires APM as loss of APM results in loss of sympathetic innervation to HFSCs. This delays anagen entry as norepinephrine, which is released by sympathetic nerves, is required for BC activation and anagen development (Pascalau and Kuruvilla, 2020). Therefore, the altered innervation of frontal follicles could be a secondary effect from the loss of APM attachment.

Moreover, in mice, upper BC, which are $Gli1^+$ $K15^-$, are multipotent stem cells regenerate the anagen hair follicle. (Shwartz *et al.*, 2020) showed that these upper $Gli1^+$ BC receive Shh from sensory neurons that wrap around the upper bulge region. Loss of sensory neurons innervating the upper bulge shifts the $Gli1^+$ $K15^-$ BC into $Gli1^-$ $K15^+$ cells and reduces their

ability to differentiate into epidermal cells. Therefore, neuronal signalling in the hair follicle macroenvironment is required to maintain BC phenotype. Decrease in nerves would result in less signalling to BC which can decrease their regenerative capacity.

It is already known that miniaturised follicles produce less VEGF which supports my findings of decreased blood vessels in the regenerating portion of the hair follicle. DP cells release VEGF which works in an autocrine and paracrine manner. Human DP cells promote proliferation of human microvascular endothelial cells (HMVECs) and increase release of VEGF from HMVECs (Bassino *et al.*, 2015). (Bassino *et al.*, 2015) also found downregulation of genes involved in blood vessel development and morphogenesis in immortalised balding DP cells compared to non-balding DP cells indicating a role of the DP in angiogenesis for hair growth. Minoxidil is a vasodilator and can increase the expression of VEGF in human DP cells (Lachgar *et al.*, 1998) suggesting vascularisation may be important to maintain hair growth effects of DP. Even though the blood capillaries of DP were not specifically observed in this study, it could be an area of further investigation to determine whether frontal and occipital DP have differential blood vasculature.

Blood vessels not only modulate the activity of DP cells, they have been shown to modulate timing of BC activation. (Lachgar *et al.*, 1998) showed that during late catagen/telogen, a horizontal vascular plexus is formed under the hair germ which keeps BC quiescent and increase in the horizontal vascular plexus delays anagen entry. They show that SHG express Runx1 at late catagen/telogen which activates expression of secreted proteins that remodel the horizontal plexus leading to less dense horizontal vascular plexus. This allows BC activation and anagen entry. Runx1 is expressed in the SHG of human telogen follicles (Hoi *et al.*, 2010) suggesting a similar mechanism of action in human hair follicles may exist. In balding follicles, $CD200^{hi}$ $ITGA6^{hi}$ progenitor cells, found in the SHG of human hair follicles, are diminished (Hoi *et al.*, 2010) suggesting loss of SHG could result in decreased expression of Runx1. This could increase the horizontal vascular plexus which could maintain hair follicles

in telogen for longer. Moreover, Runx1 has been identified as a risk loci for AGA (Garza *et al.*, 2011) suggesting Runx1 regulation of BC may be involved in pathogenesis of AGA.

Hair follicles engage in aerobic glycolysis and glutaminolysis using glucose and glutamine as their fuel source (Heilmann-Heimbach *et al.*, 2017; Pirastu *et al.*, 2017) and aerobic glycolysis produces lactate as its end product (Williams, Philpott and Kealey, 1993). Proliferating cells use aerobic glycolysis to produce energy for cell growth. Anagen is a period of rapid growth; thus, would require high levels of nutrients and oxygen. Decrease in blood vessels in frontal hair follicles may contribute to miniaturisation through reduced availability of nutrients and oxygen and poor removal of waste products such as lactate. This could limit the growth of the hair follicles, hence leading to production of smaller hair follicles. Promoting angiogenesis may help to stimulate anagen entry and rejuvenate miniaturised hair follicles.

Increase in LYVE1 intensity in the lower regenerating portion of the frontal hair follicles suggests an increase in lymphangiogenesis in AGA. Recently, (Schurr, 2017) showed that transgenic mice overexpressing VEGFC (K14-VEGFC), which stimulates lymphangiogenesis, had prolonged anagen. Peña-Jimenez et al., (2019) showed that depletion of lymphatic vessels during anagen “promoted collapse of growing” hair follicles along with increased cell death suggesting loss of lymphatic vessels during anagen promotes catagen transition, although this was not measure by the researchers. In contradiction to these papers, Gur-Cohen et al., (2019) showed that depletion of lymphatic vessels in telogen leads to precocious anagen induction. They also showed that lymphatic vessels are in close association with lower bulge at telogen which contributes to BC quiescence and telogen maintenance. This is in line with my findings which would suggest that the increase in lymphatic vessels in AGA could maintain follicles in telogen. Further research is required to delineate the exact role of lymphatic vessels during the hair cycle.

Variation in LYVE-1 intensity was seen even between follicles of same patient but frontal follicles had higher intensity of LYVE-1 in general. A co-marker with LYVE-1 could be used such as VEGFR-3 and Prox1 which has been shown to be expressed in end bulbs of mice hair follicles (Yoon *et al.*, 2019). This could be a better marker for lymphatic vessels in humans. Staining for presence of VEGF-C in human hair follicles from frontal and occipital scalp could also further solidify these findings of increased lymphatic vasculature in AGA. Observation of large lymphatic vessels were rare; perhaps, this was affected by the amount of dermis which is extracted during FUE or FUT. Therefore, to observe larger lymphatic vessels, bigger punch biopsies containing multiple hairs and larger area of dermis could be used.

Other interesting observations from this study were innervation and vascularisation of multiple follicles along with eccrine and sebaceous glands. I propose that the FU is an intricate, interconnected network consisting of hair follicles, APM, sebaceous glands, blood vessels, lymphatic vessels and nerves which all communicate with each other in order to maintain the regenerative and proper functioning of the hair follicle (Figure 4.1). Disruptions in parts of this unit could lead to impaired function of the regenerative and cycling properties of the hair follicle and could have a damaging effect on other components in the FU. Exploiting the hair follicle macroenvironment by increasing innervation and vasculature, it might lead to reversal or prevention of AGA phenotype. Developments of new treatments for AGA should take into consideration the FU and its macroenvironment in order to prevent or reverse hair loss permanently.

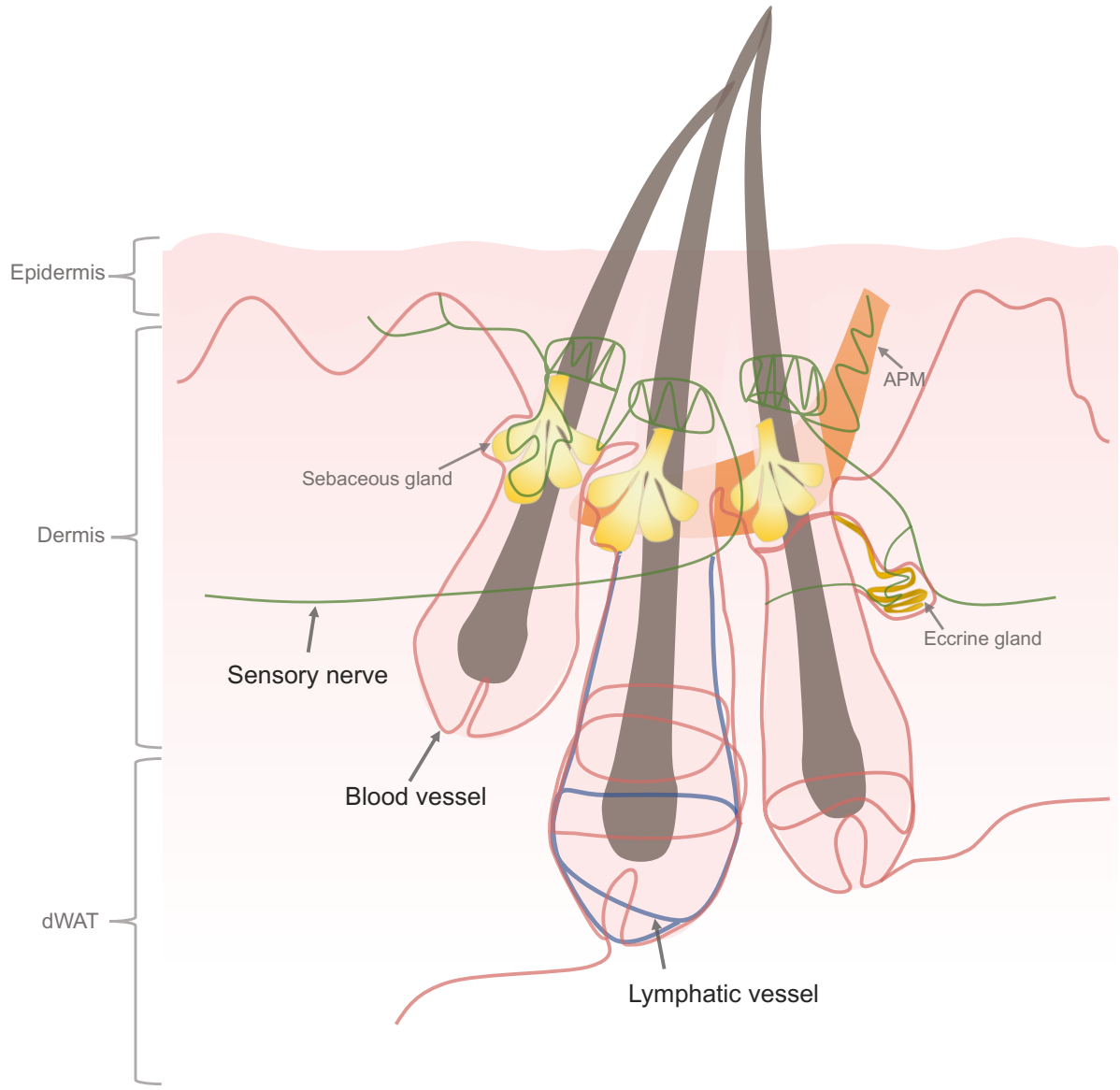


Figure 4.1: A model of hair follicle macroenvironment.

The FU consisting of primary, secondary follicles along with APM, sebaceous and eccrine glands are served by a network of nerves and blood vessels which span the whole FU.

4.2. *In vitro* models are useful to test for inductivity

AGA is the most common form of hair loss in humans affecting around 50% of adults. Treatments for AGA makes up a multi-billion dollar industry; however, minoxidil and finasteride have been shown to have moderate effects and hair transplantation surgeries are invasive (Yoon *et al.*, 2019). There is a severe unmet need to develop more drugs and treatments for AGA that could potentially stop further hair loss or increase hair growth through conversion of miniaturised follicles into terminal follicles.

In vitro models can be used as a first-line screening tool to test the efficacy of a new drug or a new treatment on growth of human hair follicles and are also good for replacing use of animals in research. Simple 2D cultures or co-cultures do not accurately reflect the complex mesenchymal-epithelial interactions that takes place in human hair follicles. Therefore, for *in vitro* models to have clinical value, they must mimic some of the mesenchymal-epithelial interactions such as the DP cell- DP cell interactions in 3D ECM and the close interaction of epithelial cells to DP which are separated by a basement membrane *in vivo*. 3D *in vitro* models are an attractive first-line screening tool as they provide cell-cell interactions within DP in an ECM and by adding epithelial cells such as ORS or BC, they can mimic mesenchymal-epithelial interactions in a controlled environment. Moreover, by using different cell types such as the skin KC or BC, these models can be used for molecular dissection of inductivity or telogen-anagen phase as similar mesenchymal-epithelial interactions are required to induce new hair growth and to regenerate hair.

In chapter 3, I developed an *in vitro* inductivity model to assess the hair inducing ability of DP cells by looking at the induction of K75 in skin KC which normally do not express it. The model showed that compared to other cell types such as PFI, RFI or KC by themselves, DP cells induce the highest expression of K75 (Figure 3.3B). Replacement of DP cells with PFI cells and addition of DP conditioned medium is also enough to induce expression of K75 to similar

levels to when DP cells were used (Figure 3.4B). These results suggested that cell contact is important for KC differentiation into follicular fate; although it did not matter the type of cell KC were in contact with if DP paracrine factors were present. This indicates that DP paracrine factors may play a bigger role in differentiation of KC into a follicular fate. A critical role of DP paracrine factors for hair inductivity was shown by (Guo *et al.*, 2017) who discovered that activin A is released by DP spheres but not DP cells in 2D. Knockdown of activin A from DP spheres resulted in decreased hair follicle induction by DP spheres suggesting DP paracrine factors are important for hair induction. Moreover, the addition of exosomes secreted by 3D DP spheres to DP spheres results in increased hair follicle neogenesis in an *in vivo* patch assay (Kwack et al., 2019). DP-derived exosomes also increased the expression of human hair growth factors IGF-1, HGF and KGF in DP cells suggesting exosomes have an autocrine effect and thus could increase or maintain inductivity of DP cells. This could explain the lack of requirement for specific DP cell contact for inductivity. DP CM may contain factors which could make PFI cells inductive. To assess this, PFI cells could be treated with DP CM first and then combined with KC to assess the induction of K75 expression in KC. This would allow us to elucidate whether DP CM is enough to reprogramme PFI cells into DP cells.

4.3. Miniaturisation can be modelled *in vitro*

In AGA, lack of epithelial progenitors through decreased differentiation of BC has been proposed as one of the changes in hair follicles which results in miniaturisation; however this has not been tested (Garza *et al.*, 2011). BC differentiation takes place during the telogen-anagen transition and signalling from the DP is important during this transition to regenerate hair. This led me to hypothesise that FDP cells have impaired ability to initiate anagen; thus, FDP cells are not able to differentiate BC as well as ODP cells. To test this hypothesis, the *in vitro* miniaturisation model was developed which combined FDP or ODP cells with BC. The *in vitro* miniaturisation model revealed that FDP cells have decreased ability to differentiate BC

into follicular KC compared to ODP cells as FDP cells induced lower K75 expression in BC (Figure 3.5F). This result correlate with the known inductive ability of FDP and ODP spheres in the patch assay (Garza *et al.*, 2011). This impairment to induce anagen could be due to effects of androgens to FDP cells which may change the paracrine factors released by FDP cells. Instead of hair-growth promoting factors, FDP cells could be releasing hair growth-inhibitory factors during the late telogen phase which could inhibit activation of BC. It is known that FDP cells release hair growth inhibitory factors in response to androgens and this induces premature catagen (Hibino & Nishiyama, 2004b; Kwack et al., 2008, 2012). However, it is not known if telogen FDP also releases hair growth inhibitory factors in response to androgens.

Moreover, these results showed that the process of miniaturisation can be modelled *in vitro* by comparing induction of K75 expression by FDP and ODP cells. K75 has been shown to be a good marker to assess the follicular fate of skin KC induced by DP cells (Roh, Tao and Lyle, 2005; Leirõs, Attorresi and Balañá, 2012; Kalabusheva, Terskikh and Vorotelyak, 2017). As cells are used, this model can also be used to assess the roles of specific genes in miniaturisation through knockdowns or overexpression in DP cells. This is useful as in organ cultured human hair follicle, it is impossible to test the loss of certain gene in DP only. With this model, specific knockdowns or overexpression can be undertaken to assess its role in miniaturisation. As these results correlate with the *in vivo* induction assay (Roh, Tao and Lyle, 2005; Leirõs, Attorresi and Balañá, 2012; Kalabusheva, Terskikh and Vorotelyak, 2017), it shows that the *in vitro* spheroid models can facilitate the replacement of animals in research.

4.4. Transcriptomic analysis of frontal and occipital hair follicle mesenchyme reveals inherent differential gene expression

Differences in anagen initiation by DP cells from different scalp sites suggests that the pattern of hair miniaturisation seen in AGA could be due to differences in the DP found at those sites. It is known that occipital hair follicles remain in the frontal scalp permanently and do not

miniaturise after transplantation suggesting occipital follicles are resistant to the effects of DHT in the frontal scalp. As DHT is thought to mediate its effect through the DP, it would suggest that ODP provides protection against DHT to prevent miniaturisation by preserving occipital follicle size, cycling and regenerative properties. Transcriptomic profiling of frontal and occipital hair follicle mesenchyme revealed inherent differences between cell types from these sites (Figure 3.6D and E) and through venn analysis, unique signature genes for each cell type (FDP, FDS, ODP and ODS) were identified (Figure 3.9A). Although only 16 genes were identified in ODP, 4 of the genes have already been shown to be DP signature genes. These were HHIP, SOSTDC1, RSPO4 and TRPS1 (Rendl, Lewis and Fuchs, 2005; Hagner *et al.*, 2020). I could not validate HHIP and SOSTDC1 expression in DP spheres. Looking through Higgins et al., (2013) dataset revealed that even though HHIP and SOSTDC1 are expressed highly in intact DP, expression of these genes is lost in culture which explains the inability to validate them (Figure 3.16). Overall, these results support the hypothesis that FDP and ODP are inherently different from one another and expression of unique ODP genes may protect occipital follicles from undergoing miniaturisation. These results are in line with previous findings by (Rendl, Lewis and Fuchs, 2005; Hagner *et al.*, 2020) who have shown that there is differential gene expression between immortalised balding and non-balding cultured DP cells.

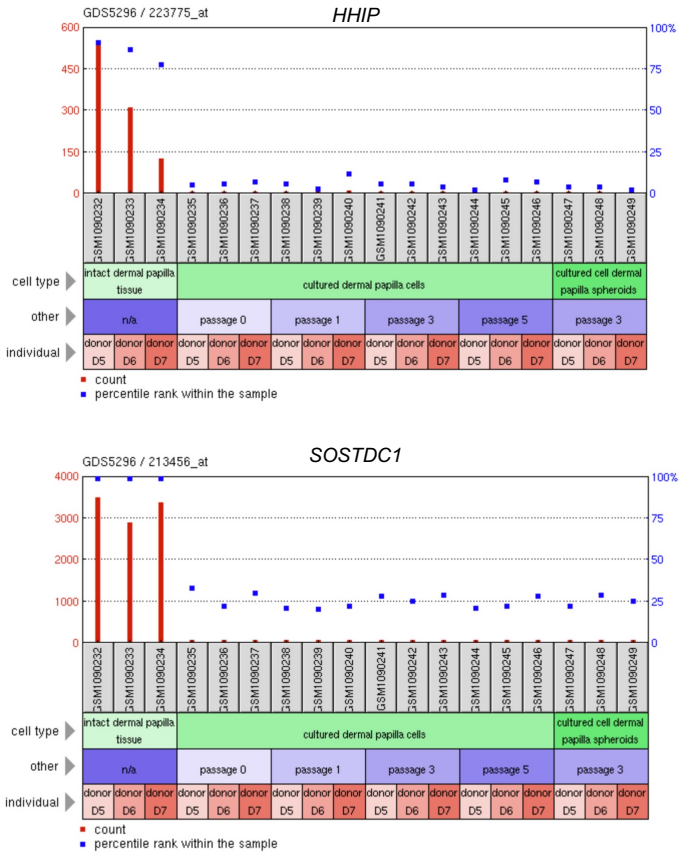


Figure 4.2: Expression of HHIP and SOSTDC1 in intact DP, cultured DP cells at P0, P1, P3, P5 and spheres. (From Higgins et al., 2013)

4.5. Potential role of TRPS1 in androgenetic alopecia

TRPS1 has been shown to have a role in hair follicle morphogenesis and downregulation of TRPS1 reduces density of vibrissae follicles during development (Fantauzzo and Christiano, 2012). In humans, autosomal dominant mutations which result in reduction of TRPS1 expression leads to TRPS type I, type II and type III which are characterised by craniofacial abnormalities and sparse scalp hair. Patients with TRPS exhibit male pattern hair loss with varying degree of hair loss (Fantauzzo and Christiano, 2012). On the other hand, position effect on TRPS1, which results in over 90% reduction in TRPS1 expression, has been associated with Ambras syndrome. In Ambras syndrome, hypertrichosis is the main

phenotype with increased vellus-type hair follicles present on the shoulders, face and ears (Rossi *et al.*, 2015). The literature suggests that TRPS1 expression could impact follicle size.

In my work, I found that the expression of TRPS1 was higher in intact ODP compared to intact FDP (Figure 3.9B) which correlates with the literature and suggests that TRPS1 expression might control follicle size. TRPS1 mRNA was significantly upregulated in ODP spheres compared to FDP spheres (Figure 3.11B). Loss of TRPS1 in ODP cells resulted in decreased expression of one of the ODP signature genes identified here, BLCAP (Figure 3.12B). This suggests that TRPS1 regulates the expression of BLCAP and loss of TRPS1 could lead to loss of DP identity in frontal hair follicles. This could result in the differential gene expression of FDP identified in this chapter. Further experiments looking at the expression of top FDP signature genes could be probed in ODP cells with TRPS1 knockout to verify that loss of TRPS1 changes ODP identity into FDP.

Knockdown of TRPS1 in ODP cells resulted in decreased K75 expression in BC suggesting a decreased ability of ODP cells to induce differentiation of BC (Figure 1.13C). This indicates that the impaired ability of FDP cells to initiate anagen could be due to decreased expression of TRPS1; thus, potentially pointing towards a role of TRPS1 in miniaturisation. Loss of TRPS1 may decrease the ability of FDP cells to initiate anagen and hence could prolong the telogen phase. On the other hand, expression of TRPS1 in ODP cells could promote differentiation of BC into follicular KC, thus allowing telogen-anagen transition and normal hair cycle to occur which leads to normal hair growth.

TRPS1 is a transcription factor and regulates the expression of several genes (Rashid and White, 2007; Fantauzzo, Tadin-Strapps, *et al.*, 2008). EGR1, which was found to be downregulated by TRPS1 in vibrissae follicles, was upregulated in my FDP vs ODP upregulated gene list. Knockdown of TRPS1 in ODP cells increased the expression of EGR1 suggesting TRPS1 represses the expression of EGR1 in human DP cells (Figure 3.14B).

Recently, EGR1 expression was detected in aged mouse DP cells and so I postulated that TRPS1 expression prevents DP ageing (Fantauzzo and Christiano, 2012). However, DNA methylation analysis of an age marker, ELOVL2, showed that TRPS1 does not infact accelerate ageing of DP cells (Figure 3.14C and D). These data must be interpreted with caution though as the patients used for the DNA methylation analysis were young (24 and 25 years old). ELOVL2 methylation analysis with ODP cells from older patients may yield different results so it would be useful to compare ELOVL2 methylation status in ODP cells from varied ages of patients (20 - 60 years old).

Aside from aged DP cells, EGR1 is overexpressed in prostate cancer, and it has been shown to bind to the AR. EGR1 can enhance translocation of AR into the nucleus (Shin *et al.*, 2020). Increased expression of EGR1 in FDP might also increase activation or inhibition of AR target genes; thus, EGR1 could have a role in AGA pathogenesis.

4.6. Androgenic regulation of TRPS1

There is strong evidence for the role of AR in AGA pathogenesis. In prostate cancer, AR has been shown to repress TRPS1 expression. CI-4AS-1 is a selective androgen receptor modulator. It has been shown to bind to AR which results in translocation of the AR/CI-4AS-1 complex to the nucleus (Chiu *et al.*, 2016). In a breast cancer cell line, activation of the AR by DHT and CI-4AS-1 leads to expression of similar genes (Chiu *et al.*, 2016) suggesting DHT and CI-4AS-1 function in a similar way. Bicalutamide is a competitive antagonist of the AR and inhibits AR activity by forming a transcriptionally inactive AR/bicalutamide complex (Ahram *et al.*, 2018).

In addition to FDP and ODP being transcriptionally different from one another, it seems that the AR in the DP from different sites on the scalp respond differently to antiandrogens. In FDP cells, CI-4AS-1 increased expression of DKK-1, which is a known to be activated by the

AR, whilst bicalutamide inhibited the expression of DKK-1. This suggests that AR activity can be inhibited by antiandrogens in FDP cells. CI-4AS-1 repressed TRPS1 expression in both FDP and ODP cells but TRPS1 expression was only elevated in ODP cells with bicalutamide treatment (Figure 3.15C and D). The AR in FDP cells may respond differently to bicalutamide suggesting impaired function of the AR. A possible explanation could be due to mutations in the AR which makes it respond differently to bicalutamide. Mutations such as W741C and W741L in the ligand-binding domain of AR have been described which makes prostate cancer cells resistant to bicalutamide (Masiello *et al.*, 2002). Polymorphisms of AR such as SNPrs6152 G>A (Hara *et al.*, 2003), rs5919324 (Cobb *et al.*, 2010) and rs2497938 (Cobb *et al.*, 2010) have been associated with AGA. Whether mutations in AR are present uniquely in FDP cells are unknown and could be an area of further investigation.

4.7. Conclusions

The hair follicle is a complex mini organ with a macroenvironment consisting of nerves, blood vessels, lymphatic vessels, APM, eccrine gland, and sebaceous gland. The macroenvironment around the hair follicle supports its growth and promotes hair cycling. The most obvious change in AGA is the miniaturisation of the hair follicles which leads to appearance of a balding scalp. It has been shown that miniaturised hairs have loss of APM attachment and fat accumulation suggesting changes in the macroenvironment of the follicle in AGA. This research aimed to investigate changes in nerves, blood vessels and lymphatic vessels in non-miniaturised frontal follicles in AGA. This study has shown that the hair follicles which are destined to miniaturise already undergo changes in their macroenvironment before miniaturisation. These frontal hair follicles have less nerves along with decrease in blood vessels and an increase in lymphatic vessels. This is important as morphologically the frontal follicles look similar in size to occipital follicles; however, these macroenvironment changes occur before miniaturisation. This raises the question why these changes are seen in frontal follicles even though they are similarly sized to occipital follicles. To better understand the

implications of these results, future studies could investigate if these same changes are seen in miniaturised follicles and if restoration of nerves and blood vessels whilst decreasing lymphatic vessels in miniaturised follicles could reverse miniaturisation.

In AGA, miniaturisation has been linked to disruptions in signalling from the DP caused by increased AR signalling. This study aimed to identify genes which are differentially expressed between FDP and ODP that could have a role in miniaturisation. Microarray analysis revealed that FDP and ODP have differential gene expression. This research focused on TRPS1 which was expressed higher in ODP compared to FDP. TRPS1 expression could be regulated by the AR suggesting a potential role of TRPS1 in AGA. The results in this thesis suggests that although frontal follicles are similar in size to occipital follicles, changes around and within it are already taking place before miniaturisation (Figure 4.3). Whether the changes within the DP and the macroenvironment occurs simultaneously or if one influences the other is unknown.

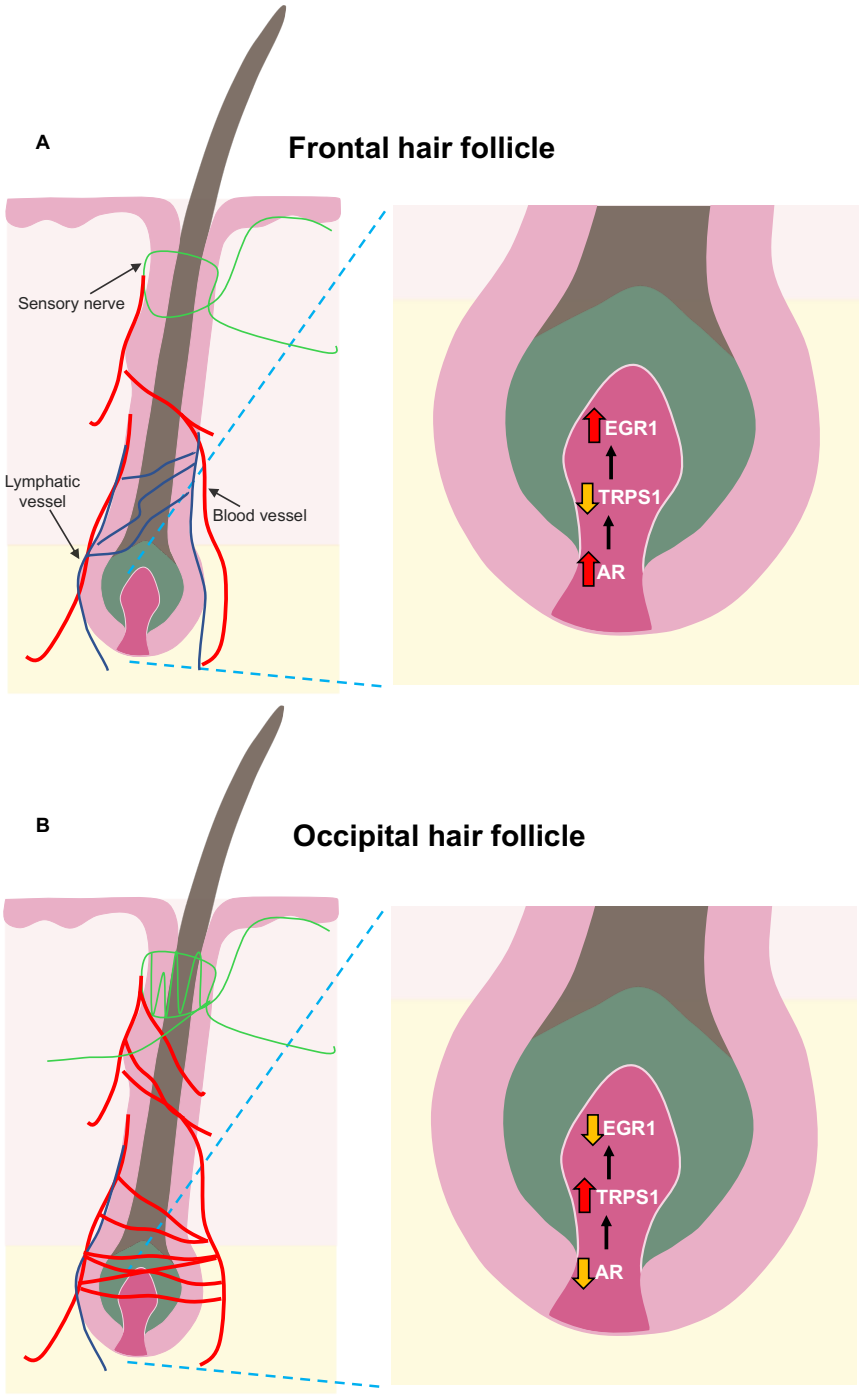


Figure 4.3: Schematic diagram of macroenvironmental and AR-dependent signalling changes in frontal and occipital follicle and DP.

A) In frontal follicles, there is a decrease in nerves and blood vessels while there is an increase in lymphatic vessels. In FDP, AR expression is higher which represses TRPS1 and leads to increase in EGR1 expression. B) In occipital follicles, opposite is seen with a rich supply of blood vessels and nerves but there is a decrease in lymphatic vessels. In the ODP, AR expression is lower which leads to upregulation of TRPS1 and downregulation of EGR1.

4.8. Future directions

Further research that could be carried out are:

- Immunostaining with other lymphatic vessel markers such as VEGFR3 and Prox1 could be conducted to support my findings of increased lymphatic vessels in AGA. The expression of VEGF-C, which promotes lymphangiogenesis, could be elucidated in human hair follicles to see if it is increased in AGA.
- As ZHX-1 has been linked to TRPS type 1 syndrome, the role of this novel transcription factor in promoting hair growth could be investigated using the *in vitro* miniaturisation model.
- The role of RSPO4 in promoting hair growth can be conducted through addition of RSPO4 to organ-cultured human hair follicles.
- Further experiments investigating the mechanism behind how TRPS1 promotes anagen initiation should be conducted. As mesenchymal-epithelial signalling is important for telogen-anagen initiation, paracrine factors released from ODP cells with TRPS1 knockdown could be added to BC to determine whether this would decrease BC differentiation.
- TRPS1 could be overexpressed in FDP cells to determine if it would rescue the K75 expression as it would indicate that TRPS1 is required for normal telogen-anagen transition.
- The results analysing the ELOVL2 methylation status were inconclusive. Further experiments with more patients and of older ages should be conducted to elucidate if loss of TRPS1 could increase ageing of DP cells.
- ELOVL2 methylation status in intact FDP and ODP could be investigated to see if FDP ‘older’ compared to ODP.
- Deep sequencing of the AR in FDP and ODP from same patients should be conducted to identify polymorphisms present in the AR that could explain the insensitivity towards antiandrogens in FDP cells.

- The transcriptomic profiling of FDS and ODS revealed differential gene expression. As HFDSCs replenish DP at the start of anagen, it would be interesting to investigate whether frontal HFDSCs have an impaired ability for self-renewal and differentiation. The blood vessels of hair follicles are present close to the dermal sheath. FDS and ODS genes could reveal novel factors that could also affect the vascularisation of hair follicles.

References

Adams, J. U. (2011) 'Raising hairs Companies are trying to translate the burgeoning science of hair into', *Nature Publishing Group*. Nature Publishing Group, 29(6), pp. 474–476. doi: 10.1038/nbt0611-474.

Adamson, E. D. and Mercola, D. (2002) 'Egr1 transcription factor: Multiple roles in prostate tumor cell growth and survival', *Tumor Biology*, 23(2), pp. 93–102. doi: 10.1159/000059711.

Ahram, M. *et al.* (2018) 'The cellular and molecular effects of the androgen receptor agonist, Cl-4AS-1, on breast cancer cells', *Endocrine Research*. Taylor & Francis, 43(3), pp. 203–214. doi: 10.1080/07435800.2018.1455105.

Alonso, L. and Fuchs, E. (2006) 'The hair cycle', *Journal of Cell Science*, 119(3), pp. 391–393. doi: 10.1242/jcs02793.

Amoretti, A., Laydner, H. and Bergfeld, W. (2013) 'Androgenetic alopecia and risk of prostate cancer: A systematic review and meta-analysis', *Journal of the American Academy of Dermatology*. Mosby, 68(6), pp. 937–943. doi: 10.1016/J.JAAD.2012.11.034.

Andl, T. *et al.* (2002) 'WNT signals are required for the initiation of hair follicle development', *Developmental cell*. Dev Cell, 2(5), pp. 643–653. doi: 10.1016/S1534-5807(02)00167-3.

Azaripour, A. *et al.* (2016) 'A survey of clearing techniques for 3D imaging of tissues with special reference to connective tissue', *Progress in Histochemistry and Cytochemistry*. Urban & Fischer, 51(2), pp. 9–23. doi: 10.1016/J.PROGHI.2016.04.001.

Baluk, P. and McDonald, D. M. (2008) 'Markers for microscopic imaging of lymphangiogenesis and angiogenesis', *Annals of the New York Academy of Sciences*,

1131(May), pp. 1–12. doi: 10.1196/annals.1413.001.

Bassino, E. *et al.* (2015) 'Paracrine crosstalk between human hair follicle dermal papilla cells and microvascular endothelial cells', *Experimental and Therapeutic Medicine*, 24, pp. 381–400. doi: 10.1111/exd.12670.

Bekaert, B. *et al.* (2015) 'Improved age determination of blood and teeth samples using a selected set of DNA methylation markers', *https://doi.org/10.1080/15592294.2015.1080413*. Taylor & Francis, 10(10), pp. 922–930. doi: 10.1080/15592294.2015.1080413.

Bi, Y. *et al.* (2021) 'The characteristics and roles of β-TrCP1/2 in carcinogenesis', *FEBS Journal*, 288(11), pp. 3351–3374. doi: 10.1111/febs.15585.

Biggs, L. C. *et al.* (2018) 'Hair follicle dermal condensation forms via FGF20 primed cell cycle exit, cell motility, and aggregation', *eLife*. eLife Sciences Publications Ltd, 7. doi: 10.7554/ELIFE.36468.

Blaydon, D. C. *et al.* (2006) 'The gene encoding R-spondin 4 (RSPO4), a secreted protein implicated in Wnt signaling, is mutated in inherited anonychia', *Nature Genetics 2006 38:11*. Nature Publishing Group, 38(11), pp. 1245–1247. doi: 10.1038/ng1883.

Botchkarev, V. A. *et al.* (1997) *Hair Cycle-Dependent Plasticity of Skin and Hair Follicle Innervation in Normal Murine Skin*, *J. Comp. Neurol*. Wiley-Liss, Inc. doi: 10.1002/(SICI)1096-9861(19970929)386:3.

Botchkareva, N. V., Ahluwalia, G. and Shander, D. (2006) 'Apoptosis in the Hair Follicle', *Journal of Investigative Dermatology*. Elsevier, 126(2), pp. 258–264. doi: 10.1038/SJ.JID.5700007.

Brockschmidt, F. F. *et al.* (2011a) 'Susceptibility variants on chromosome 7p21.1 suggest HDAC9 as a new candidate gene for male-pattern baldness', *British Journal of Dermatology*, 165(6), pp. 1293–1302. doi: 10.1111/j.1365-2133.2011.10708.x.

Brockschmidt, F. F. *et al.* (2011b) 'Susceptibility variants on chromosome 7p21.1 suggest HDAC9 as a new candidate gene for male-pattern baldness', *British Journal of Dermatology*, 165(6), pp. 1293–1302. doi: 10.1111/j.1365-2133.2011.10708.x.

Brownell, I. *et al.* (2011) 'Nerve-derived sonic hedgehog defines a niche for hair follicle stem

cells capable of becoming epidermal stem cells', *Cell stem cell*. Cell Stem Cell, 8(5), pp. 552–565. doi: 10.1016/J.STEM.2011.02.021.

Cai, R. *et al.* (2019) 'Panoptic imaging of transparent mice reveals whole-body neuronal projections and skull-meninges connections', *NATuRE NEuRoSCIENCE* |, 22, pp. 317–327. doi: 10.1038/s41593-018-0301-3.

Castronovo, V. and Belotti, D. (1996) 'TNP-470 (AGM-1470): Mechanisms of action and early clinical development', *European Journal of Cancer Part A*, 32(14), pp. 2520–2527. doi: 10.1016/S0959-8049(96)00388-7.

Chang, G. T. G. *et al.* (2000) 'Characterization of a zinc-finger protein and its association with apoptosis in prostate cancer cells', *Journal of the National Cancer Institute*, 92(17), pp. 1414–1421. doi: 10.1093/jnci/92.17.1414.

Chang, G. T. G. *et al.* (2002) 'Structure and function of GC79/TRPS1, a novel androgen-repressible apoptosis gene', *Apoptosis 2002 7:1*. Springer, 7(1), pp. 13–21. doi: 10.1023/A:1013504710343.

Chase, H. B. (1954) 'Growth of the hair', *Physiological reviews*, 34(1), pp. 113–126. doi: 10.1152/PHYSREV.1954.34.1.113.

Chase, H. B., Montagna, W. and Malone, J. D. (1953) 'Changes in the skin in relation to the hair growth cycle', *Anat Rec*, 116, pp. 75–82.

Chen, C. L. *et al.* (2020) 'Functional complexity of hair follicle stem cell niche and therapeutic targeting of niche dysfunction for hair regeneration', *Journal of Biomedical Science*. BioMed Central Ltd., 27(1). doi: 10.1186/S12929-020-0624-8.

Chen, C. P. *et al.* (2015) 'Prenatal diagnosis and array comparative genomic hybridization characterization of interstitial deletions of 8q23.3–q24.11 and 8q24.13 associated with Langer-Giedion syndrome, Cornelia de Lange syndrome and haploinsufficiency of TRPS1, RAD21 and EXT1', *Taiwanese Journal of Obstetrics and Gynecology*. Elsevier, 54(5), pp. 592–596. doi: 10.1016/J.TJOG.2015.08.013.

Chen, D. *et al.* (2012) 'Dermal β-catenin activity in response to epidermal Wnt ligands is required for fibroblast proliferation and hair follicle initiation', *Development*. The Company of

Biologists, 139(8), pp. 1522–1533. doi: 10.1242/DEV.076463.

Chew, E. G. Y. *et al.* (2016) 'Differential Expression between Human Dermal Papilla Cells from Balding and Non-Balding Scalps Reveals New Candidate Genes for Androgenetic Alopecia', *Journal of Investigative Dermatology*, 136(8), pp. 1559–1567. doi: 10.1016/j.jid.2016.03.032.

Chi, W., Wu, E. and Morgan, B. A. (2013) 'Dermal papilla cell number specifies hair size, shape and cycling and its reduction causes follicular decline', *Development (Cambridge)*, 140(8), pp. 1676–1683. doi: 10.1242/dev.090662.

Chiu, C. L. *et al.* (2016) 'Intracellular kinetics of the androgen receptor shown by multimodal Image Correlation Spectroscopy (mICS)', *Scientific Reports*. Nature Publishing Group, 6(December 2015), pp. 1–13. doi: 10.1038/srep22435.

Choi, S. J. *et al.* (2013) 'Effects of glucocorticoid on human dermal papilla cells in vitro', *Journal of Steroid Biochemistry and Molecular Biology*. Elsevier Ltd, 135(1), pp. 24–29. doi: 10.1016/j.jsbmb.2012.11.009.

Choong, C. S. *et al.* (1996) 'Reduced androgen receptor gene expression with first exon CAG repeat expansion', *Molecular endocrinology (Baltimore, Md.)*. Mol Endocrinol, 10(12), pp. 1527–1535. doi: 10.1210/MEND.10.12.8961263.

Cobb, J. E. *et al.* (2010) 'Evidence for two independent functional variants for androgenetic alopecia around the androgen receptor gene', *Experimental Dermatology*, 19, pp. 1020–1028. doi: 10.1111/j.1600-0625.2010.01132.x.

Cobb, J. E. *et al.* (2011) 'Evidence of increased DNA methylation of the androgen receptor gene in occipital hair follicles from men with androgenetic alopecia', *British Journal of Dermatology*, 165(1), pp. 210–213. doi: 10.1111/j.1365-2133.2011.10335.x.

Courtois, M. *et al.* (1994) 'Hair Cycle and Alopecia', *Skin Pharmacology and Physiology*. Karger Publishers, 7(1–2), pp. 84–89. doi: 10.1159/000211279.

Cranwell, W. and Sinclair, R. (2016) 'Male androgenetic alopecia', *Hair, Hair Growth and Hair Disorders*, pp. 159–170. doi: 10.1007/978-3-540-46911-7_9.

Dalsgaard, C.-J. *et al.* (1984) *Distribution of neurofilament-immunoreactive nerve fibers in*

human skin, *Histochemistry*.

Dargie, H. J., Dollery, C. T. and Daniel, J. (1977) 'MINOXIDIL IN RESISTANT HYPERTENSION', *The Lancet*. Elsevier, 310(8037), pp. 515–518. doi: 10.1016/S0140-6736(77)90660-2.

Davey, R. A. and Grossmann, M. (2016) 'Androgen Receptor Structure, Function and Biology: From Bench to Bedside', *The Clinical Biochemist Reviews*. Australasian Association for Clinical Biochemistry and Laboratory Medicine, 37(1), p. 3. Available at: /pmc/articles/PMC4810760/ (Accessed: 13 December 2021).

Dhouailly, D. (1973) 'Dermo-epidermal interactions between birds and mammals: differentiation of cutaneous appendages', *Development*. The Company of Biologists, 30(3), pp. 587–603. doi: 10.1242/DEV.30.3.587.

Dinh, H. V., Sinclair, R. D. and Martinick, J. (2008) 'Donor site dominance in action: Transplanted hairs retain their original pigmentation long term', *Dermatologic Surgery*, 34(8), pp. 1108–1111. doi: 10.1111/j.1524-4725.2008.34228.x.

Driskell, R. *et al.* (2013) 'Distinct fibroblast lineages determine dermal architecture in skin development and repair', *Nature*. Nature Publishing Group, 504(7479), pp. 277–281. doi: 10.1038/nature12783.

DuBois, J. *et al.* (2021) 'Setipiprant for Androgenetic Alopecia in Males: Results from a Randomized, Double-Blind, Placebo-Controlled Phase 2a Trial', *Clinical, Cosmetic and Investigational Dermatology*. Dove Press, 14, pp. 1507–1517. doi: 10.2147/CCID.S319676.

Duclot, F. and Kabbaj, M. (2017) 'The role of early growth response 1 (EGR1) in brain plasticity and neuropsychiatric disorders', *Frontiers in Behavioral Neuroscience*, 11(March), pp. 1–20. doi: 10.3389/fnbeh.2017.00035.

Duverger, O. and Morasso, M. I. (2014) 'To grow or not to grow: Hair morphogenesis and human genetic hair disorders', *Seminars in Cell and Developmental Biology*. Elsevier Ltd, 25–26, pp. 22–33. doi: 10.1016/j.semcdb.2013.12.006.

Elliott, K., Stephenson, T. J. and Messenger, A. G. (1999) *Differences in Hair Follicle Dermal Papilla Volume are Due to Extracellular Matrix Volume and Cell Number: Implications for the*

Control of Hair Follicle Size and Androgen Responses, *Journal of Investigative Dermatology*. doi: 10.1046/j.1523-1747.1999.00797.x.

Ellis, J. A., Stebbing, M. and Harrap, S. B. (2001) 'Polymorphism of the Androgen Receptor Gene is Associated with Male Pattern Baldness', *Journal of Investigative Dermatology*. Elsevier, 116(3), pp. 452–455. doi: 10.1046/J.1523-1747.2001.01261.X.

Ellis, R. A. and Moretti, G. (1959) 'VASCULAR PATTERNS ASSOCIATED WITH CATAGEN HAIR FOLLICLES IN THE HUMAN SCALP', *Annals of the New York Academy of Sciences*, 83(3), pp. 448–457. doi: 10.1111/J.1749-6632.1960.TB40918.X/FORMAT/PDF.

Fabbrocini, G. *et al.* (2018) 'Female pattern hair loss: A clinical, pathophysiologic, and therapeutic review', *International Journal of Women's Dermatology*, 4(4), pp. 203–211. doi: 10.1016/j.ijwd.2018.05.001.

Fan, D. G. *et al.* (2011) 'BLCAP induces apoptosis in human Ewing's sarcoma cells:', *https://doi.org/10.1258/ebm.2011.010315*. SAGE PublicationsSage UK: London, England, 236(9), pp. 1030–1035. doi: 10.1258/EBM.2011.010315.

Fantauzzo, K. A., Tadin-Strapps, M., *et al.* (2008) 'A position effect on TRPS1 is associated with Ambras syndrome in humans and the Koala phenotype in mice', *Human Molecular Genetics*, 17(22), pp. 3539–3551. doi: 10.1093/hmg/ddn247.

Fantauzzo, K. A., Bazzi, H., *et al.* (2008) 'Dynamic expression of the zinc-finger transcription factor Trps1 during hair follicle morphogenesis and cycling', *Gene Expression Patterns*, 8(2), pp. 51–57. doi: 10.1016/j.modgep.2007.10.006.

Fantauzzo, K. A. and Christiano, A. M. (2012) 'Trps1 activates a network of secreted Wnt inhibitors and transcription factors crucial to vibrissa follicle morphogenesis', *Development*, 139(1), pp. 203–214. doi: 10.1242/dev.069971.

Fawzi, M. M. T. *et al.* (2016) 'Assessment of tissue levels of dickkopf-1 in androgenetic alopecia and alopecia areata', *Journal of cosmetic dermatology*. J Cosmet Dermatol, 15(1), pp. 10–15. doi: 10.1111/JOCD.12171.

Feng, Q. and He, B. (2019) 'Androgen Receptor Signaling in the Development of Castration-Resistant Prostate Cancer', *Frontiers in Oncology*, 9(September), pp. 1–10. doi:

10.3389/fonc.2019.00858.

Fenner, J. and Clark, R. A. F. (2016) *Anatomy, Physiology, Histology, and Immunohistochemistry of Human Skin*, *Skin Tissue Engineering and Regenerative Medicine*. Elsevier Inc. doi: 10.1016/B978-0-12-801654-1.00001-2.

Gai, Z., Gui, T. and Muragaki, Y. (2011) 'The function of TRPS1 in the development and differentiation of bone, kidney, and hair follicles', *Histology and Histopathology*, 26(7), pp. 915–921. doi: 10.14670/HH-26.915.

Garagnani, P. *et al.* (2012) 'Methylation of ELOVL2 gene as a new epigenetic marker of age', *Aging Cell*, 11(6), pp. 1132–1134. doi: 10.1111/acel.12005.

Garza, L. A. *et al.* (2011) 'Bald scalp in men with androgenetic alopecia retains hair follicle stem cells but lacks CD200-rich and CD34-positive hair follicle progenitor cells', *Journal of Clinical Investigation*, 121(2), pp. 613–622. doi: 10.1172/JCI44478.

Garza, L. A. *et al.* (2012) 'Prostaglandin D2 inhibits hair growth and is elevated in bald scalp of men with androgenetic alopecia', *Sci Transl Med*, 4(126). doi: 10.1126/scitranslmed.3003122.Prostaglandin.

Geyfman, M. *et al.* (2015) 'Resting no more: re-defining telogen, the maintenance stage of the hair growth cycle', *Biological reviews of the Cambridge Philosophical Society*. NIH Public Access, 90(4), p. 1179. doi: 10.1111/BRV.12151.

Giles, G. G. *et al.* (2002) 'Androgenetic Alopecia and Prostate Cancer: Findings from an Australian Case-Control Study 1'.

Goldman, C. K. *et al.* (1995) 'Loss of Vascular Endothelial Growth Factor in Human Alopecia Hair Follicles'. doi: 10.1038/jid.1995.40.

Gómez-Gaviro, M. V. *et al.* (2020) 'Biomedical Applications of Tissue Clearing and Three-Dimensional Imaging in Health and Disease', *iScience*. Elsevier, 23(8), p. 101432. doi: 10.1016/J.ISCI.2020.101432.

Gormley, G. J. *et al.* (1992) 'The Effect of Finasteride in Men with Benign Prostatic Hyperplasia', *New England Journal of Medicine*. Massachusetts Medical Society, 327(17), pp. 1185–1191. doi: 10.1056/NEJM199210223271701.

Greco, V. *et al.* (2009) ‘A Two-Step Mechanism for Stem Cell Activation during Hair Regeneration’, *Cell Stem Cell*, 19(4). doi: 10.1016/j.stem.2008.12.009. A.

Griffith, E. C. *et al.* (1997) ‘Methionine aminopeptidase (type 2) is the common target for angiogenesis inhibitors AGM-1470 and ovalicin’, *Chemistry & biology*. Chem Biol, 4(6), pp. 461–471. doi: 10.1016/S1074-5521(97)90198-8.

de Groot, S. C. *et al.* (2021) ‘Back to the Future: From Appendage Development Toward Future Human Hair Follicle Neogenesis’, *Frontiers in Cell and Developmental Biology*. Frontiers Media S.A., 9, p. 840. doi: 10.3389/FCELL.2021.661787/BIBTEX.

Guarrera, M. and Rebora, A. (2019) ‘The Higher Number and Longer Duration of Kenogen Hairs Are the Main Cause of the Hair Rarefaction in Androgenetic Alopecia’, *Skin Appendage Disorders*. Karger Publishers, 5(3), pp. 152–154. doi: 10.1159/000493587.

Guo, H. *et al.* (2017) ‘Experimental and early investigational drugs for androgenetic alopecia’, *Expert Opinion on Investigational Drugs*. Taylor & Francis, 26(8), pp. 917–932. doi: 10.1080/13543784.2017.1353598.

Gur-Cohen, S. *et al.* (2019) ‘Stem cell – driven lymphatic remodeling coordinates tissue regeneration’, *Science*, 366, pp. 1218–1225.

Haber, R. S. *et al.* (2019) ‘Finasteride for androgenetic alopecia is not associated with sexual dysfunction: a survey-based, single-centre, controlled study’, *Journal of the European Academy of Dermatology and Venereology*. Blackwell Publishing Ltd, 33(7), pp. 1393–1397. doi: 10.1111/JDV.15548.

Hagenaars, S. P. *et al.* (2017) ‘Genetic prediction of male pattern baldness’, *PLoS Genetics*. Public Library of Science, 13(2). doi: 10.1371/JOURNAL.PGEN.1006594.

Hagner, A. *et al.* (2020) ‘Transcriptional Profiling of the Adult Hair Follicle Mesenchyme Reveals R-spondin as a Novel Regulator of Dermal Progenitor Function’, *iScience*. Elsevier Inc., 23(4), p. 101019. doi: 10.1016/j.isci.2020.101019.

Halata, Z. (1993) ‘Sensory innervation of the hairy skin (light-and electronmicroscopic study)’, *Journal of Investigative Dermatology*, 101(1 SUPPL.). doi: 10.1016/0022-202X(93)90505-C.

Hamilton, J. B. (1942) ‘Male Hormone Stimulation is a Prerequisite and Incitant in Common Baldness’, *Journal of Investigative Dermatology*, 5(6), pp. 451–480. doi: 10.1038/jid.1942.62.

Han, J. H. *et al.* (2004) ‘Effect of minoxidil on proliferation and apoptosis in dermal papilla cells of human hair follicle’, *Journal of Dermatological Science*, 34(2), pp. 91–98. doi: 10.1016/j.jdermsci.2004.01.002.

Hao, T. *et al.* (2021) ‘Predicting human age by detecting DNA methylation status in hair’, *Electrophoresis*, 42(11), pp. 1255–1261. doi: 10.1002/elps.202000349.

Hara, T. *et al.* (2003) ‘Novel Mutations of Androgen Receptor: A Possible Mechanism of Bicalutamide Withdrawal Syndrome’, *CANCER RESEARCH*, 63, pp. 149–153.

Hardy, M. H. (1992) ‘The secret life of the hair follicle’, *Trends in Genetics*, 8(2), pp. 55–61. doi: 10.1016/0168-9525(92)90350-D.

Hashimoto, K., Ito, M. and Suzuki, Y. (1990) ‘Innervation and Vasculature of the Hair Follicle’, *Hair and Hair Diseases*, (1966), pp. 117–147. doi: 10.1007/978-3-642-74612-3_6.

Hato, T., Tabata, M. and Oike, Y. (2008) ‘The Role of Angiopoietin-Like Proteins in Angiogenesis and Metabolism’, *Trends in Cardiovascular Medicine*. Elsevier, 18(1), pp. 6–14. doi: 10.1016/J.TCM.2007.10.003.

Havlickova, B. *et al.* (2009) ‘A human folliculoid microsphere assay for exploring epithelial-mesenchymal interactions in the human hair follicle’, *Journal of Investigative Dermatology*, 129(4), pp. 972–983. doi: 10.1038/jid.2008.315.

Heilmann-Heimbach, S. *et al.* (2017) ‘Meta-analysis identifies novel risk loci and yields systematic insights into the biology of male-pattern baldness’, *Nature Communications 2017 8:1*. Nature Publishing Group, 8(1), pp. 1–8. doi: 10.1038/ncomms14694.

Heilmann, S. *et al.* (2013) ‘Evidence for a polygenic contribution to androgenetic alopecia’, *British Journal of Dermatology*. John Wiley & Sons, Ltd, 169(4), pp. 927–930. doi: 10.1111/BJD.12443.

Heitman, N. *et al.* (2020) ‘Dermal sheath contraction powers stem cell niche relocation during hair cycle regression’, *Science*, 367(6474), pp. 161–166. doi:

10.1126/science.aax9131.

Hibberts, N. A., Howell, A. E. and Randall, V. A. (1998) 'Balding hair follicle dermal papilla cells contain higher levels of androgen receptors than those from non-balding scalp', *Journal of Endocrinology*, 156(1), pp. 59–65. doi: 10.1677/joe.0.1560059.

Hibino, T. and Nishiyama, T. (2004) 'Role of TGF-β2 in the human hair cycle', *Journal of Dermatological Science*. Elsevier, 35(1), pp. 9–18. doi: 10.1016/J.JDERMSCI.2003.12.003.

Higgins, C. A. *et al.* (2010) 'Modelling the hair follicle dermal papilla using spheroid cell cultures', *Experimental Dermatology*, 19(6), pp. 546–548. doi: 10.1111/J.1600-0625.2009.01007.X.

Higgins, C. A. *et al.* (2013) 'Microenvironmental reprogramming by threedimensional culture enables dermal papilla cells to induce de novo human hair-follicle growth', *Proceedings of the National Academy of Sciences of the United States of America*. National Academy of Sciences, 110(49), pp. 19679–19688. doi: 10.1073/pnas.1309970110.

Higgins, C. A. *et al.* (2014) 'FGF5 is a crucial regulator of hair length in humans', *Proceedings of the National Academy of Sciences of the United States of America*. National Academy of Sciences, 111(29), pp. 10648–10653. doi: 10.1073/PNAS.1402862111/-/DCSUPPLEMENTAL.

Hillmer, A. M. *et al.* (2008) 'Susceptibility variants for male-pattern baldness on chromosome 20p11', *Nature Genetics*, 40(11), pp. 1279–1281. doi: 10.1038/ng.228.

Hochfeld, L. M. *et al.* (2021) 'Evidence for a functional interaction of WNT10A and EBF1 in male-pattern baldness', *PLOS ONE*. Public Library of Science, 16(9), p. e0256846. doi: 10.1371/JOURNAL.PONE.0256846.

Hoi, C. S. L. *et al.* (2010) 'Runx1 Directly Promotes Proliferation of Hair Follicle Stem Cells and Epithelial Tumor Formation in Mouse Skin', *Molecular and Cellular Biology*, 30(10), pp. 2518–2536. doi: 10.1128/mcb.01308-09.

Hordinsky, M. K. and Ericson, M. E. (1996) 'Relationship between follicular nerve supply and alopecia', *Dermatologic Clinics*, 14(4), pp. 651–660. doi: 10.1016/S0733-8635(05)70391-0.

Huang, S. *et al.* (2012) 'Wls Is Expressed in the Epidermis and Regulates Embryonic Hair

Follicle Induction in Mice', *PLOS ONE*. Public Library of Science, 7(9), p. e45904. doi: 10.1371/JOURNAL.PONE.0045904.

Huelsken, J. *et al.* (2001) 'beta-Catenin controls hair follicle morphogenesis and stem cell differentiation in the skin', *Cell*. Cell, 105(4), pp. 533–545. doi: 10.1016/S0092-8674(01)00336-1.

Inamatsu, M. *et al.* (1998) 'Establishment of rat dermal papilla cell lines that sustain the potency to induce hair follicles from afollicular skin', *Journal of Investigative Dermatology*. Elsevier Masson SAS, 111(5), pp. 767–775. doi: 10.1046/j.1523-1747.1998.00382.x.

Inui, S. *et al.* (2002) 'Androgen-inducible TGF-beta1 from balding dermal papilla cells inhibits epithelial cell growth: a clue to understand paradoxical effects of androgen on human hair growth', *The FASEB journal : official publication of the Federation of American Societies for Experimental Biology*.

Irvine, R. A. *et al.* (1995) 'The CAG and GGC Microsatellites of the Androgen Receptor Gene Are in Linkage Disequilibrium in Men with Prostate Cancer', *Cancer Research*, 55(9).

Irwig, M. S. and Kolukula, S. (2011) 'Persistent Sexual Side Effects of Finasteride for Male Pattern Hair Loss', *Journal of Sexual Medicine*, 8(6), pp. 1747–1753. doi: 10.1111/j.1743-6109.2011.02255.x.

Ishii, Y. *et al.* (2008) 'Mutations in R-Spondin 4 (RSPO4) Underlie Inherited Anonychia', *Journal of Investigative Dermatology*. Elsevier, 128(4), pp. 867–870. doi: 10.1038/SJ.JID.5701078.

Itami, S. *et al.* (1995) 'Interaction between dermal papilla cells and follicular epithelial cells in vitro: Effect of androgen', *British Journal of Dermatology*. Blackwell Publishing Ltd, 132(4), pp. 527–532. doi: 10.1111/J.1365-2133.1995.TB08706.X/FORMAT/PDF.

Jahoda, C. A. (1992) 'Induction of follicle formation and hair growth by vibrissa dermal papillae implanted into rat ear wounds: vibrissa-type fibres are specified', *Development*. The Company of Biologists, 115(4), pp. 1103–1109. doi: 10.1242/DEV.115.4.1103.

Jahoda, C. A. B. (1998) 'Cellular and developmental aspects of androgenetic alopecia', *Experimental Dermatology*, 7(5), pp. 235–248. doi: 10.1111/j.1600-0625.2007.00666.x.

Jahoda, C. A. B. and Oliver, R. F. (1981) ‘The growth of vibrissa dermal papilla cells in vitro’, *British Journal of Dermatology*, 105(6), pp. 623–627. doi: 10.1111/J.1365-2133.1981.TB00971.X.

Jahoda, C. A. B. and Oliver, R. F. (1984) ‘Vibrissa dermal papilla cell aggregative behaviour in vivo and in vitro’, *Journal of Embryology and Experimental Morphology*.

Jahoda, C.A.B., Reynolds, A. J. and Oliver, R. F. (1993) ‘Induction of hair growth in ear wounds by cultured dermal papilla cells’, *Journal of Investigative Dermatology*, 101(4), pp. 584–590. doi: 10.1111/1523-1747.ep12366039.

Jahoda, Colin A.B., Reynolds, A. J. and Oliver, R. F. (1993) ‘Induction of hair growth in ear wounds by cultured dermal papilla cells’, *Journal of Investigative Dermatology*, 101(4), pp. 584–590. doi: 10.1111/1523-1747.ep12366039.

Jimenez, F. *et al.* (2021) ‘Hair Transplantation: Basic Overview’, *Journal of the American Academy of Dermatology*. American Academy of Dermatology, Inc. doi: 10.1016/j.jaad.2021.03.124.

Kalabusheva, E., Terskikh, V. and Vorotelyak, E. (2017) ‘Hair germ model in vitro via human postnatal keratinocyte-dermal papilla interactions: Impact of hyaluronic acid’, *Stem Cells International*, 2017. doi: 10.1155/2017/9271869.

Kamberov, Y. G. *et al.* (2015) ‘A genetic basis of variation in eccrine sweat gland and hair follicle density’, *Proceedings of the National Academy of Sciences*. National Academy of Sciences, 112(32), pp. 9932–9937. doi: 10.1073/PNAS.1511680112.

Kang, B. M. *et al.* (2012) ‘Sphere formation increases the ability of cultured human dermal papilla cells to induce hair follicles from mouse epidermal cells in a reconstitution assay’, *Journal of Investigative Dermatology*. Elsevier, pp. 237–239. doi: 10.1038/jid.2011.250.

Kim, J. N. *et al.* (2014) ‘Morphological and morphometric study of the androgenetic alopecic scalp using two- and three-dimensional analysis comparing regional differences’, *The British journal of dermatology*. Br J Dermatol, 170(6), pp. 1313–1318. doi: 10.1111/BJD.12842.

Kimura-Ueki, M. *et al.* (2012) ‘Hair Cycle Resting Phase Is Regulated by Cyclic Epithelial FGF18 Signaling’, *Journal of Investigative Dermatology*. Elsevier, 132(5), pp. 1338–1345.

doi: 10.1038/JID.2011.490.

Kishimoto, J., Burgeson, R. E. and Morgan, B. A. (2000) 'Wnt signaling maintains the hair-inducing activity of the dermal papilla', *Genes and Development*, 14(10), pp. 1181–1185. doi: 10.1101/gad.14.10.1181.

Kolarsick, P. A. J. and Goodwin, C. (2018) 'Anatomy and physiology of the skin', *Journal of the Dermatology Nurses' Association*, 3(4), pp. 203–213. doi: 10.1007/978-3-319-78310-9_2.

Komiya, Y. and Habas, R. (2008) 'Wnt signal transduction pathways', *Organogenesis*. Taylor & Francis, 4(2), p. 68. doi: 10.4161/ORG.4.2.5851.

Kozlowska, U. *et al.* (1998) 'Expression of vascular endothelial growth factor (VEGF) in various compartments of the human hair follicle', *Archives of Dermatological Research 1998 290:12*. Springer, 290(12), pp. 661–668. doi: 10.1007/S004030050370.

Kruger, E. A. and Figg, W. D. (2005) 'TNP-470: an angiogenesis inhibitor in clinical development for cancer TNP-470: an angiogenesis inhibitor in clinical development for cancer', *Expert Opinion on Investigational Drugs*, 9(6), pp. 1383–1396. doi: 10.1517/13543784.9.6.1383.

Kure, K., Isago, T. and Hirayama, T. (2015) *Changes in the sebaceous gland in patients with male pattern hair loss (androgenic alopecia)*, *Journal of Cosmetic Dermatology*.

Kwack, M. H. *et al.* (2008) 'Dihydrotestosterone-inducible dickkopf 1 from balding dermal papilla cells causes apoptosis in follicular keratinocytes', *Journal of Investigative Dermatology*. Elsevier Masson SAS, 128(2), pp. 262–269. doi: 10.1038/sj.jid.5700999.

Kwack, M. H. *et al.* (2011) 'Minoxidil activates β-catenin pathway in human dermal papilla cells: A possible explanation for its anagen prolongation effect', *Journal of Dermatological Science*. Elsevier, 62(3), pp. 154–159. doi: 10.1016/J.JDERMSCI.2011.01.013.

Kwack, M. H. *et al.* (2012) 'Dihydrotestosterone-Inducible IL-6 Inhibits Elongation of Human Hair Shafts by Suppressing Matrix Cell Proliferation and Promotes Regression of Hair Follicles in Mice', *Journal of Investigative Dermatology*. Elsevier, 132(1), pp. 43–49. doi: 10.1038/JID.2011.274.

Kwack, M. H. *et al.* (2016) 'SFRP2 augments Wnt/β-catenin signalling in cultured dermal papilla cells', *Experimental Dermatology*. John Wiley & Sons, Ltd, 25(10), pp. 813–815. doi: 10.1111/EXD.12993.

Kwack, M. H. *et al.* (2017) 'Dickkopf-1 is involved in dexamethasone-mediated hair follicle regression', *Experimental Dermatology*. John Wiley & Sons, Ltd, 26(10), pp. 952–954. doi: 10.1111/EXD.13308.

Kwack, Mi H. *et al.* (2019) 'Exosomes derived from human dermal papilla cells promote hair growth in cultured human hair follicles and augment the hair-inductive capacity of cultured dermal papilla spheres', *Experimental Dermatology*. Blackwell Publishing Ltd, 28(7), pp. 854–857. doi: 10.1111/EXD.13927.

Kwack, Mi Hee *et al.* (2019) 'Overexpression of alkaline phosphatase improves the hair-inductive capacity of cultured human dermal papilla spheres', *Journal of Dermatological Science*. Elsevier Ireland Ltd, pp. 126–129. doi: 10.1016/j.jdermsci.2019.07.008.

Kwon, R. J. *et al.* (2016) 'ZHX1 Promotes the proliferation, migration and invasion of cholangiocarcinoma cells', *PLoS ONE*, 11(11), pp. 1–15. doi: 10.1371/journal.pone.0165516.

Lachgar, S. *et al.* (1998) 'Minoxidil upregulates the expression of vascular endothelial growth factor in human hair dermal papilla cells', *British Journal of Dermatology*, 138(3), pp. 407–411. doi: 10.1046/j.1365-2133.1998.02115.x.

Lai-Cheong, J. E. and McGrath, J. A. (2017) 'Structure and function of skin, hair and nails', *Medicine*. Elsevier, 45(6), pp. 347–351. doi: 10.1016/J.MPMED.2017.03.004.

Lattanand, A. and Johnson, W. C. (1975) 'Male Pattern Alopecia A Histopathologic and Histochemical Study', *Journal of Cutaneous Pathology*, 2(2), pp. 58–70. doi: 10.1111/j.1600-0560.1975.tb00209.x.

de Lau, W. B. M., Snel, B. and Clevers, H. C. (2012) 'The R-spondin protein family', *Genome Biology*. BioMed Central, 13(3), pp. 1–10. doi: 10.1186/GB-2012-13-3-242/FIGURES/4.

Lechner, S. G. and Lewin, G. R. (2013) 'Hairy sensation', *Physiology*, 28(3), pp. 142–150.

doi: 10.1152/PHYSIOL.00059.2012/ASSET/IMAGES/MEDIUM/PHY0031301570001.JPEG.

Leirõs, G. J., Attorresi, A. I. and Balañá, M. E. (2012) 'Hair follicle stem cell differentiation is inhibited through cross-talk between Wnt/β-catenin and androgen signalling in dermal papilla cells from patients with androgenetic alopecia', *British Journal of Dermatology*, 166(5), pp. 1035–1042. doi: 10.1111/j.1365-2133.2012.10856.x.

Lertkiatmongkol, P. *et al.* (2016) 'Endothelial functions of PECAM-1 (CD31)', *Current Opinion in Hematology*, 23(3), pp. 253–259. doi: 10.1097/MOH.0000000000000239.

Li, K. N. *et al.* (2019) 'Skin vasculature and hair follicle cross- talking associated with stem cell activation and tissue homeostasis', *eLife*, 8, pp. 1–27. doi: 10.7554/eLife.45977.

Li, L. *et al.* (2011) 'The functional organization of cutaneous low-threshold mechanosensory neurons', *Cell*. Elsevier Inc., 147(7), pp. 1615–1627. doi: 10.1016/j.cell.2011.11.027.

Li, R. *et al.* (2012) 'Six Novel Susceptibility Loci for Early-Onset Androgenetic Alopecia and Their Unexpected Association with Common Diseases', *PLoS Genet*, 8(5). doi: 10.1371/journal.pgen.1002746.

Lin, K. K. *et al.* (2004) 'Identification of hair cycle-associated genes from time-course gene expression profile data by using replicate variance', *Proceedings of the National Academy of Sciences of the United States of America*. National Academy of Sciences, 101(45), pp. 15955–15960. doi: 10.1073/PNAS.0407114101/SUPPL_FILE/07114TABLE4.XLS.

Lindner, G. *et al.* (1997) 'Analysis of apoptosis during hair follicle regression (catagen)', *The American Journal of Pathology*. American Society for Investigative Pathology, 151(6), pp. 1601–1617. Available at: /pmc/articles/PMC1858357/?report=abstract (Accessed: 20 November 2021).

Lindner, G. *et al.* (2011) 'De novo formation and ultra-structural characterization of a fiber-producing human hair follicle equivalent in vitro', *Journal of Biotechnology*, 152(3), pp. 108–112. doi: 10.1016/j.jbiotec.2011.01.019.

Maas, S. *et al.* (1993) *Trichorhinophalangeal Syndrome*. University of Washington, Seattle, Seattle (WA). Available at: http://europepmc.org/books/NBK425926.

Madaan, A. *et al.* (2018) 'Review of Hair Follicle Dermal Papilla cells as in vitro screening

model for hair growth', *International Journal of Cosmetic Science*. John Wiley & Sons, Ltd, 40(5), pp. 429–450. doi: 10.1111/ICS.12489.

Malgouries, S., Thibaut, S. and Bernard, B. A. (2008) 'Proteoglycan expression patterns in human hair follicle', *British Journal of Dermatology*, 158(2), pp. 234–342. doi: 10.1111/j.1365-2133.2007.08339.x.

Martino, P. A., Heitman, N. and Rendl, M. (2021) 'The dermal sheath: An emerging component of the hair follicle stem cell niche', *Experimental Dermatology*. John Wiley & Sons, Ltd, 30(4), pp. 512–521. doi: 10.1111/EXD.14204.

Masiello, D. *et al.* (2002) 'Bicalutamide Functions as an Androgen Receptor Antagonist by Assembly of a Transcriptionally Inactive Receptor *', *Journal of Biological Chemistry*. Elsevier, 277(29), pp. 26321–26326. doi: 10.1074/JBC.M203310200.

Maurer, Marcus *et al.* (1998) *Intact hair follicle innervation is not essential for anagen induction and development*, *Arch Dermatol Res*.

Mecklenburg, L. *et al.* (2000) 'Active hair growth (anagen) is associated with angiogenesis', *Journal of Investigative Dermatology*. Blackwell Publishing Inc., 114(5), pp. 909–916. doi: 10.1046/j.1523-1747.2000.00954.x.

Mella, J. M. *et al.* (2010) 'Efficacy and safety of finasteride therapy for androgenetic alopecia: A systematic review', *Archives of Dermatology*, 146(10), pp. 1141–1150. doi: 10.1001/archdermatol.2010.256.

Messenger, A. (1984) 'The culture of dermal papilla cells from human hair follicles', *British Journal of Dermatology*, 110, pp. 685–689. doi: 10.1111/j.1365-2133.1984.tb04705.x.

Messenger, A. G. *et al.* (1991) 'Expression of basement membrane proteins and interstitial collagens in dermal papillae of human hair follicles', *Journal of Investigative Dermatology*, 96(1), pp. 93–97. doi: 10.1111/1523-1747.ep12515907.

Messenger, A. G. and Rundegren, J. (2004) 'Minoxidil: Mechanisms of action on hair growth', *British Journal of Dermatology*, 150(2), pp. 186–194. doi: 10.1111/j.1365-2133.2004.05785.x.

Midorikawa, T. *et al.* (2004) 'Different gene expression profile observed in dermal papilla

cells related to androgenic alopecia by DNA macroarray analysis', *Journal of Dermatological Science*. Elsevier, 36(1), pp. 25–32. doi: 10.1016/J.JDERMSCI.2004.05.001.

Mok, K. W. *et al.* (2019) 'Dermal Condensate Niche Fate Specification Occurs Prior to Formation and Is Placode Progenitor Dependent', *Developmental Cell*. Cell Press, 48(1), pp. 32-48.e5. doi: 10.1016/J.DEVCEL.2018.11.034.

Molbay, M. *et al.* (2021) 'A guidebook for DISCO tissue clearing', *Molecular Systems Biology*. EMBO, 17(3), p. e9807. doi: 10.15252/msb.20209807.

Montagna, W. and Ellis, R. A. (1957) 'Histology and Cytochemistry of Human Skin. XIII. The Blood Supply of the Hair Follicle', *Journal of the National Cancer Institute*, 19(3). Available at: https://academic.oup.com/jnci/article/19/3/451/1015181 (Accessed: 11 December 2021).

Moore, L. D., Le, T. and Fan, G. (2012) 'DNA Methylation and Its Basic Function', *Neuropsychopharmacology 2013 38:1*. Nature Publishing Group, 38(1), pp. 23–38. doi: 10.1038/npp.2012.112.

Morgan, B. A. (2014) 'The dermal papilla: An instructive niche for epithelial stem and progenitor cells in development and regeneration of the hair follicle', *Cold Spring Harbor Perspectives in Medicine*, 4(7), pp. 1–14. doi: 10.1101/cshperspect.a015180.

Müller-Röver, S. *et al.* (2001) 'A Comprehensive Guide for the Accurate Classification of Murine Hair Follicles in Distinct Hair Cycle Stages', *Journal of Investigative Dermatology*. Elsevier, 117(1), pp. 3–15. doi: 10.1046/J.0022-202X.2001.01377.X.

Naue, J. *et al.* (2021) 'Analysis of age-dependent DNA methylation changes in plucked hair samples using massive parallel sequencing', *Rechtsmedizin*. Springer, pp. 1–8. doi: 10.1007/s00194-021-00487-4.

Nguyen, M. B. *et al.* (2018) 'FGF signalling controls the specification of hair placode-derived SOX9 positive progenitors to Merkel cells', *Nature Communications*. Nature Publishing Group, 9(1). doi: 10.1038/S41467-018-04399-Y.

Nicu, C. *et al.* (2018) 'A guide to studying human dermal adipocytes in situ', *Experimental Dermatology*, 27(6), pp. 589–602. doi: 10.1111/exd.13549.

Niehrs, C. (2012) 'The complex world of WNT receptor signalling', *Nature Reviews*

Molecular Cell Biology 2012 13:12. Nature Publishing Group, 13(12), pp. 767–779. doi: 10.1038/nrm3470.

Nyholt, D. R. *et al.* (2003) 'Genetic Basis of Male Pattern Baldness', *Journal of Investigative Dermatology*. Elsevier, 121(6), pp. 1561–1564. doi: 10.1111/J.1523-1747.2003.12615.X.

Oh, J. W., Kloepper, J., Langan, Ewan A, *et al.* (2016) 'A Guide to Studying Human Hair Follicle Cycling In Vivo', *Journal of Investigative Dermatology*, 136, pp. 34–44. doi: 10.1038/JID.2015.354.

Oh, J. W., Kloepper, J., Langan, Ewan A., *et al.* (2016) 'A Guide to Studying Human Hair Follicle Cycling In Vivo', *Journal of Investigative Dermatology*. Elsevier, 136(1), pp. 34–44. doi: 10.1038/JID.2015.354.

Ohyama, M. *et al.* (2012) 'Restoration of the intrinsic properties of human dermal papilla in vitro', *Journal of Cell Science*, 125, pp. 4114–4125. doi: 10.1242/jcs.105700.

Oliver, R. F. (1966) 'Whisker growth after removal of the dermal papilla and lengths of follicle in the hooded rat.', *Journal of Embryology and Experimental Morphology*, 15(3), pp. 331–347.

Oliver, R. F. (1967) 'The experimental induction of whisker growth in the hooded rat by implantation of dermal papillae.', *Journal of Embryology and Experimental Morphology*, 18(1), pp. 43–51.

Oliver, R. F. (1970) 'The induction of hair follicle formation in the adult hooded rat by vibrissa dermal papillae', *Development*. The Company of Biologists, 23(1), pp. 219–236. doi: 10.1242/DEV.23.1.219.

Olson, W. *et al.* (2016) 'The specification and wiring of mammalian cutaneous low-threshold mechanoreceptors', *Wiley Interdisciplinary Reviews: Developmental Biology*, 5(3), pp. 389–404. doi: 10.1002/wdev.229.

Orentreich, N. (1959) 'AUTOGRAFTS IN ALOPECIAS AND OTHER SELECTED DERMATOLOGICAL CONDITIONS', *Annals of the New York Academy of Sciences*, 83(3), pp. 463–479. doi: 10.1111/J.1749-6632.1960.TB40920.X.

Pallotti, F. *et al.* (2020) 'Androgenetic alopecia: effects of oral finasteride on hormone profile,

reproduction and sexual function', *Endo*, 68, pp. 688–694. doi: 10.1007/s12020-020-02219-2.

Panati, K., Suneetha, Y. and Narala, V. R. (2016) 'Irisin/FNDC5 - An updated review', *European Review for Medical and Pharmacological Sciences*, 20(4), pp. 689–697.

Panteleyev, A. A. (2018) 'Functional anatomy of the hair follicle: The Secondary Hair Germ', *Experimental Dermatology*. John Wiley & Sons, Ltd, 27(7), pp. 701–720. doi: 10.1111/EXD.13666.

Pantelireis, N. and Higgins, C. A. (2018) 'A bald statement — Current approaches to manipulate miniaturisation focus only on promoting hair growth', *Experimental Dermatology*, 27(9), pp. 959–965. doi: 10.1111/exd.13690.

Pascalau, R. and Kuruvilla, R. (2020) 'A Hairy End to a Chilling Event', *Cell*. Cell Press, 182(3), pp. 539–541. doi: 10.1016/J.CELL.2020.07.004.

Peluso, A. M. *et al.* (1997) 'Diffuse hypertrichosis during treatment with 5% topical minoxidil', *British Journal of Dermatology*. Wiley, 136, pp. 118–120. doi: 10.1046/J.1365-2133.1997.D01-1156.X.

Peña-Jimenez, D. *et al.* (2019) ' Lymphatic vessels interact dynamically with the hair follicle stem cell niche during skin regeneration in vivo ', *The EMBO Journal*, 38(19), pp. 1–17. doi: 10.15252/embj.2019101688.

Peters, E. M. J. *et al.* (2001) 'Hair-cycle-associated remodeling of the peptidergic innervation of murine skin, and hair growth modulation by neuropeptides', *Journal of Investigative Dermatology*. Blackwell Publishing Inc., 116(2), pp. 236–245.

Pirastu, N. *et al.* (2017) 'GWAS for male-pattern baldness identifies 71 susceptibility loci explaining 38% of the risk', *Nature Communications*, 8(1584). doi: 10.1038/s41467-017-01490-8.

Plikus, M. V. *et al.* (2008) 'Cyclic dermal BMP signalling regulates stem cell activation during hair regeneration', *Nature 2008 451:7176*. Nature Publishing Group, 451(7176), pp. 340–344. doi: 10.1038/nature06457.

Plikus, M. V. (2012) 'New activators and inhibitors in the hair cycle clock: targeting stem

cells' state of competence', *The Journal of investigative dermatology*. NIH Public Access, 132(5), p. 1321. doi: 10.1038/JID.2012.38.

Poblet, E. *et al.* (2018) 'Eccrine sweat glands associate with the human hair follicle within a defined compartment of dermal white adipose tissue', *British Journal of Dermatology*. John Wiley & Sons, Ltd, 178(5), pp. 1163–1172. doi: 10.1111/BJD.16436.

Praveen, K. *et al.* (2022) 'ANGPTL7, a therapeutic target for increased intraocular pressure and glaucoma', *Communications Biology 2022 5:1*. Nature Publishing Group, 5(1), pp. 1–15. doi: 10.1038/s42003-022-03932-6.

Qiao, J. *et al.* (2009) 'Hair follicle neogenesis induced by cultured human scalp dermal papilla cells', *Regenerative Medicine*. doi: 10.2217/rme.09.50.

Rahmani, W. *et al.* (2014) 'Hair Follicle Dermal Stem Cells Regenerate the Dermal Sheath, Repopulate the Dermal Papilla, and Modulate Hair Type', *Developmental Cell*. Elsevier Inc., 31(5), pp. 543–558. doi: 10.1016/j.devcel.2014.10.022.

Rashid, R. M. and White, L. E. (2007) 'A hairy development in hypertrichosis: A brief review of Ambras syndrome', *Dermatology Online Journal*, 13(3). doi: 10.5070/D3542884MC.

Ratner, P. *et al.* (2017) 'Efficacy and safety of setipiprant in seasonal allergic rhinitis: Results from Phase 2 and Phase 3 randomized, double-blind, placebo- and active-referenced studies', *Allergy, Asthma and Clinical Immunology*. BioMed Central Ltd., 13(1), pp. 1–15. doi: 10.1186/S13223-017-0183-Z/FIGURES/5.

Rebora, A. and Guarrera, M. (2002) 'Kenogen. A new phase of the hair cycle?', *Dermatology (Basel, Switzerland)*, 205(2), pp. 108–110. doi: 10.1159/000063908.

Reddy, S. *et al.* (2001) 'Characterization of Wnt gene expression in developing and postnatal hair follicles and identification of Wnt5a as a target of Sonic hedgehog in hair follicle morphogenesis', *Mechanisms of Development*. Elsevier, 107(1–2), pp. 69–82. doi: 10.1016/S0925-4773(01)00452-X.

Rendl, M., Lewis, L. and Fuchs, E. (2005) 'Molecular dissection of mesenchymal-epithelial interactions in the hair follicle', *PLoS Biology*, 3(11), pp. 1910–1924. doi: 10.1371/journal.pbio.0030331.

Rendl, M., Polak, L. and Fuchs, E. (2008) ‘BMP signaling in dermal papilla cells is required for their hair follicle-inductive properties’, *Genes & Development*. Cold Spring Harbor Laboratory Press, 22(4), pp. 543–557. doi: 10.1101/GAD.1614408.

Renier, N. *et al.* (2014) ‘IDISCO: A simple, rapid method to immunolabel large tissue samples for volume imaging’, *Cell*. Elsevier Inc., 159(4), pp. 896–910. doi: 10.1016/j.cell.2014.10.010.

Reveles Jensen, K. H. and Berg, R. W. (2017) ‘Advances and perspectives in tissue clearing using CLARITY’. doi: 10.1016/j.jchemneu.2017.07.005.

Reynolds, A. J. and Jahoda, C. A. B. (1992) ‘Cultured dermal papilla cells induce follicle formation and hair growth by transdifferentiation of an adult epidermis’, *Development*, 115, pp. 587–593.

Richards, J. B. *et al.* (2008) ‘Male-pattern baldness susceptibility locus at 20p11’, *Nature Genetics*, 40(11), pp. 1282–1284. doi: 10.1038/ng.255.

Richardson, D. S. and Lichtman, J. W. (2015) ‘Clarifying Tissue Clearing’, *Cell*. NIH Public Access, 162(2), p. 246. doi: 10.1016/J.CELL.2015.06.067.

Roh, C., Tao, Q. and Lyle, S. (2005) ‘Dermal papilla-induced hair differentiation of adult epithelial stem cells from human skin’, *Physiological Genomics*, 19, pp. 207–217. doi: 10.1152/physiolgenomics.00134.2004.

Rossi, A. *et al.* (2015) ‘Conditions simulating androgenetic alopecia’, *Journal of the European Academy of Dermatology and Venereology*, 29(7), pp. 1258–1264. doi: 10.1111/JDV.12915.

Sawaya, M. E. and Price, V. H. (1997) ‘Different Levels of 5α-Reductase Type I and II, Aromatase, and Androgen Receptor in Hair Follicles of Women and Men with Androgenetic Alopecia’, *Journal of Investigative Dermatology*. Elsevier, 109(3), pp. 296–300. doi: 10.1111/1523-1747.EP12335779.

Schiewer, M. J. and Knudsen, K. E. (2021) ‘Basic Science and Molecular Genetics of Prostate Cancer Aggressiveness’, *Urologic Clinics of North America*. Elsevier, 48(3), pp. 339–347. doi: 10.1016/J.UCL.2021.04.004.

Schneider, M. R., Schmidt-Ullrich, R. and Paus, R. (2009) 'The Hair Follicle as a Dynamic Miniorgan', *Current Biology*. Elsevier, 19(3), pp. R132–R142. doi: 10.1016/J.CUB.2008.12.005.

Schurr, A. (2017) 'Lactate, Not Pyruvate, Is the End Product of Glucose Metabolism via Glycolysis', *Carbohydrate*. IntechOpen. doi: 10.5772/66699.

Seo, C. H. *et al.* (2017) 'Activin A-induced signalling controls hair follicle neogenesis', *Experimental Dermatology*, 26(2), pp. 108–115. doi: 10.1111/exd.13234.

Shin, W. *et al.* (2020) 'Dysfunction of Hair Follicle Mesenchymal Progenitors Contributes to Age-Associated Hair Loss', *Developmental Cell*. Elsevier Inc., 53(2), pp. 185-198.e7. doi: 10.1016/j.devcel.2020.03.019.

Shwartz, Y. *et al.* (2020) 'Cell Types Promoting Goosebumps Form a Niche to Regulate Hair Follicle Stem Cells', *Cell*. Elsevier, 182(3), pp. 578-593.e19. doi: 10.1016/j.cell.2020.06.031.

Sick, S. *et al.* (2006) 'WNT and DKK determine hair follicle spacing through a reaction-diffusion mechanism', *Science*, 314, pp. 1447–1451.

Sinclair, R. D. (2004) 'Male androgenetic alopecia', *jmhg*, 1(4), pp. 319–327. doi: 10.1007/978-3-540-46911-7_9.

Sinclair, R., Torkamani, N. and Jones, L. (2015) 'Androgenetic alopecia: new insights into the pathogenesis and mechanism of hair loss', *F1000Research*. Faculty of 1000 Ltd, 4(F1000 Faculty Rev). doi: 10.12688/F1000RESEARCH.6401.1.

Soma, T. *et al.* (1998) 'Analysis of Apoptotic Cell Death in Human Hair Follicles In Vivo andIn Vitro', *Journal of Investigative Dermatology*. Elsevier, 111(6), pp. 948–954. doi: 10.1046/J.1523-1747.1998.00408.X.

Song, W. C. *et al.* (2006) 'A new model for the morphology of the arrector pili muscle in the follicular unit based on three-dimensional reconstruction', *Journal of Anatomy*. Wiley-Blackwell, 208(5), p. 643. doi: 10.1111/J.1469-7580.2006.00575.X.

Sousa, I. C. V. D. de and Tosti, A. (2013) 'New investigational drugs for androgenetic alopecia', *Expert Opinion on Investigational Drugs*. Taylor & Francis, 22(5), pp. 573–589. doi: 10.1517/13543784.2013.784743.

Stenn, K. S. and Paus, R. (2001) ‘Controls of hair follicle cycling’, *Physiological Reviews*. American Physiological Society, 81(1), pp. 449–494. doi: 10.1152/PHYSREV.2001.81.1.449/ASSET/IMAGES/LARGE/9J0110123003.JPEG.

Swartz, M. A. (2001) ‘The physiology of the lymphatic system’, *Advanced Drug Delivery Reviews*. Elsevier, 50(1–2), pp. 3–20. doi: 10.1016/S0169-409X(01)00150-8.

Teama, S. (2018) ‘DNA Polymorphisms: DNA-Based Molecular Markers and Their Application in Medicine’, *Genetic Diversity and Disease Susceptibility*. IntechOpen. doi: 10.5772/INTECHOPEN.79517.

Topouzi, H. *et al.* (2017) ‘Methods for the isolation and 3D culture of dermal papilla cells from human hair follicles’, *Experimental Dermatology*. Wiley-Blackwell, 26(6), p. 491. doi: 10.1111/EXD.13368.

Topouzi, H. and Higgins, C. A. (2016) ‘Changing faces: can a new identity stop balding?’, *Experimental Dermatology*, 25(10), pp. 765–766. doi: 10.1111/exd.13094.

Torkamani, N. *et al.* (2014) ‘Destruction of the arrector pili muscle and fat infiltration in androgenic alopecia* Funding sources’, *British Journal of Dermatology level one*. doi: 10.1111/bjd.12921.

Tosti, A., Piraccini, B. and Soli, M. (2001) ‘Evaluation of sexual function in subjects taking finasteride for the treatment of androgenetic alopecia’, *Journal of the European Academy of Dermatology and Venereology*. John Wiley & Sons, Ltd, 15(5), pp. 418–421. doi: 10.1046/J.1468-3083.2001.00315.X.

Traish, A. M. (2020) ‘Post-finasteride syndrome: a surmountable challenge for clinicians’, *Fertility and Sterility*. Elsevier, 113(1), pp. 21–50. doi: 10.1016/J.FERTNSTERT.2019.11.030.

Trüeb, R. M. (2002) ‘Molecular mechanisms of androgenetic alopecia’, *Experimental Gerontology*, 37(8–9), pp. 981–990.

Tsai, S. Y. *et al.* (2014) ‘Wnt/β-catenin signaling in dermal condensates is required for hair follicle formation’, *Developmental Biology*. Academic Press, 385(2), pp. 179–188. doi: 10.1016/J.YDBIO.2013.11.023.

Visscher, P. M. *et al.* (2017) ‘10 Years of GWAS Discovery: Biology, Function, and Translation’, *The American Journal of Human Genetics*. Cell Press, 101(1), pp. 5–22. doi: 10.1016/J.AJHG.2017.06.005.

Wen, L. *et al.* (2021) ‘Establishment of an Efficient Primary Culture System for Human Hair Follicle Stem Cells Using the Rho-Associated Protein Kinase Inhibitor Y-27632’, *Frontiers in Cell and Developmental Biology*, 9(March), pp. 1–16. doi: 10.3389/fcell.2021.632882.

Whiting, D. A. (2001) ‘Possible mechanisms of miniaturization during androgenetic alopecia or pattern hair loss’, *Journal of the American Academy of Dermatology*, 45(3 SUPPL.), pp. 81–86. doi: 10.1067/mjd.2001.117428.

Williams, R., Philpott, M. P. and Kealey, T. (1993) ‘Metabolism of freshly isolated human hair follicles capable of hair elongation: A glutaminolytic, aerobic glycolytic tissue’, *Journal of Investigative Dermatology*. Elsevier Masson SAS, 100(6), pp. 834–840. doi: 10.1111/1523-1747.ep12476744.

De Winter, J. A. R. *et al.* (1991) ‘Androgen Receptor Expression in Human Tissues: An Immunohistochemical Study’, *Printedin USA*, 39(7), pp. 927–936.

Woo, W. M., Zhen, H. H. and Oro, A. E. (2012) ‘Shh maintains dermal papilla identity and hair morphogenesis via a Noggin-Shh regulatory loop’, *Genes and Development*. Cold Spring Harbor Laboratory Press, 26(11), pp. 1235–1246. doi: 10.1101/gad.187401.112.

Xiao, Y. *et al.* (2015) ‘ANGPTL7 regulates the expansion and repopulation of human hematopoietic stem and progenitor cells’, *Haematologica*. Ferrata Storti Foundation, 100(5), p. 585. doi: 10.3324/HAEMATOL.2014.118612.

Yanez, S., Hernandez-Vincente, I. and Armijo, M. (1992) ‘Tricho-rhino-phalangeal syndrome’, *International Journal of Dermatology*, 31(10), pp. 706–709. doi: 10.1159/000250894.

Yang, H. *et al.* (2017) ‘Epithelial-Mesenchymal Micro-niches Govern Stem Cell Lineage Choices’, *Cell*. Cell, 169(3), pp. 483-496.e13. doi: 10.1016/J.CELL.2017.03.038.

Yang, S. Z. and Abdulkadir, S. A. (2003) ‘Early Growth Response Gene 1 Modulates Androgen Receptor Signaling in Prostate Carcinoma Cells *’, *Journal of Biological*

Chemistry. Elsevier, 278(41), pp. 39906–39911. doi: 10.1074/JBC.M307250200.

Yano, K., Brown, L. F. and Detmar, M. (2001) 'Control of hair growth and follicle size by VEGF-mediated angiogenesis', *Journal of Clinical Investigation*. The American Society for Clinical Investigation, 107(4), pp. 409–417. doi: 10.1172/JCI11317.

Yao, J. *et al.* (2006) 'Overexpression of BLCAP induces S phase arrest and apoptosis independent of p53 and NF-κB in human tongue carcinoma', *Molecular and Cellular Biochemistry 2006 297:1*. Springer, 297(1), pp. 81–92. doi: 10.1007/S11010-006-9332-2.

Yazdabadi, A. *et al.* (2012) 'Miniaturized hairs maintain contact with the arrector pili muscle in alopecia areata but not in androgenetic alopecia: A model for reversible miniaturization and potential for hair regrowth', *International Journal of Trichology*, 4(3), pp. 154–157. doi: 10.4103/0974-7753.100069.

Yen, C. M., Chan, C. C. and Lin Sung Jan, S. J. (2010) 'High-throughput reconstitution of epithelial-mesenchymal interaction in folliculoid microtissues by biomaterial-facilitated self-assembly of dissociated heterotypic adult cells', *Biomaterials*. Elsevier Ltd, 31(15), pp. 4341–4352. doi: 10.1016/j.biomaterials.2010.02.014.

Yoon, S. Y. *et al.* (2019) 'An important role of cutaneous lymphatic vessels in coordinating and promoting anagen hair follicle growth', *PLoS ONE*. Public Library of Science, 14(7). doi: 10.1371/journal.pone.0220341.

Yoshida, Y., Soma, T. and Kishimoto, J. (2019) 'Characterization of human dermal sheath cells reveals CD36-expressing perivascular cells associated with capillary blood vessel formation in hair follicles', *Biochemical and Biophysical Research Communications*. Academic Press, 516(3), pp. 945–950. doi: 10.1016/J.BBRC.2019.06.146.

Yuan, A. *et al.* (2012) 'Neurofilaments at a glance', *Journal of Cell Science*, 125(14), pp. 3257–3263. doi: 10.1242/jcs.104729.

Zbieć-Piekarska, R. *et al.* (2015) 'Examination of DNA methylation status of the ELOVL2 marker may be useful for human age prediction in forensic science', *Forensic Science International: Genetics*. Elsevier Ireland Ltd, 14, pp. 161–167. doi: 10.1016/j.fsigen.2014.10.002.

Zhang, Y. *et al.* (2000) 'Cell cycle inhibition by the anti-angiogenic agent TNP-470 is mediated by p53 and p21WAF1/CIP1', *Proceedings of the National Academy of Sciences of the United States of America*. National Academy of Sciences, 97(12), pp. 6427–6432. doi: 10.1073/PNAS.97.12.6427/ASSET/64E30C79-4808-46C2-A6DC-C02F60BC10BD/ASSETS/GRAPHIC/PQ1200625004.JPEG.

Zhang, Y. *et al.* (2009a) 'Reciprocal requirements for EDA/EDAR/NF-kappaB and Wnt/beta-catenin signaling pathways in hair follicle induction', *Developmental cell*. Dev Cell, 17(1), pp. 49–61. doi: 10.1016/J.DEVCEL.2009.05.011.

Zhang, Y. *et al.* (2009b) 'Reciprocal Requirements for EDA/EDAR/NF-κB and Wnt/β-Catenin Signaling Pathways in Hair Follicle Induction', *Developmental Cell*. Elsevier, 17(1), pp. 49–61. doi: 10.1016/j.devcel.2009.05.011.

Zheng, M. *et al.* (2019) 'Hypoxia improves hair inductivity of dermal papilla cells via nuclear NADPH oxidase 4-mediated reactive oxygen species generation'*', *British Journal of Dermatology*, 181, pp. 523–534. doi: 10.1111/bjd.17706.

Zheng, Y. *et al.* (2005) 'Organogenesis From Dissociated Cells: Generation of Mature Cycling Hair Follicles From Skin-Derived Cells', *Journal of Investigative Dermatology*. Elsevier, 124(5), pp. 867–876. doi: 10.1111/J.0022-202X.2005.23716.X.

Zuo, Z. *et al.* (2006) 'Functional Analysis of Bladder Cancer-Related Protein Gene: A Putative Cervical Cancer Tumor Suppressor Gene in Cervical Carcinoma', *Tumor Biol*, 27, pp. 221–226. doi: 10.1159/000093057.

Appendix

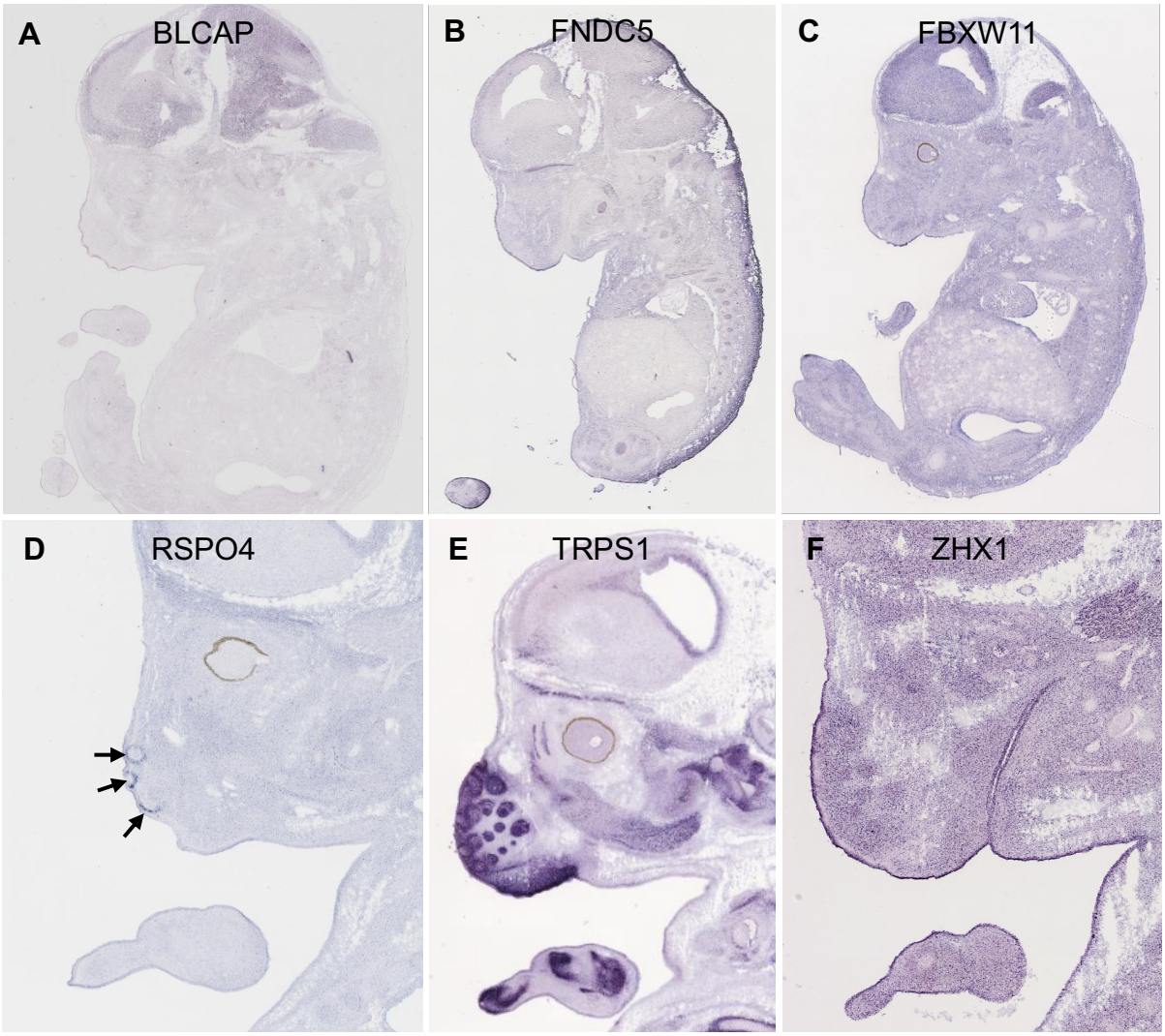


Figure A.1. In situ hybridisation of ODP signature genes.

In situ hybridisation to detect mRNA expression of BLCAP (A), FNDC5 (B), FBXW11 (C), RSPO4 (black arrows to show the expression, D), TRPS1 (E) and ZHX1 (F). Images obtained from GenePaint (https://gp3.mpg.de/).

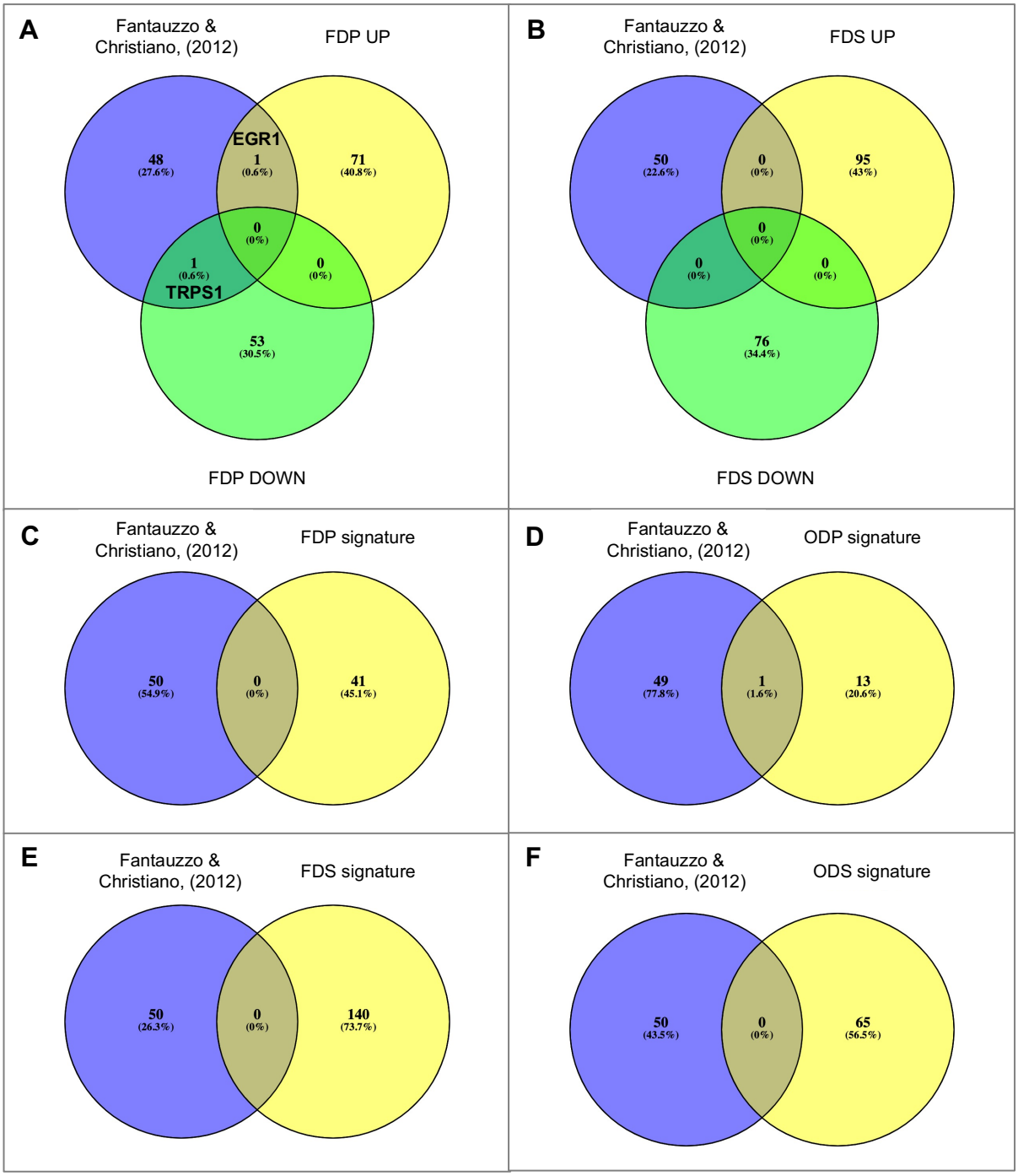


Figure A.2. Venn diagram to identify TRPS1 regulated genes in the follicular mesenchyme.

Comparison of TRPS1 regulated genes published by Fantauzzo and Christiano, (2012) with FDP vs ODP upregulated and downregulated genes (A), FDS vs ODS upregulated and downregulated genes (B), FDP signature (C), ODP signature (D), FDS signature (E) and ODS signature genes (F).